INTERNATIONAL DOCTORAL
SCHOOL OF THE USC

David Mateo
Fouz Varela

PhD Thesis

# A holistic methodology for the planning of hydrokinetic energy projects in coastal regions: Application to the Shannon Estuary (W Ireland)

Lugo, 2024

Doctoral Programme in Engineering for Rural and Civil Development

ESCOLA DE DOUTORAMENTO
INTERNACIONAL DA USC

DOCTORAL THESIS

# A holistic methodology for the planning of hydrokinetic energy projects in coastal regions: Application to the Shannon Estuary (W Ireland)

David Mateo Fouz Varela

Supervisors: Prof. Dr. Rodrigo Carballo Sánchez & Prof. Dr. Gregorio Iglesias Rodríguez

Tutor: Prof. Dr. Rodrigo Carballo Sánchez

**PHD PROGRAMME IN ENGINEERING FOR RURAL AND CIVIL DEVELOPMENT**

LUGO

2024

*A diente de sierra se despliega la vida. La cima es sólo de algunos. Para los que se mueven por la parte baja, para los que nunca llegan al pico, el desamparo gregario, la náusea de lo cotidiano.*

*Debe ser hermoso haberse en la cumbre. ¿Cómo se conseguirá cobijo ahí arriba? ¿No se temerá la caída? ¿No se sentirá el vértigo de la soledad cuando estás tan alto que se aligera el propio peso?*

*Los del valle sin embargo son ignorantes, no saben nada de cumbres nevadas, ni de aires frescos, no, de miradas infinitas. El valle abotarga los sentidos, retiene la prisa, borra la diferencia o la sitúa en el filo del diente: allí donde no se llega, donde se degüella a aquellos que pretendan subir a horcajadas y sin estilo.*

*El secreto de los dientes de sierra es que cortan, y que sólo se mueven bien por ellos los que se han revestido con corazas.*

*El caracol vive en el valle. Y el mar. Y yo.*

*(Hay noches en que me sueño sobrevolando cumbres).*

José Domingo de Prada. *Vértigo*

*Á memoria dos meus avós e avoas.*
*A David e Isabel e á familia que formaron,*
*por todo o seu esforzo.*

# ACKNOWLEDGEMENTS (IN GALICIAN)

*Vio, en fin, agradecido, los rostros de quienes lo habían hecho lo que era, y también lo que sería durante el resto de su vida.*

Arturo Pérez-Reverte. *Revolución*

Comezando polo **ámbito académico**, en primeiro lugar, gustaríame expresar o meu máis sincero afecto e gratitude ós directores desta tese, o Prof. Dr. Rodrigo Carballo e o Prof. Dr. Gregorio Iglesias, xa que sen eles e a súa inestimable axuda non podería ter completado esta etapa da vida académica. A Gregorio débolle a súa disposición e voluntariedade ó ter aceptado a dirección desta tese e a súa involucración na mesma sen case coñecerme previamente, máxime a distancia, e especialmente nunha situación na que non debera ter motivos ou necesidade de asumir esa carga de traballo adicional e parcialmente descoñecida. A Rodrigo débolle todo o traballo e a implicación do día a día, comezando pola posibilidade de poder comezar esta aventura, e rematando pola finalización desta tese, apoiándome constantemente durante todo o seu transcurso, tanto no plano académico como, máis importante se cabe, no persoal. Non sei se algún día serei quen de devolver todo isto, aínda que me sinto orgulloso e agradecido de poder dicir que nesta etapa non foi só un director, senón tamén un amigo.

Meu especial agradecemento ó Prof. Dr. Iván López, por exercer en todo momento coma se fose un terceiro director, sempre disposto a axudar e a perder parte do seu tempo en facer as cousas máis sinxelas ós demais ca súa enorme calidade científica e investigadora, pero especialmente ca súa inmensa calidade humana e o seu gran sentido do humor. Igualmente, estou tremendamente contento de poder dicir que para min, máis que un compañeiro, sempre será un amigo.

En terceiro lugar, o meu afectuoso agradecemento ó derradeiro dos coautores dos artigos que compoñen esta tese, o Prof. Dr. Xesús Pablo González, por estar sempre disposto a aportar e a botar unha man cando é máis necesario. Foi, en gran medida, determinante nos meus inicios nesta Universidade, e non o foi menos na culminación desta etapa académica.

O meu agradecemento ó resto de compañeiros cos que compartín esta etapa, xa que todos aportaron algo de seu, fundamentalmente no plano persoal, para que o meu paso pola Universidade fose tremendamente entretido e divertido: Dr. Miguel Álvarez, Dr. Víctor Ramos, Dr. Marcos Sánchez, Néstor Aréan e, final e especialmente, a Borja Álvarez, co que me une, ademais de algunha que outra aventura internacional, unha gran afinidade persoal e amizade.

No **ámbito persoal**, gustaríame comezar cunha mención especial a meus avós e avoas, Benigno, Pepa, Luis e Lina, que aínda que xa non están, ocuparon, ocupan e ocuparán sempre un lugar destacado na miña vida, xa que sen eles e as privacións que pasaron, eu non podería estar hoxe escribindo isto. Esta tese está dedicada á súa memoria.

O maior de todos estes agradecementos só pode ser para meu pai e miña nai, David e Isabel, por ser para min unha inmensa e inesgotable fonte de amor, respecto e exemplo. Esta tese está dedicada a eles, a todo o seu esforzo e á familia que formaron.

A miña irmá, Sandra, por apoiarme en todos e cada un dos momentos da miña vida, e por ter sempre unha inmensa fe en min, pensado que podo resolver practicamente todos os problemas das nosas vidas, incluso, en ocasións, a distancia.

Ós meus amigos e amigas, ós que nunca poderei devolver todos os sorrisos que me sacaron durante esta etapa, algún deles cando máis falta facía, e por ser, en todo momento e situación, unha parte imprescindible da miña vida: Laura, Diego e Uxío; Javi e Vero; Segade; Clemente, Natalia, Sara e Paula; Copa e Uxía.

Por último, pero non menos importante, a Tania. Por todo: polo pasado, polo presente e, sobre todo, polo futuro.

*Seguro que non están todos os que son, pero son todos os que están.*

Parte do traballo realizado nesta tese foi financiado co proxecto PORTOS, co-financiado polo Programa *Interreg Atlantic Area* a través do Fondo Europeo de Desenvolvemento Rexional (FEDER) [EAPA_784/2018]. Ademais, a realización desta tese obtivo financiación da Convocatoria de contratos predoutorais do Campus de Especialización Campus Terra financiada pola Consellería de Cultura, Educación, Formación Profesional e Universidades da Xunta de Galicia (8042-272B-64100).

# PUBLICATIONS DERIVED FROM THIS THESIS

This thesis includes in its main body the following research articles, corresponding with Chapters 4, 5 and 6, respectively:

Fouz, D. M., Carballo, R., López, I., & Iglesias, G. (2022). Tidal stream energy potential in the Shannon Estuary. *Renewable Energy*, *185*, 61-74. 10.1016/j.renene.2021.12.055
(Impact factor, IF = 8.700; First quartile, Q1, position 26/119 of *Energy & Fuels*; 2022).

Fouz, D. M., Carballo, R., López, I., & Iglesias, G. (2022). A holistic methodology for hydrokinetic energy site selection. *Applied Energy*, *317*, 119155. 10.1016/j.apenergy.2022.119155
(Impact factor, IF = 11.200; First quartile, Q1, position 15/119 of *Energy & Fuels*; 2022).

Fouz, D. M., Carballo, R., López, I., González, X. P., & Iglesias, G. (2023). A methodology for cost-effective analysis of hydrokinetic energy projects. *Energy*, *282*, 128373. 10.1016/j.energy.2023.128373
(Impact factor, IF = 9.000; First quartile, Q1, position 24/170 of *Energy & Fuels*; 2023).

# ABSTRACT

This thesis develops a comprehensive methodology for the exploitation of the hydrokinetic energy resource in coastal regions —a specific type of marine renewable energy (MRE)—, overcoming the limitations of the currently available procedures, and whose application to a coastal area of interest will provide the required information for an informed decision-making process. The methodology comprises three different procedures, each of them providing a specific index designed to analyse different stages of hydrokinetic energy farm planning, from initial designs to full scale MRE projects, increasing in complexity and accuracy as planning progresses: (i) Tidal Stream Exploitability index adapted to non-depth-limited areas, $TSE_{ndl}$ index, for projects at preliminary stages; (ii) Integrated Hydrokinetic Energy index, IHE index, for projects at early stages; and (iii) Cost-Effective Analysis (CEA) in terms of Levelized Costs of Energy based on the IHE index, $LCOE_{IHE}$, for projects at final stages. These procedures resort to high-resolution hydrodynamic numerical modelling and advanced geospatial analysis techniques and algorithms, being illustrated through their application to a case study in the Shannon Estuary (W Ireland), a non-depth-limited macrotidal estuary subject to significant fluvial discharges and renowned for its potential for hydrokinetic energy exploitation.

Keywords: marine renewable energy; hydrokinetic energy; resource characterisation; integrated coastal zone management; cost-effective analysis.

# RESUMO

Esta tese desenvolve unha metodoloxía integral para a explotación do recurso enerxético hidrocinético en rexións costeiras —un tipo específico de enerxía renovable mariña (ERM)—, superando as limitacións dos procedementos actualmente dispoñibles, e cuxa aplicación a unha zona costeira de interese proporcionará a información necesaria para un proceso de toma de decisións informado. A metodoloxía comprende tres procedementos diferentes, cada un dos cales proporciona un índice específico deseñado para analizar diferentes etapas da planificación de parques de enerxía hidrocinética, desde deseños iniciais ata proxectos de ERM a escala real, aumentando en complexidade e precisión a medida que avanza a planificación: (i) *Tidal Stream Exploitability index adapted to non-depth-limited areas*, índice $TSE_{ndl}$, para proxectos en fases preliminares; (ii) *Integrated Hydrokinetic Energy index*, índice IHE, para proxectos en fases iniciais; e (iii) *Cost-Effective Analysis* (CEA) *in terms of Levelized Costs of Energy based on the* IHE *index*, $LCOE_{IHE}$, para proxectos en fases finais. Estes procedementos recorren á modelaxe numérica hidrodinámica de alta resolución e a técnicas e algoritmos avanzados de análise xeoespacial, sendo ilustrados mediante a súa aplicación a un caso de estudo no estuario do Shannon (Oeste de Irlanda), un estuario macromareal non limitado pola profundidade sometido a importantes descargas fluviais e coñecido polo seu potencial para a explotación da enerxía hidrocinética.

Palabras chave: enerxías renovables mariñas; enerxía hidrocinética; caracterización de recurso; xestión integrada da zona costeira; análise custo-beneficio.

# RESUMEN

Esta tesis desarrolla una metodología integral para la explotación del recurso energético hidrocinético en regiones costeras —un tipo específico de energía renovable marina (ERM)—, superando las limitaciones de los procedimientos actualmente disponibles, y cuya aplicación a una zona costera de interés proporcionará la información necesaria para un proceso de toma de decisiones informado. La metodología comprende tres procedimientos diferentes, cada uno de los cuales proporciona un índice específico diseñado para analizar diferentes etapas de la planificación de parques de energía hidrocinética, desde diseños iniciales hasta proyectos de ERM a escala real, aumentando en complejidad y precisión a medida que avanza la planificación: (i) *Tidal Stream Exploitability index adapted to non-depth-limited areas*, índice $TSE_{ndl}$, para proyectos en fases preliminares; (ii) *Integrated Hydrokinetic Energy index*, índice IHE, para proyectos en fases iniciales; y (iii) *Cost-Effective Analysis* (CEA) *in terms of Levelized Costs of Energy based on the* IHE *index*, $LCOE_{IHE}$, para proyectos en fases finales. Estos procedimientos recurren a la modelización numérica hidrodinámica de alta resolución y a técnicas y algoritmos avanzados de análisis geoespacial, siendo ilustrados mediante su aplicación a un caso de estudio en el estuario del Shannon (Oeste de Irlanda), un estuario macromareal no limitado por la profundidad sometido a importantes descargas fluviales y conocido por su potencial para la explotación de la energía hidrocinética.

Palabras clave: energías renovables marinas; energía hidrocinética; caracterización de recurso; gestión integrada de la zona costera; análisis coste-beneficio.

# CONTENTS

# 1 INTRODUCTION

## 1.1 MOTIVATION AND THEORETICAL FRAMEWORK OF THE THESIS

Climate change and global warming have focused the interest of 21st-century societies on two key environmental aspects: (i) greenhouse gas emissions and (ii) air pollution. These issues hold particular significance in coastal areas, characterized by an intense socioeconomic activity, and consequently by a high energy consumption (Bailey & Solomon, 2004; Lonati et al., 2010). Within this framework, the interest in carbon-free energy sources has experienced an exponential growth, with marine renewable energies (MREs) gaining recognition as a significant contributor to the green energy sector and holding the potential to significantly reduce greenhouse gas emissions and thereby mitigate climate change (Ramos et al., 2021).

Among MREs, hydrokinetic energy emerges as a significant option. It represents a specific type of hydropower, primarily resulting from the combined action of tidal currents and barotropic flows resulting from river discharges (Fouz et al., 2019), which highlights for its predictability (Carballo et al., 2009), high-quality electricity output (Lewis et al., 2019), and minimal environmental impact (Brooks, 2011). Estuaries, characterized by strong tidal currents and, in some cases, large fluvial discharges, represent promising locations for hydrokinetic energy exploitation (Fouz et al., 2019; Iglesias, I. et al., 2021). In recent years, significant efforts have been made for developing hydrokinetic energy converters (HECs), particularly hydrokinetic turbines (Kamal & Saini, 2022; Khan et al., 2009), and identifying optimal areas for their operation. Typically, site-selection procedures are conducted on the basis of the available energy resource (e.g., Carballo et al., 2009; Fouz et al., 2019; Mejía-Olivares et al., 2018; Ramos et al., 2014; Robins et al., 2015; Sánchez et al., 2014; Yang et al., 2021), with only a handful of studies incorporating geomorphological parameters such as water depth (e.g., Iglesias, G. et al., 2012). However, as projects develop, additional considerations such as socioeconomic and environmental factors become crucial. In this context, ensuring the coexistence of energy exploitation with other marine activities, along with considering site-specific installation and operational costs (Castro-Santos et al., 2018), are of a paramount importance, particularly in estuarine areas where several locations may have potential for the deployment of hydrokinetic farms (Vázquez & Iglesias, 2016a). Given these complexities, more comprehensive studies are required for an informed decision-making. Thus, reliable metrics must be developed to support this process, ensuring both technical and economic viability, even at early project stages, allowing investors to reduce the uncertainties inherent to hydrokinetic energy projects and farm planning.

The development of accurate metrics is not straightforward and requires a comprehensive description of all the relevant aspects associated with the installation and operation of a hydrokinetic farm in a specific coastal area. This description must encompass not only techno-economic considerations (e.g., technical requirements and constraints, cost structure, reliability, maintenance, etc.) but also hydrodynamic factors. A detailed characterisation of coastal hydrodynamics is particularly crucial, especially in estuaries subject to significant fluvial discharges, where their influence on the variability of the available energy resource (e.g., intra-annual variability or seasonality) and their interaction with tidal flows have not been adequately investigated.

Extensive research has tried to address the challenge of tidal stream farm siting in tidally driven coastal areas, where the hydrodynamics are primarily dominated by the action of the tide and the variability of the energy resource is virtually negligible. Although fluvial discharges are usually present in these coastal areas, they generally play a secondary role, resulting from their reduced importance in comparison to the tidal prism; however, they may have significant importance in specific sites, which needs to be addressed. Moreover, these studies typically focus on depth-limited areas (e.g., inner and middle parts of shallow estuaries) where the geomorphology and coastal configuration, and especially the water depth, are crucial aspects in defining the best locations for hydrokinetic energy exploitation. Nevertheless, in the case of deep estuaries, water depth does not play the same role, and its influence on site selection procedures has not been thoroughly analysed, usually resulting in the overestimation of energy availability.

**This thesis presents a methodology whose application to a coastal area will lead to an informed decision-making process for the exploitation of hydrokinetic energy resource, overcoming the aforementioned limitations of the currently available studies.** The methodology comprises three different procedures, each yielding a different metric or index designed to analyse specific stages of hydrokinetic energy farm planning, from initial designs to full-scale projects, increasing in complexity and accuracy as planning progresses. These procedures, based on high-resolution hydrodynamic numerical modelling and advanced geospatial analysis techniques and algorithms, are illustrated through their application to a case study in the Shannon Estuary (Western Ireland), a non-depth-limited water body subject to significant fluvial discharges and renowned for its potential for hydrokinetic energy exploitation.

The methodology and procedures herein presented summarises the results resulting from a series of research articles published in peer-reviewed journals, constituting the core of this thesis. Each article represents a fundamental step towards achieving the final goal of this work: to make available a feasible and reliable methodology that, when applied to a given coastal region, provides the required information for appropriate decision-making regarding hydrokinetic energy exploitation.

### 1.2 JUSTIFICATION OF THE UNITY AND COHERENCE OF THE THESIS

This thesis is structured in eight chapters as follows. First, the present Chapter 1 provides an overall perspective of this work. Then, in Chapter 2, the main hypothesis along with the final and intermediate objectives are briefly presented, the latter being defined according to the different tasks and coherent steps required so as to fulfil the proposed final objective. Next, in Chapter 3, the main methodological aspects of this thesis are briefly introduced in close connection with the intermediate objective and the research article in which they are developed and implemented. The three following chapters (Chapters 4 to 6) correspond to respective publications in peer-reviewed journals constituting the main body of this thesis. Each of them represents a piece of research whose integration represents a whole through which a methodology for the decision-making process of hydrokinetic energy projects is developed. For this purpose, each publication deals with one of the three intermediate objectives as stated in Chapter 2.

In **Chapter 4 – *Tidal stream energy potential in the Shannon Estuary***, a procedure is developed to characterise the available hydrokinetic energy resource in a coastal area of interest which, together with the analysis of geomorphological parameters, leads to the selection of large areas of interest for MRE projects at preliminary stages, suitable of requiring further analysis at subsequent project stages. To this end, the Tidal Stream Exploitability (TSE) index

is adapted to the analysis of estuaries with non-depth-limited areas ($TSE_{ndl}$), and then used to select the hotspots with potential for hydrokinetic energy farm sitting. For this purpose, a new depth penalty-limiting function is defined to avoid overestimating the available energy potential in areas with depths greater than those required for hydrokinetic energy converter operation. The implementation of this procedure is illustrated through a case study covering the whole Shannon Estuary (W Ireland). This chapter has been published in *Renewable Energy* in 2022, journal indexed in the Journal Citation Reports with an impact factor, IF, of 8.700, and belonging to the first quartile (Q1) of this category (*Energy & Fuels*) (2022).

In **Chapter 5 – *A holistic methodology for hydrokinetic energy site selection***, a comprehensive procedure is developed with the aim of selecting the optimum locations for hydrokinetic energy exploitation in a coastal area of interest, by considering all the relevant aspects which affect the decision-making process, with application to MRE projects at early stages, thereby reducing the uncertainties of these phases. This brand-new procedure is centred around a novel holistic index, the Integrated Hydrokinetic Energy (IHE) index, which considers: (i) the exploitable resource, (ii) the costs of installation, and (iii) the socioeconomic and environmental aspects. The approach is illustrated again through a case study in the Shannon Estuary, showing the capabilities of this procedure to facilitate the planning and reduce the uncertainties in the development of a hydrokinetic farm project. This chapter has been published in *Applied Energy* in 2022, journal indexed in the Journal Citation Reports with an IF of 11.200 and belonging to the first quartile (Q1) of this category (*Energy & Fuels*) (2022).

In **Chapter 6 – *A methodology for cost-effective analysis of hydrokinetic energy projects***, a novel approach is developed in order to select the most appropriate HEC-site combination within a coastal area of interest, leading to its detailed analysis in MRE projects at final stages, with the accurate computation of the cost-effective analysis parameters as the cornerstone for final decision-making. This approach, which is illustrated again through a case study in the Shannon Estuary, encompasses four models, namely: (i) HEC-site selection model, (ii) energy production model, (iii) CAPEX model, and (iv) OPEX model. By avoiding simplistic assumptions, the proposed approach improves on current procedures and enables developers to accurately compute any cost-effective parameter of interest. In particular, operation and maintenance costs are considered, along with economies of scale, which are typically disregarded in existing procedures. This chapter has been published in *Energy* in 2023, journal indexed in the Journal Citation Reports with an IF of 9.000 and belonging to the first quartile (Q1) of this category (*Energy & Fuels*) (2023).

All in all, the original research articles composing the main body of this thesis are profoundly connected, each of them constituting a coherent step towards the fulfilment of the intermediate objectives of this research —which in turn lead to the achievement of the final objective— and therefore providing coherence and unity to this thesis.

Then, in Chapter 7, an integrated analysis of the results obtained in the preceding chapters (Chapters 4 to 6) is conducted so as to properly describe their significance within the general context of this work, thereby ensuring the reader's understanding of the present research as a whole. Finally, in Chapter 8, the main contributions and findings are synthetically presented along with the planned future research, part of which is currently under development.

# 2 HYPOTHESIS AND OBJECTIVES

Hydrokinetic energy exploitation in coastal areas presents a wide range of complexities, especially when considering large fluvial discharges or non-depth-limited waterbodies, where the currently available procedures lead to several limitations, and their application could result in an inappropriate decision-making. On this basis, and considering the relevant background provided in Chapter 1, the following **starting hypothesis** (H1 to H3) are established:

H1. Site-selection procedures are usually based on resource assessments lacking accuracy, especially in the case of: (i) coastal areas where fluvial discharges are significant in comparison with the tidal prism, resulting in a marked intra-annual variability; (ii) non-depth-limited coastal areas; and (iii) complex bathymetric configurations.

H2. Socioeconomic and environmental aspects have shown to be of the uttermost importance for selecting the best sites for hydrokinetic energy exploitation, and they should be analysed through the implementation of geospatial approaches.

H3. Techno-economic aspects related to the installation and operation of hydrokinetic energy farms, which are closely connected with coastal hydrodynamics, should be accurately considered.

With this in view, the **final objective of thesis is to develop a comprehensive methodology that defines specific procedures for hydrokinetic energy exploitation within a coastal region of interest**. The application of these procedures is illustrated through their implementation to the Shannon Estuary, thereby providing the required information for proper site-selection and operation for hydrokinetic energy exploitation throughout this waterbody. The application of each procedure results in a corresponding index for hydrokinetic energy site-selection, increasing in complexity and accuracy as project planning progresses, from the preliminary definition of areas of interest for initial designs to the assessment of specific locations for full-scale project installations. To achieve this final objective, the following **intermediate objectives** (O1 to O3) are established, each corresponding to a publication in a peer-reviewed journal (i.e., Chapters 4, 5 and 6 attain O1, O2 and O3, respectively) constituting the main body of this work:

O1. To develop and apply to a coastal region of interest an index allowing the selection of large areas of interest for MRE projects at preliminary stages, including non-depth limited regions, based on: (i) the available energy resource and (ii) geomorphological features.

**Taks involved**: to develop a methodology whose application in a coastal area provides the definition of different areas suitable for hydrokinetic energy exploitation with various levels of interest, which are selected according to their available energy resource and geomorphology and then are fully characterised by means of high resolution spatiotemporal analysis; to apply Geographic Information System (GIS) techniques for easily managing the geospatial data generated (e.g., hydrodynamic numerical results and geomorphological data); to apply the procedure to the Shannon Estuary.

**Addressed in**: **Chapter 4 –** ***Tidal stream energy potential in the Shannon Estuary***.



O2. To define and apply a comprehensive methodology, leading to the identification of the most suitable area for hydrokinetic energy exploitation in a coastal region, designed for

its application to MRE projects at early stages, independently of the type of energy converter or farm layout, and therefore reducing their uncertainties, by considering: (i) the exploitable resource, (ii) the costs of installation, and (iii) socioeconomic and environmental aspects.

**Taks involved**: to conduct a thorough characterisation of the exploitable energy resource; to develop a geospatial penalty function leading to a penalisation of those areas where the costs of hydrokinetic energy exploitation are higher; to assess the suitability of the coexistence of the main socioeconomic and environmental water uses with hydrokinetic energy exploitation, leading to an additional geospatial penalty function; the integration of previous results in order to provide a reliable indicator showing the viability of hydrokinetic energy exploitation throughout a coastal region; to apply the procedure to the Shannon Estuary.

**Addressed in**: **Chapter 5 – *A holistic methodology for hydrokinetic energy site selection***.

O3. To define and apply a new approach to identify best HEC-site combination within a coastal area of interest, whose application leads to its detailed analysis in MRE projects at final stages based on accurately cost-effective analyses (CEA) (i.e., techno-economic assessment).

**Taks involved**: to develop an HEC-site selection model, which employs the methods and results made available in O2 along with spatial analysis algorithms to define different HEC-site combinations, allowing for economies of scale; to compute the energy production of the different HEC-site combinations previously defined; to define a Capital Expenditures (CAPEX) model; to develop an Operation Expenditures (OPEX) model, considering Operation and Maintenance (O&M) procedures; the integration of previous results to provide reliable CEA parameters for the different HEC-site combinations, leading to the selection of the best alternative; to apply the procedure to the Shannon Estuary.

**Addressed in**: **Chapter 6 – *A methodology for cost-effective analysis of hydrokinetic energy projects***.

# 3 METHODOLOGY: A GENERAL OVERVIEW

With the aim of achieving the general and intermediate objectives described in Chapter 2, a common methodological approach is defined by developing and applying the procedures previously introduced and described in Chapters 4, 5 and 6, each of them corresponding with a publication in a peer reviewed journal, and specifically designed to attain each intermediate objective (i.e., Chapters 4, 5 and 6 attain O1, O2 and O3, respectively). This section constitutes only a brief description of the main methodological approaches developed in this thesis. The reader is referred to Chapters 4, 5 and 6 for a detailed description of these procedures.

In **Chapter 4 – *Tidal stream energy potential in the Shannon Estuary***, the first procedure made available in this thesis is presented. It consists in developing and applying the $TSE_{ndl}$ index, a revised version of the Tidal Stream Exploitability (TSE) index (Iglesias, G. et al., 2012), adapted for its application to non-depth-limited coastal regions. Prior to the application of this procedure to a coastal region of interest, a detailed characterisation of its hydrodynamics is required, including: (i) a detailed characterisation of river discharges, considering the intra-annual variability of river-induced currents resulting from the seasonality of the hydrological regime of rivers (Álvarez et al., 2017; Fouz et al., 2019; Iglesias, G. & Carballo, 2009); (ii) the assessment of the hydrokinetic (i.e., tidal and river in-stream) energy potential through hydrodynamic numerical modelling, for which the case studies considered should capture the variability of not only tidal stream energy resource, but also the variability induced by river discharges. To this end, four seasonal scenarios are analysed by considering a baseline period covering a complete mean spring neap tidal cycle (i.e., ≈ 14.75 days) and seasonal riverine discharges. The resulting information allows the understanding of the general patterns of the magnitude and distribution of the hydrokinetic energy resource along with the influence of the river discharges on the total available resource. Furthermore, an annual scenario considering mean monthly river discharges is also analysed to accurately compute the total available resource along with other parameters of interest (Álvarez et al., 2020).

Once the numerical results are made available, the $TSE_{ndl}$ index is computed in a tidal cycle during spring tides and mean river discharges and thermohaline conditions, based on which large areas of interest for MRE projects at preliminary stages are selected by considering different thresholds according to their level of interest from an energy resource standpoint: (i) locations of interest, with $TSE_{ndl}$ over 1, and (ii) locations of high interest, with $TSE_{ndl}$ over 2. Then, the areas of interest are analysed in greater detail by means of high-resolution spatiotemporal numerical modelling by computing the time distribution of the available resource over a complete mean spring-neap tidal cycle under mean river discharges and thermohaline conditions. This preliminary site-selection is done by physical interpretation of the $TSE_{ndl}$ index thresholds as follows. A $TSE_{ndl} = 1$ can be interpreted as the average available tidal stream power at mid-ebb and mid-flood at a given location corresponding with a tidal current with characteristic velocity and water depth (e.g., 1.5 $ms^{-1}$ at 5 m, respectively). Although the resulting information provides a valuable information at initial stages, in the case of areas with interest for hydrokinetic energy exploitation, the final decision regarding the installation of a hydrokinetic energy farm should be conducted under an integrated approach, considering not only the resource, but also Marine Spatial Planning, and in particular the

environmental and socioeconomic factors (including the computation of hydrokinetic energy farm expenditures), which will be addressed Chapter 5.

Next, in **Chapter 5 – *A holistic methodology for hydrokinetic energy site selection***, the second procedure made available in this thesis is presented. It consists in developing and applying an integrated site-selection process, which is conducted by means of the definition and application of the novel Integrated Hydrokinetic Energy (IHE) index. Based on a holistic approach, the IHE index integrates the three main aspects affecting the installation of hydrokinetic energy farms (Vázquez & Iglesias, 2016b): (i) the exploitable resource, i.e., the resource that can be effectively harnessed by HECs, which is computed on the basis of the high-resolution numerical results obtained from Chapter 4; (ii) the geomorphological configuration, for which the main Capital Expenditures (CAPEX) of a hydrokinetic farm are parameterised according to water depth and shoreline distance; and finally, (iii) the socioeconomic activities (aquaculture, shellfish, and shipping) and environmental uses (Special Areas of Conservation, SACs, Special Protection Areas, SPAs) which are considered by analysing and parameterising a large amount of geospatial data.

As a result, the physical interpretation of the IHE index is straightforward. The higher the IHE index, the better the site for hydrokinetic energy exploitation, with values above 1 indicating suitability for hydrokinetic energy exploitation, which would correspond with a site with IHE=1 (minimum value for suitability), and without any penalisation in terms of CAPEX and socioeconomic or environmental aspects. The results of implementing the IHE index will support the procedure for selecting the most appropriate locations for hydrokinetic energy conversion in a coastal region, reducing the uncertainties in the planning of commercial projects at their early stage. The final design of the farm configuration in subsequent stages would require a detailed cost-effective analysis of the selected HEC-site combinations, which is addressed in Chapter 6.

Finally, in **Chapter 6 – *A methodology for cost-effective analysis of hydrokinetic energy projects***, the last procedure made available in this thesis is presented. It consists in developing and applying a novel approach for accurately computing the CEA parameters of hydrokinetic energy projects, leading to the selection of the optimum HEC-site combination for installing a hydrokinetic farm in a coastal area (Bahaj et al., 2008; Si et al., 2022). In the present application, the CEA parameters are computed in terms of Levelized Costs of Energy (LCOE) based on the results of the IHE index, leading to the computation of the $LCOE_{IHE}$ index. This approach encompasses four aspects, namely: (i) the definition of feasible HEC-site combinations, which is based on the spatial analysis of the IHE index and the large areas of interest selected on its basis (Chapter 5); (ii) the assessment of the energy production of the different alternatives defined in (i), computed by means of high-resolution numerical results (Chapter 5), which are rearranged in order to appropriately consider the spatial variability of the energy resource and avoid inaccurate figures of energy yield; (iii) the detailed analysis of farm's CAPEX, including management-engineering, manufacturing and installation costs, along with the effects of economies of scale, which is conducted by combining a reliable breakdown of unitary costs, representative of generic designs of HECs and parametric analyses of proposed hydrokinetic farms, respectively; and finally, (iv) the computation of farm's OPEX, including insurances and fixed costs, scheduled or preventive maintenance and unscheduled or corrective maintenance, by considering reliability HEC data, the definition of weather windows based on high-resolution hydrodynamic numerical modelling (Chapter 5), and several O&M procedures depending on the configuration of the farm.

As a result, the interpretation of the $LCOE_{IHE}$ index is straightforward: the lower the value of the $LCOE_{IHE}$ index, the better the HEC-site combination for hydrokinetic energy

exploitation. In sum, the proposed approach addresses the major difficulties and uncertainties when computing the main aspects affecting the CEA of hydrokinetic energy farms, avoiding simplistic and unreliable assumptions which can result in a significant overestimation of OPEX, especially in the case of large farms, and overall improving on the current procedures.

# 4 TIDAL STREAM ENERGY POTENTIAL IN THE SHANNON ESTUARY

This chapter corresponds with the following research article:


- **Tittle:** Tidal stream energy potential in the Shannon Estuary
- **Journal:** Renewable Energy, Volume 185, February 2022, Pages 61-74
- **Editorial:** Elsevier
- **ISSN:** 1879-0682
- **DOI:** https://doi.org/10.1016/j.renene.2021.12.055


- **Authors:** D.M. Fouz[a], R. Carballo[a], I. López[a], G. Iglesias [b, c]
- **Institutions:**
  - [a]Departamento de Enxeñaría Agroforestal, Universidade de Santiago de Compostela, EPSE, Rúa Benigno Ledo s/n, 27002, Lugo, Spain
  - [b]School of Engineering and Architecture & MaREI, Environmental Research Institute, University College Cork, Ireland
  - [c]School of Engineering, Computing and Mathematics, University of Plymouth, UK

- **CRediT authorship contribution statement:**
  - **D.M. Fouz:** Conceptualization, Methodology, Investigation, Formal analysis, Visualization, Writing – original draft
  - **R. Carballo:** Conceptualization, Methodology, Writing – review & editing, Supervision, Project administration, Funding acquisition
  - **I. López:** Formal analysis, Visualization, Writing – review & editing, Supervision
  - **G. Iglesias:** Conceptualization, Methodology, Writing – review & editing, Supervision
- **Indicators (2022):** Impact factor, IF = 8.700; First quartile (Q1; 26/119) of this category (*Energy & Fuels*)
- **Authorization of the publisher**: This paper has been published as an open access article under a Creative Commons licence (CC BY 4.0) (https://creativecommons.org/licenses/by/4.0/), which permits its unrestricted use, distribution and reproduction in any medium or format, for any purpose, without the need for specific permission. Likewise, according to the copyright policies of Elsevier (https://www.elsevier.com/about/policies-and-standards/copyright), the publisher of the article, the authors have the right to use and share their works for scholarly purposes, including in a thesis or dissertation

Renewable Energy 185 (2022) 61–74

Contents lists available at ScienceDirect

Renewable Energy

journal homepage: www.elsevier.com/locate/renene

# Tidal stream energy potential in the Shannon Estuary

D.M. Fouz [a], R. Carballo [a, *], I. López [a], G. Iglesias [b, c]

[a] Departamento de Enxeñaría Agroforestal, Universidade de Santiago de Compostela, EPSE, Rúa Benigno Ledo s/n, 27002, Lugo, Spain
[b] School of Engineering and Architecture & MaREI, Environmental Research Institute, University College Cork, Ireland
[c] School of Engineering, Computing and Mathematics, University of Plymouth, UK

ARTICLE INFO

*Article history:*
Received 14 May 2021
Received in revised form
25 November 2021
Accepted 13 December 2021
Available online 15 December 2021

*Keywords:*
Tidal stream energy
River in-stream energy
Non-depth-limited areas
Numerical modelling
Resource assessment

ABSTRACT

The tidal and river in-stream energy resource in the Shannon Estuary (W Ireland) is investigated using of high-resolution numerical modelling and spatial analysis. Although freshwater discharges are large, their influence on the available resource is found to be all but negligible, the tide being the main driver of estuarine circulation. The Tidal Stream Exploitability (TSE) index is adapted to the analysis of estuaries with non-depth-limited areas ($TSE_{ndl}$), such as the Shannon Estuary, and then used to select the hotspots with potential for a tidal stream farm. For this purpose, a new depth penalty-limiting function is defined to avoid overestimating the available energy potential in areas with depths greater than those required for tidal energy converter operation. Seven hotspots are identified based on the revised index. The approach followed in this study illustrates the applicability of high-resolution numerical modelling and spatial analysis for identifying the most appropriate areas for tidal stream energy conversion. Finally, the potential of tidal stream energy to contribute to the much-needed decarbonisation of the energy mix in Ireland is emphasized.



## 1. Introduction

Climate change and global warming have drawn attention to two environmental priorities of 21st century societies – greenhouse gas emissions and air pollution [1–4]. These are paramount priorities in coastal areas, where socioeconomic activity is intense, resulting in high energy consumption [5–8]. This is the case of the Shannon Estuary, the largest estuary in Ireland (Fig. 1), which harbours six commercial maritime terminals managed by the Shannon Foynes Port Company (SFPC): (from East to West) Limerick Docks, Shannon Airport, Aughinish, Port of Foynes, Tarbert and Moneypoint.

The high energy consumption in coastal areas coexists with a vast Marine Renewable Energy (MRE) resource, which emerges as a promising alternative for diversifying and decarbonising the energy supply [9–15]. In particular, tidal stream energy is significant in certain estuarine areas, mainly because it is predictable and has a relatively low environmental impact [16–22]. Its large tidal range (up to 5.5 m in spring tides, i.e., macrotidal) makes the Shannon Estuary a potential source for hydrokinetic energy conversion. The tidal regime is semidiurnal, with a form factor $F = 0.082$ [23]. The estuary tapers gradually from widths of ~15 km (water depths of ~40 m) at its mouth to less than 100 m (and water depths less than 5 m) in the inner estuary, including large intertidal areas [24].

The River Shannon, the longest in Ireland, the River Feale, and others, flow into the estuary, which has a total catchment area of 16,865 $km^2$ (or one sixth of the area of Ireland). Of its total length of ~400 km, ~100 km correspond to its estuary. The large river discharges may have an effect on the available resource, and as a result, on hydrokinetic energy farm operation.

This study examines the hydrokinetic (tidal and river in-stream) energy resources in the Shannon Estuary, with a focus on supplying part of the electricity demand of several coastal facilities. The first step is to accurately characterize all the tidal and river flows in the estuary. A high-resolution shallow-water numerical model is implemented to simulate the hydrodynamics. Then, the distribution of the hydrokinetic energy resource is analysed by considering different case studies. An accurate river in-stream resource characterization for this requires an intra-annual analysis of river-induced currents, including the variability of the hydrological regime of the rivers discharging into it [17,25,26].

Thus, the present study is developed by analysing different cases capturing the variability of both the tidal and river in-stream energy resource. First, four characteristic seasonal

* Corresponding author.
*E-mail address:* rodrigo.carballo@usc.es (R. Carballo).

https://doi.org/10.1016/j.renene.2021.12.055

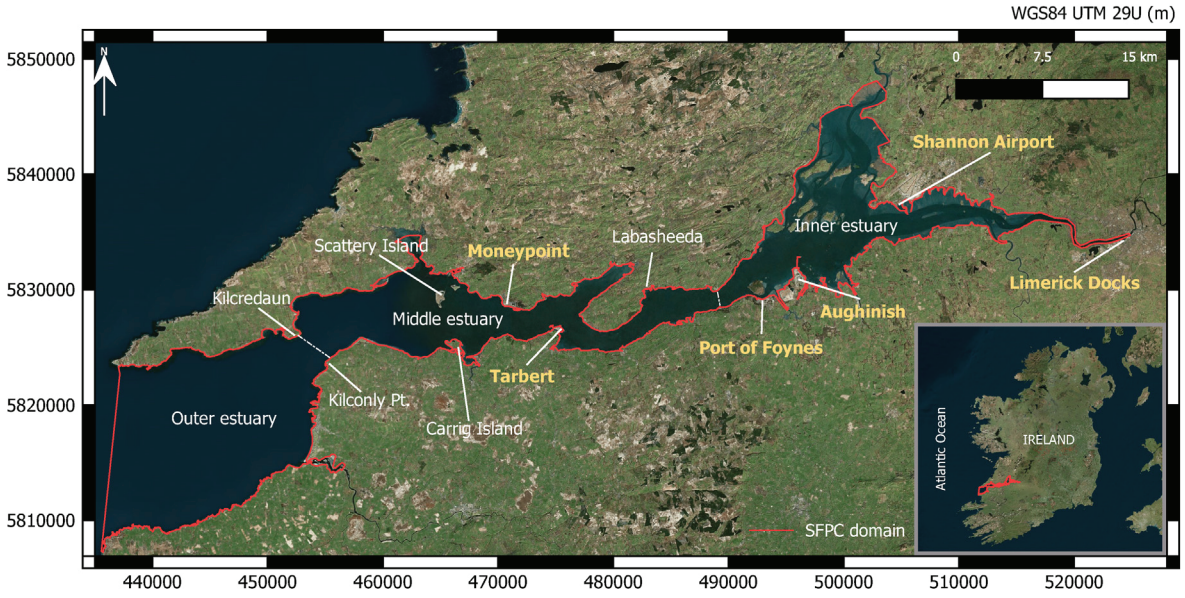


**Fig. 1.** Location of the Shannon Estuary, with the SFPC limits and port facilities.

scenarios are analysed for a baseline period covering a complete mean spring-neap tidal cycle and seasonal riverine discharges. The resulting dataset provides a general picture of the magnitude and distribution of the hydrokinetic energy resource, as well as the extent of riverine influx contributions to the resource. Then, a complete annual scenario is simulated for computation of the total available hydrokinetic resource. On this basis, a new ad hoc version of the Tidal Stream Exploitability (TSE) index [27] is defined for non-depth-limited estuaries ($TSE_{ndl}$), such as the Shannon Estuary. This new version of the index is used to select the areas of interest for hydrokinetic energy exploitation, which are then examined in greater detail. The results form the basis for a plan for hydrokinetic power supply for the Shannon Estuary facilities.

## 2. Materials and methods

### 2.1. Model implementation

A high-resolution hydrodynamic numerical model of the Shannon Estuary was implemented and validated with field data. The model, Delft3D-FLOW, is a finite-difference code that approximates the Navier-Stokes equations under the Shallow Water and Boussinesq assumptions, coupled with the transport equation, which enables the spatial distribution of the temperature, salinity, and thereby density, to be computed. Density may not be irrelevant in view of the large river inflows in this estuary. Delft3D-FLOW can be implemented either as a 3D model [28,29] or in its 2DH form (depth integrated). The 2DH form is used in this study based on previous hydrokinetic energy analyses [17,30–33]. Under these assumptions, the model equations can be expressed as [31,32,34]:

$$\frac{\partial \zeta}{\partial t}+\frac{\partial[(d+\zeta)U]}{\partial x}+\frac{\partial[(d+\zeta)V]}{\partial y}=S, \tag{1}$$

$$\left.\begin{aligned}\frac{\partial U}{\partial t}+U\frac{\partial U}{\partial x}+V\frac{\partial U}{\partial y}-fV&=-g\frac{\partial \zeta}{\partial x}-\frac{g}{\rho_0}\int_{-d}^{\zeta}\frac{\partial \rho'}{\partial x}dz+\frac{\tau_{sx}-\tau_{bx}}{\rho_0(d+\varsigma)}+\upsilon_h\nabla^2 U\\ \frac{\partial U}{\partial t}+U\frac{\partial V}{\partial x}+V\frac{\partial V}{\partial y}+fU&=-g\frac{\partial \zeta}{\partial y}-\frac{g}{\rho_0}\int_{-d}^{\zeta}\frac{\partial \rho'}{\partial y}dz+\frac{\tau_{sy}-\tau_{by}}{\rho_0(d+\varsigma)}+\upsilon_h\nabla^2 V\end{aligned}\right\}, \tag{2}$$

$$\frac{\partial(\zeta+d)c}{\partial t}+\frac{\partial[(\zeta+d)Uc]}{\partial x}+\frac{\partial[(\zeta+d)Vc]}{\partial y}=D_h\nabla^2 c-\lambda_d(d+\zeta)c+C, \tag{3}$$

where the conservation of mass and momentum in the $x$- and $y$-directions correspond to equations (1) and (2), respectively, and the spatial distribution of salinity and temperature (and as a result density) is computed by equation (3). In these expressions, $d$ and $\zeta$ represent the water depth and water level, respectively; $U$ and $V$ are the depth-integrated velocity components in $x$ and $y$ directions, respectively; $\rho'$ and $\rho_0$ represent the sea water anomaly and reference density, respectively; $f$ is the Coriolis parameter; $S$ is the source of mass; $\upsilon_h$ expresses the horizontal eddy viscosity; $\tau_{bx}$ and $\tau_{by}$ are the shear stress at the bottom in $x$ and $y$ directions; $\tau_{sx}$ and $\tau_{sy}$ represent the wind stress acting on the sea surface in $x$ and $y$ directions, respectively; $c$ is any constituent (here, both salinity and temperature); $D_h$ stands for the horizontal eddy diffusivity; $C$ is the source term of each constituent; and finally, $\lambda_d$ is first order decay.

The model grid in this application not only covers the whole Shannon Estuary but also extends to the 100 m isobath, roughly 30 km offshore, to prevent spurious numerical disturbances from affecting the area of interest. The resulting grid is composed of 69,649 cells of varying-size resolution: 100 m × 100 m resolution within the estuary, gradually increasing up to 100 × 300 m from the mouth of the estuary to the ocean boundary. Bathymetry data was obtained from the INFOMAR programme (Integrated Mapping For the Sustainable Development of Ireland's Marine Resource) [35], and supplemented with topographic data to fully describe this

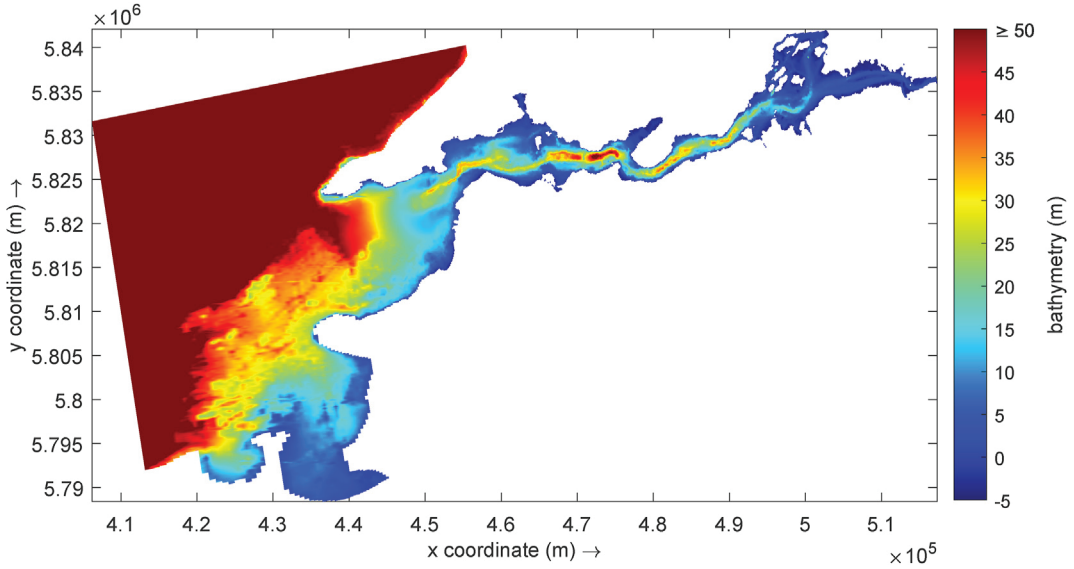


**Fig. 2.** Bathymetric and topographic configuration of the Shannon Estuary and its surroundings.

estuary's extensive shallows (Fig. 2).

The initial model conditions are zero free surface elevation and water velocity throughout the computational domain (*cold start*). In addition, a one-month spin-up period [36,37] is considered to ensure that the initial conditions do not affect the numerical results [26]. A Dirichlet boundary condition is applied to the open boundaries by imposing the main astronomical tidal constituents and the thermohaline conditions based on field measurements. Finally, null flow and free slip conditions (i.e., zero shear stress) are imposed on closed boundaries.

### 2.2. Field data and model validation

The model is forced and validated with a large set of field data. At the open boundaries the model is forced by the tide through its major harmonics, obtained from the TOPEX/Poseidon database [38,39], and by the thermohaline conditions of the oceanic water mass, using wave buoy data provided by the Irish Marine Institute (MI). As the Shannon Estuary receives large freshwater inflows, baroclinic and barotropic forcing may be significant [40]. An accurate characterization of the hydrological regime of freshwater inputs is therefore required. Freshwater inputs are obtained from gauging stations operated by the Irish Office of Public Works (OPW) which enables to include the intra-annual variability in the discharge of the most important rivers flowing into the estuary: Shannon, Fergus, Feale, Mulkear, Killimor, Deel, Maigue, Ollatrim and Killimor. The average monthly discharges of these freshwater inputs are shown in Fig. 3. Their variability can be characterized seasonally, with a rather constant contribution of the River Shannon to the total discharge (Table 1).

A second dataset for model validation consists of flow velocity field measurements as recorded by Acoustic Doppler Current Profilers (ADCP) deployed at two sites (Table 2) in the inner and middle estuary over different time periods.

ADCP measurements were taken at a sampling frequency of 30 min and 10 min at stations S1 and S2, respectively, during about one month at S1 and four days at S2. These measurements were denoised by a low-pass filter designed ad hoc [41] and vertically averaged for comparison with model results.

Fig. 4 shows a comparison of the magnitude of flow velocity computed by the model to measured data from S1 and S2. Overall, the agreement is excellent, with coefficients of determination, $R^2$, of 0.81 and 0.92, and root mean square errors, RMSE, of 0.211 and

**Table 1**
Seasonal variability of freshwater inputs to the Shannon Estuary.

| Season | Total river discharge ($m^3s^{-1}$) | Contribution of River Shannon (%) |
|---|---|---|
| **Winter** | 668.14 | 75 |
| **Spring** | 501.24 | 86 |
| **Summer** | 334.16 | 79 |
| **Autumn** | 390.70 | 68 |

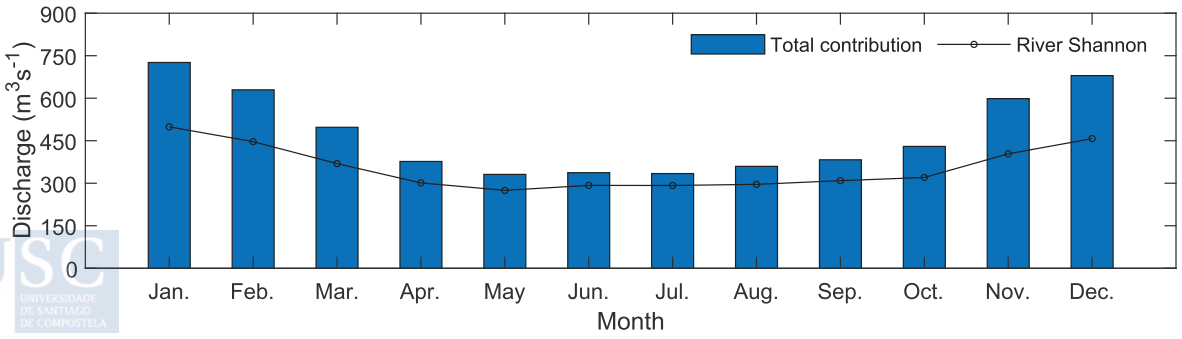


**Fig. 3.** Total monthly freshwater inputs in the Shannon estuary (blue bars) and contribution of the River Shannon (black line).

**Table 2**
Location of deployment points for ADCP.

| Location | ID | X-Coordinate (m) WGS84 UTM 29U | Y-Coordinate (m) WGS84 UTM 29U | Water depth (m) low tide |
|---|---|---|---|---|
| **Scattery Island** | S1 | 464655 | 5827265 | 14.0 |
| **River Fergus** | S2 | 500607 | 5836220 | 10.0 |

0.079 $ms^{-1}$, for S1 and S2, respectively, showing that the model can accurately predict the hydrodynamics of this estuary.

### 2.3. Spatial analysis of the $TSE_{ndl}$ index

The Tidal Stream Exploitability (TSE) index was designed for tidal stream energy conversion site selection in areas with limited water depth [27]. It may be expressed as:

$$TSE = \frac{\xi}{2V_0^3 h_0}\left(V_f^3 + V_e^3\right)h, \tag{4}$$

where $V_0$ and $h_0$ represent the characteristic velocity and characteristic water depth, respectively, which are usually set as 1.5 $ms^{-1}$ ($V_0$) and 5 m ($h_0$); $V_f$ and $V_e$ are the average velocities at mid-flood and mid-ebb, respectively; $h$ is the water depth at mid-tide; finally, $\xi$ is a penalty function which depends on the water depth and computed as:

$$\xi = \begin{cases} 0, \; h - \dfrac{\Delta h}{2} \le h_1 \\ \dfrac{1}{h_2 - h_1}\left(h - \dfrac{\Delta h}{2} - h_1\right), \; h_1 < h - \dfrac{\Delta h}{2} < h_2 \\ 1, \; h - \dfrac{\Delta h}{2} \ge h_2 \end{cases}, \tag{5}$$

where $\Delta h$ is the maximum tidal range in the study area; $h_1$ and $h_2$ represent the lower and upper limits of the depth penalty range, usually set as 2 m ($h_1$) and 5 m ($h_2$), respectively. For further information on the TSE index, see Ref. [27].

As the TSE index was designed for shallow and intermediate water depths, where the depth is a major constraint for the selection of potential tidal stream energy conversion sites [27,32,42,43], it should be modified for its application to deep estuaries, such as the Shannon Estuary, where depth does not have the same role. In this work, a new version of this index adapted to non-depth-limited estuaries, $TSE_{ndl}$, is proposed (Eq. (6)). To this end, the analysis of the areas with water depths over a given threshold depth is analysed by considering an additional resource-limiting expression in the above penalty function, leading to the new penalty-limiting function, $\xi_{ndl}$ (Eq. (7)). The objective of this new function is not to overestimate the energy potential of areas with large water depths and, more specifically, areas with depths in excess than those required for the operation of the majority of Tidal Energy Converters (TECs). This is done by considering a new range in the function, given by the threshold $h_3$, above which $TSE_{ndl}$ values are limited to those corresponding to water depths of $h_3$.

$$TSE_{ndl} = \frac{\xi_{ndl}}{2V_0^3 h_0}\left(V_f^3 + V_e^3\right)h\,, \tag{6}$$

$$\xi_{ndl} = \begin{cases} 0, \; h - \dfrac{\Delta h}{2} \le h_1 \\ \dfrac{1}{h_2 - h_1}\left(h - \dfrac{\Delta h}{2} - h_1\right), \; h_1 < h - \dfrac{\Delta h}{2} < h_2 \\ 1, \; h_2 \le h - \dfrac{\Delta h}{2} < h_3 \\ \dfrac{1}{h}\left(h_3 + \dfrac{\Delta h}{2}\right), \; h - \dfrac{\Delta h}{2} \ge h_3 \end{cases}. \tag{7}$$

Based on the characteristics of current available commercial technologies, $h_3 = 16$ m [44–46]. It is worth of mentioning that the bounds $h_1$, $h_2$ and $h_3$ are strongly dependent on the maturity of energy conversion systems and could therefore be adapted to future developments.

The $TSE_{ndl}$ index is computed based on the information from the numerical model and analysed through spatial analysis [47,48], leading to the delimitation of the most suitable areas for hydrokinetic energy exploitation. This is done by physical interpretation of the $TSE_{ndl}$ index thresholds as follows. A $TSE_{ndl} = 1$ means that the average available tidal stream power at mid-ebb and mid-flood at a given location corresponds to a tidal current with characteristic velocity ($V_0 = 1.5$ $ms^{-1}$) in a characteristic water depth ($h_0 = 5$ m). Thus, and based on [49,50], it can be established that $TSE_{ndl}$ over 1 indicates locations of interest for tidal stream energy conversion, and over 2 are of high interest. These thresholds are retained for analysis in Section 4.

### 2.4. Case studies

The hydrokinetic energy potential of the Shannon Estuary is assessed, and thereby identified the best areas for its conversion, by analysing a number of case studies. First, a preliminary analysis is made of the distribution of the available resource considering both tide and river discharges (in addition to the thermohaline conditions at the open boundaries and resulting baroclinic flows) for a complete mean spring-neap tidal cycle (≈14.75 days). Seasonal river discharges (Fig. 3) during this period are used to define four case studies: winter (CS1), spring (CS2), summer (CS3), autumn (CS4). Once the general resource distribution has been analysed, the combined effects of the interaction of both energy resources are assessed over a long period (a complete year) (CS5) to accurately determine the total available energy. Average monthly river discharges (Fig. 3) are input to the model to this end. Even though the above information would have been sufficient to identify the areas with the largest energy resource, the most suitable areas for its conversion also depend on other variables, such as the magnitude of peak velocities or water depth. Thus, the $TSE_{ndl}$ index is computed for a tidal cycle during spring tides and mean river discharges and thermohaline conditions (CS6). Several large areas of interest (hotspots) are delimited based on the results. This delimitation is defined by establishing the $TSE_{ndl}$ thresholds defined in Section 2.3. Within each of these large areas, two locations are

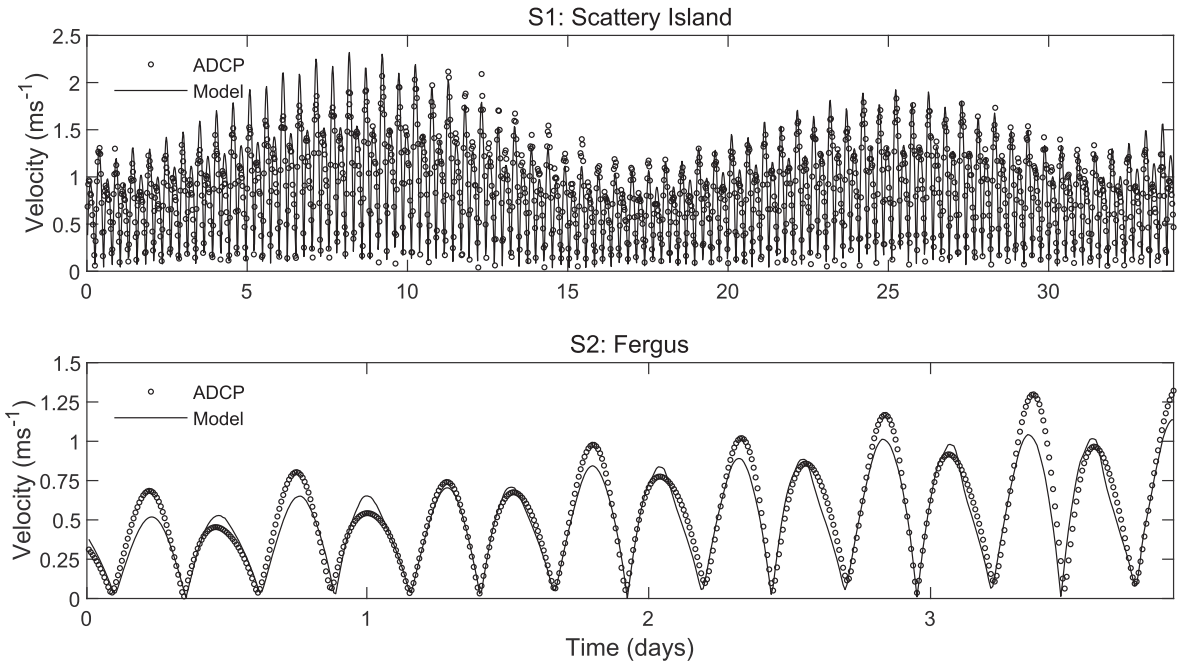


**Fig. 4.** Comparison of the flow velocity from numerical modelling and ADCP measurements at S1 and S2.

selected for high-resolution analysis, one with the highest $TSE_{ndl}$, and a representative location with the mean $TSE_{ndl}$ for the area.

Finally, the time distribution of the available resource is analysed at the selected locations for a complete mean spring-neap tidal cycle under mean river discharges and thermohaline conditions (CS7).

## 3. General resource distribution

Following the procedure described in Section 2, the results of the general spatial distribution of the available resource obtained from the simulations corresponding to case studies CS1-CS4 are analysed. A preliminary key point is to investigate for the first time the influence of the freshwater inputs on the total available resource. Having analysed the large amount of information obtained, the spatial distribution of the flow field is presented at mid-ebb and mid-flood of a mean spring tide only for CS1 (winter) and CS3 (summer) for the sake of clarity (Fig. 5 and Fig. 6). These are the case studies corresponding to the seasons with the largest and least freshwater inputs.

The maximum current speeds occur in the surroundings of Tarbert, with values of up to 2.30 ms$^{-1}$ and 1.96 ms$^{-1}$ at mid-ebb and mid-flood, respectively, during the winter season (Fig. 5). Nevertheless, the greater fluvial discharges in winter are not capable of significantly modifying the general resource distribution, as it is apparent from the comparison between Fig. 5 (winter or CS1) and Fig. 6 (summer or CS3). The results for autumn and spring present virtually identical flow patterns and, therefore, are omitted.

In addition to the surroundings of Tarbert, there exist other areas with high current velocities that could be of interest for distributed energy generation across the estuary: the surroundings of Kilcredaun, close to the mouth, with velocities of 1.88 ms$^{-1}$ and 1.45 ms$^{-1}$ at mid-ebb and mid-flood, respectively; the constriction between Scattery Island and Carrig Island, in the middle estuary, with similar figures (2.08 ms$^{-1}$ and 1.45 ms$^{-1}$ at mid-ebb and mid-flood, respectively). Other areas of interest, with somewhat lower velocities, are the surroundings of Moneypoint (with velocities of 1.36 ms$^{-1}$ and 1.21 ms$^{-1}$ at mid-ebb and mid-flood, respectively) and the area close to the Port of Foynes and Aughinish (1.41 ms$^{-1}$ and 1.11 ms$^{-1}$ at mid-ebb and mid-flood, respectively). These areas might be of interest with a view to the energetic supply of the nearby SFPC facilities.

Based on the previous results, a clear ebb dominance [51] is apparent, probably as a result of the complex interaction of the tide with the bottom contours. This effect is complemented by the river discharges in specific areas of the inner estuary – even though their influence on the general circulation patterns is more limited than might have been expected a priori.

In order to have a more detailed knowledge of the distribution of the available resource, the results of CS5, a numerical simulation of a complete year considering the intra-annual variability of the river inputs in terms of monthly discharges, are used to accurately compute the spatial distribution of the mean power density (Fig. 7).

The areas with the greatest values of mean power density correspond to those with maximum velocities – the Tarbert area, with approx. 1.84 kWm$^{-2}$, followed by the channel between Scattery Island and Carrig Island, and Kilcredaun area, with 1.23 and 1.05 kWm$^{-2}$, respectively; and finally, the surroundings of Port of Foynes and Aughinish, and Moneypoint with 0.46 and 0.44 kWm$^{-2}$, respectively.

## 4. Selection of areas based on $TSE_{ndl}$ index

The available energy resource in terms of power density provides valuable information for pinpointing the areas of interest for hydrokinetic energy exploitation. Nevertheless, there exist other factors which affect the operation of a hydrokinetic farm, such as the available water depth. With this in view, in order to have a clearer understanding of the exploitable resource, the spatial distribution of the $TSE_{ndl}$ index is computed as defined in Section 2 (CS6) (Fig. 8 and Fig. 9).

The results of the $TSE_{ndl}$ index follow a rather similar spatial distribution pattern to that provided by the power density

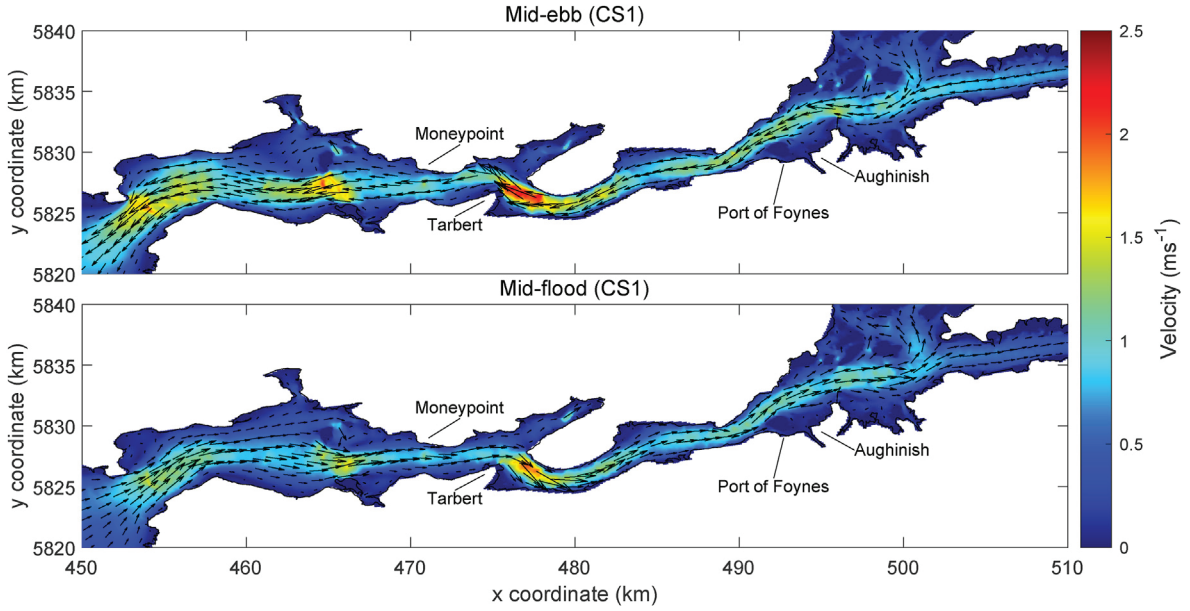


**Fig. 5.** Flow pattern at mid-ebb (top) and mid-flood (bottom) in CS1 (winter).

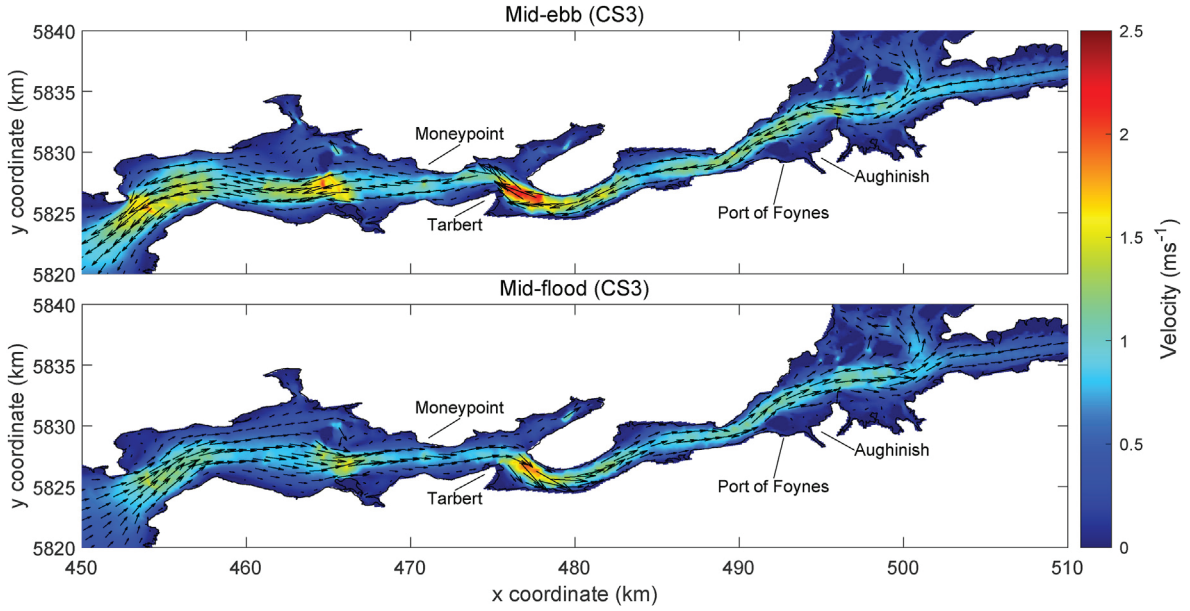


**Fig. 6.** Flow pattern at mid-ebb (top) and mid-flood (bottom) in CS3 (summer).

distribution. The greatest figures occur close to Tarbert, 9.36, followed, in the middle and outer estuary, by the surroundings of Kilcredaun, with 5.70, the channel between Scattery Island and Carrig Island with 5.50, and the surroundings of Moneypoint with 2.50. In the case of the inner part of the estuary, the $TSE_{ndl}$ values range between minimums of 1.10 and maximums of 2.80 (in some specific zones) over a large area, which roughly corresponds to the central channel, attaining 2.1 close to the Port of Foynes and Aughinish.

Having analysed the spatial distribution of the $TSE_{ndl}$ index, it emerges that extensive areas may be suitable for hydrokinetic energy exploitation. However, the installation of a hydrokinetic farm requires the accurate delimitation of the areas suited for its operation. To this end, following the approach described in Section 2, the values of the $TSE_{ndl}$ index are analysed by applying spatial analysis techniques. More specifically, the areas above two thresholds of $TSE_{ndl}$ ($TSE_{ndl} = 1$ and $TSE_{ndl} = 2$) are delimited (Figs. 9 and 10).

The resulting areas are plotted in Fig. 9. A total of seven areas (Area I to VII) are identified in the Shannon Estuary, whose main characteristics are provided in Table 3.

The results show that all the identified areas are of interest for hydrokinetic energy exploitation, in particular areas I, II and IV. However, areas I and II are far away from SFPC facilities. Nearer to SFPC facilities, but with a somewhat lower resource, are: Area III (close to Moneypoint), Area VI (close to the Port of Foynes) and Area VII (near Aughinish). On this basis, Areas III, IV, VI and VII are retained for further analysis in the following section.

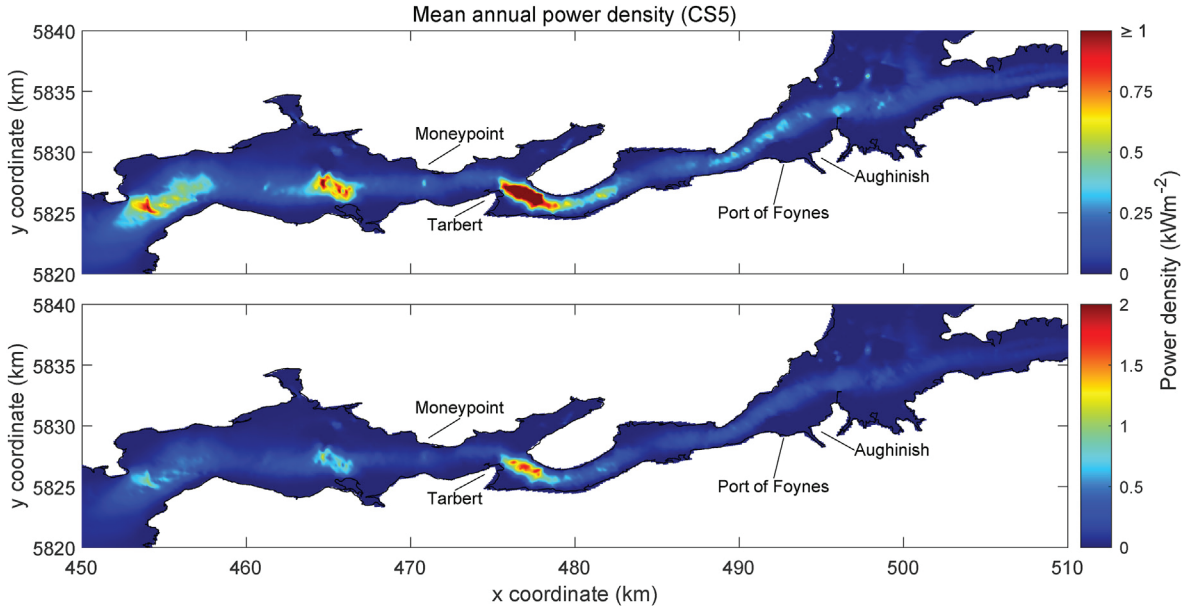


**Fig. 7.** Spatial distribution of the mean annual power density as obtained from CS5. The colour scale is adapted to appropriately describe the power density distribution throughout the estuary (top) and the maximum values attained (bottom).

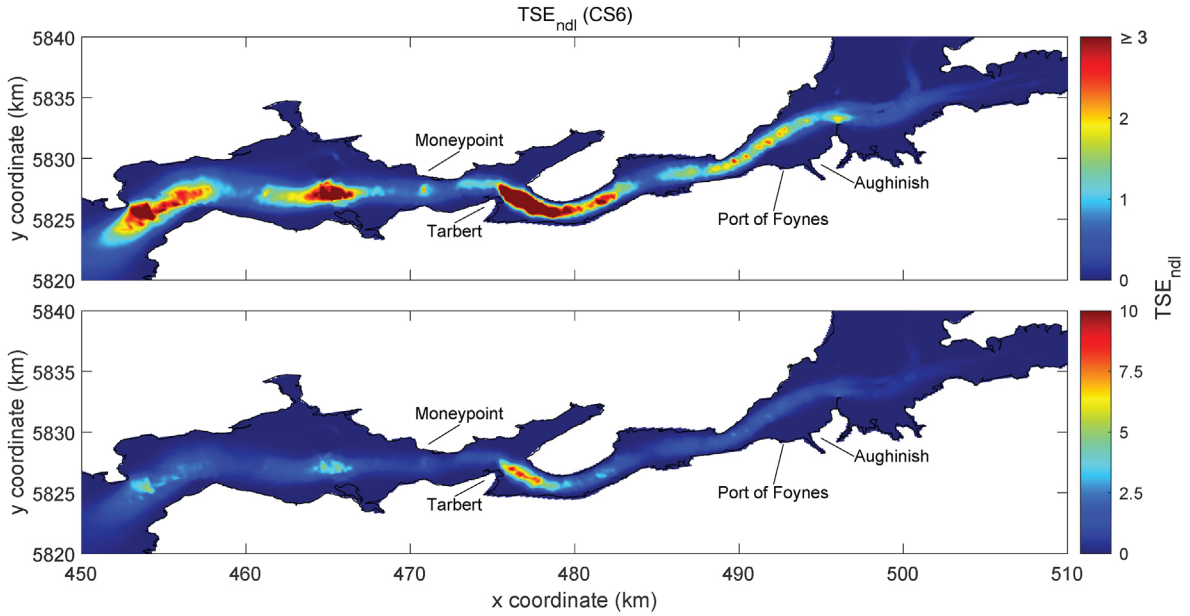


**Fig. 8.** Spatial distribution of the $TSE_{ndl}$ as obtained from CS6. The colour scale is adapted to appropriately describe the $TSE_{ndl}$ distribution throughout the estuary (top) and the maximum values attained (bottom).

## 5. High-resolution spatiotemporal analysis of the selected areas

In this section, in order to provide further information of interest for the operation of a tidal energy farm within the previously selected areas (III, IV, VI and VII), their analysis is conducted by focusing on two representative locations which correspond to: (i) the mean value of the $TSE_{ndl}$ within the delimited areas, or $L_{mean,i}$, and (ii) the maximum value of the $TSE_{ndl}$ within the delimited areas, or $L_{max,i}$, with the index *i* denoting the Area (III, IV, VI or VII).The selected locations are pinpointed in Fig. 10.

At the selected points, the time distribution of the current velocity and power density are analysed throughout a 14.75-day mean spring-neap tidal cycle under mean river discharge (CS7) (Fig. 11–14).

In Area III, mean and peak values of the current velocity of

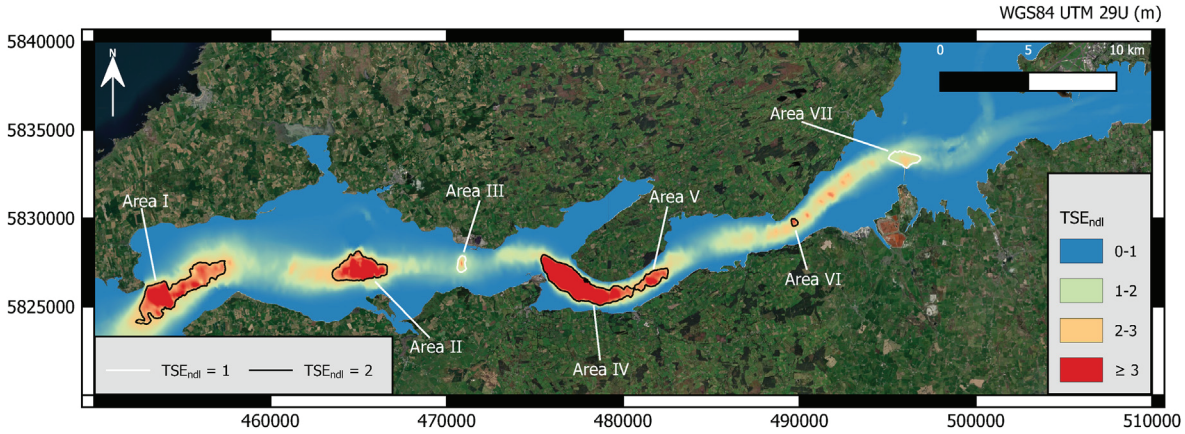


**Fig. 9.** Delimitation of the areas of interest for hydrokinetic energy exploitation based on the $TSE_{ndl}$. The lines corresponding to $TSE_{ndl}$ values of 2 and 1 delimit the areas exceeding these thresholds.

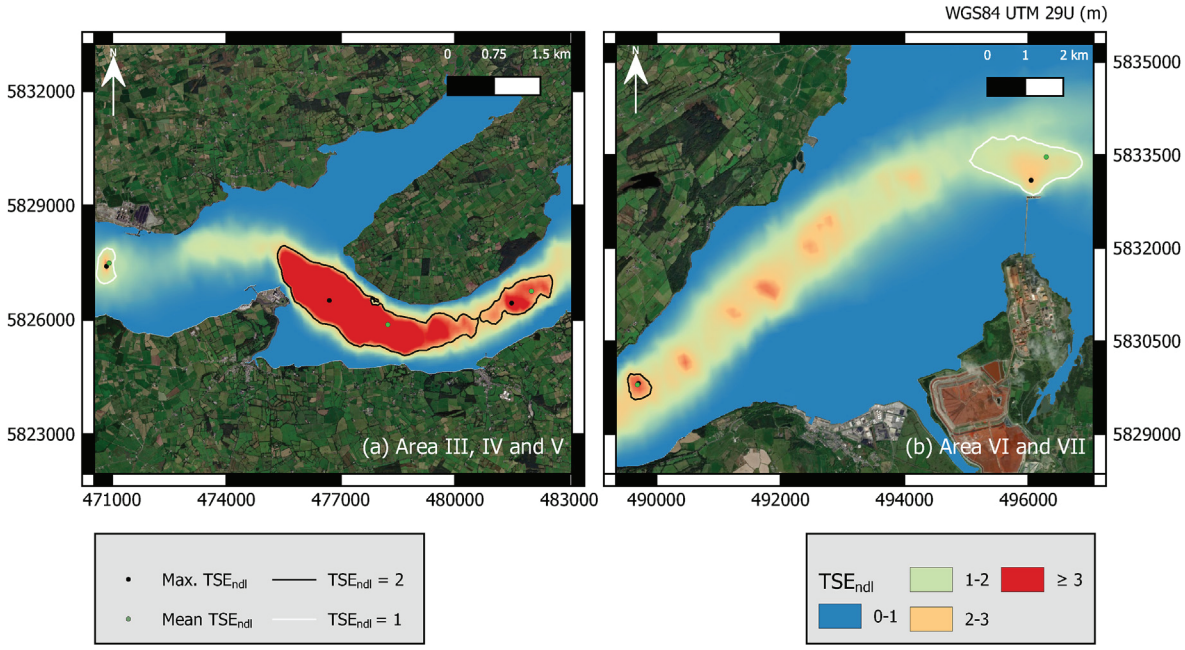


**Fig. 10.** Detailed view of the selected areas, identifying the representative points (maximum $TSE_{ndl}$ and mean $TSE_{ndl}$) selected for high-resolution analysis.

**Table 3**
Main characteristics of hydrokinetic selected sites.

| Area | Surface ($km^2$) | Mean water depth (m) | Mean $TSE_{ndl}$ | Maximum $TSE_{ndl}$ |
|---|---|---|---|---|
| **I** | 6.1 | 23.0 | 2.7 | 5.7 |
| **II** | 3.3 | 17.4 | 3.0 | 5.5 |
| **III** | 0.4 | 26.4 | 1.4 | 2.5 |
| **IV** | 5.7 | 18.7 | 4.4 | 9.4 |
| **V** | 1.1 | 30.0 | 2.5 | 3.7 |
| **VI** | 0.1 | 23.2 | 2.3 | 2.8 |
| **VII** | 1.0 | 12.6 | 1.4 | 2.1 |

0.61 $ms^{-1}$ and 1.17 $ms^{-1}$, respectively, are attained at $L_{mean,III}$, with somewhat larger figures at $L_{max,III}$, 0.71 $ms^{-1}$ and 1.37 $ms^{-1}$, respectively. There exist significant differences between the *x*- and *y*-direction velocities, with the latter presenting much weaker values, which shows how the geographical configuration of the middle estuary influences its hydrodynamics, and therefore the most likely configuration of a hydrokinetic energy farm in this area. With respect to the power density, as expected, the differences between locations are more apparent than in the case of the velocity magnitude, with average and peak values of 0.20 $kWm^{-2}$ and 0.82 $kWm^{-2}$, respectively at $L_{mean,III,}$ and 0.31 $kWm^{-2}$ and 1.30 $kWm^{-2}$ at $L_{max,III}$.

As for Area IV, mean and maximum values of flow magnitude of 1.06 $ms^{-1}$ and 2.04 $ms^{-1}$, respectively, are present at $L_{mean,IV}$, which are again similar to those at $L_{max,IV}$, 1.14 $ms^{-1}$ and 2.21 $ms^{-1}$. The *x*-direction flow remains stronger, but less so than in Area III. Both sites provide similar figures of power density, with mean values of 1.03 $kWm^{-2}$ and 1.28 $kWm^{-2}$, and peak values of 4.28 $kWm^{-2}$ and 5.49 $kWm^{-2}$ at $L_{mean,IV}$ and $L_{max,IV}$, respectively.

In the case of Area VI, the flow field of the central channel in the middle-inner estuary up to Aughinish does not present marked spatial variations. This feature, together with the relatively reduced surface of this area (with roughly 12 $hm^2$ above $TSE_{ndl} = 2$), results

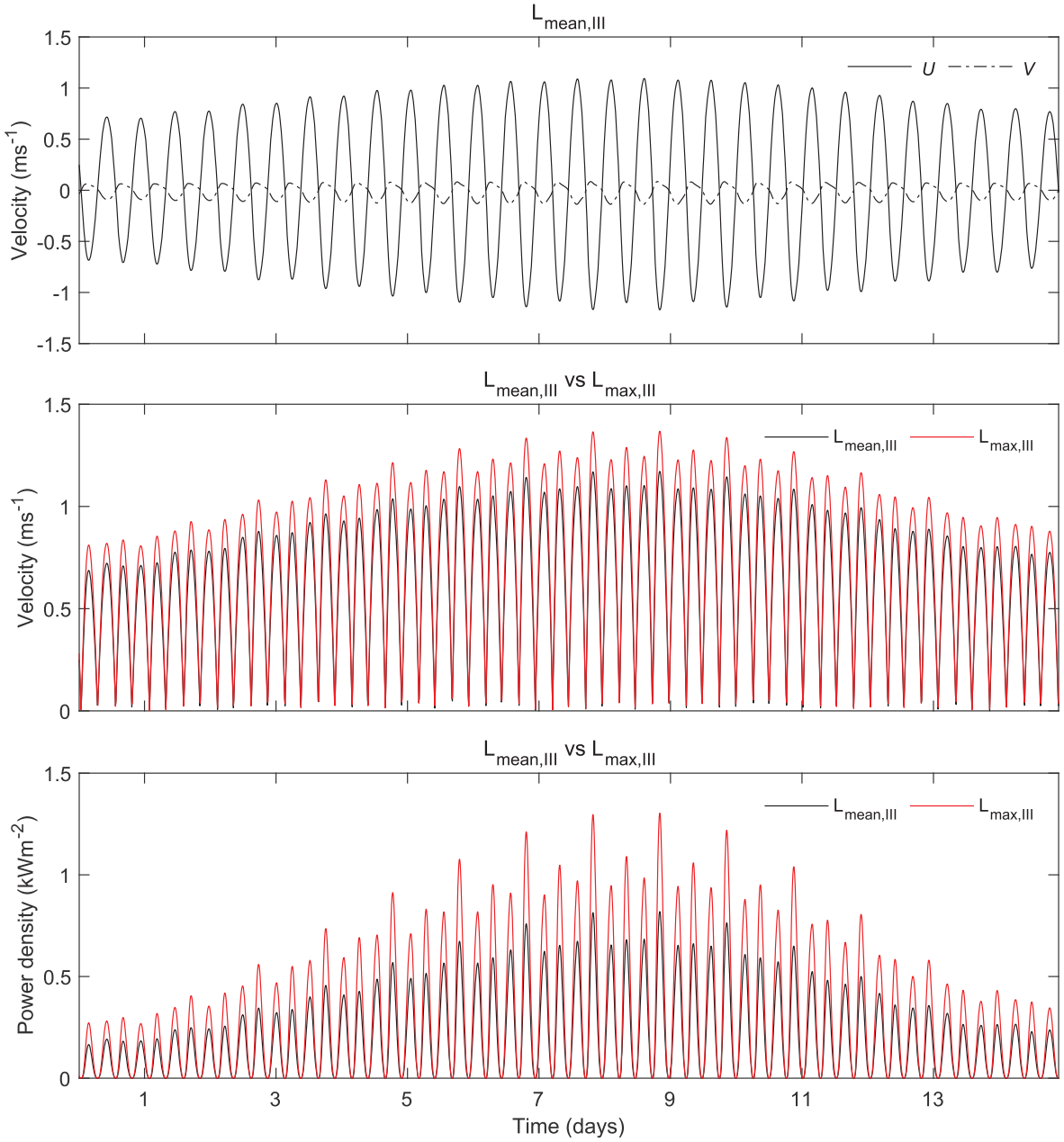


**Fig. 11.** High-resolution analysis in Area III showing the time distribution of the current velocity components, *U* and *V*, at $L_{mean,III}$ (above), the magnitude of current velocity at $L_{mean,III}$ and $L_{max,III}$ (intermediate), and the power density at $L_{mean,III}$ and $L_{max,III}$ (bottom).

in similar figures at both representative points, $L_{mean,VI}$ and $L_{max,VI}$, with mean current speeds of 0.69 and 0.71 $ms^{-1}$, and peak values of 1.41 and 1.45 $ms^{-1}$, respectively. The power density available at both locations is therefore similar, with mean values of 0.28 and 0.32 $kWm^{-2}$ and maximum values of 1.41 and 1.54 $kWm^{-2}$ at $L_{mean,VI}$ and $L_{max,VI}$, respectively.

Finally, in the uppermost area, Area VII, the mean magnitude of the current velocity at both representative locations is again similar, of 0.62 $ms^{-1}$ at $L_{mean,VII}$ and 0.64 $ms^{-1}$ at $L_{max,VII}$. In the case of the peak values, the differences are more apparent, with values of 1.13 $ms^{-1}$ and 1.39 $ms^{-1}$, respectively. In addition, the change in the alignment of the main axis of the estuary in this area causes the *y*-axis velocity component to all but vanish. Regarding the power density, similar average values are obtained at both locations, with 0.20 $kWm^{-2}$ at $L_{mean,VII}$ and 0.24 $kWm^{-2}$ at $L_{max,VII}$, with much larger differences however in the maximum values, 0.74 $kWm^{-2}$ and 1.37 $kWm^{-2}$, respectively.

For the sake of clarity, the previous results are summarized in Table 4, in which the values of the mean and peak velocities and power density for the period analysed at the selected locations are provided.

## 6. Conclusions

This study used a high-resolution analysis to characterize the tidal and river in-stream energy resource throughout the Shannon Estuary to identify the most suitable areas for its conversion. The resource is examined in a number of case studies (CS1 to CS7)

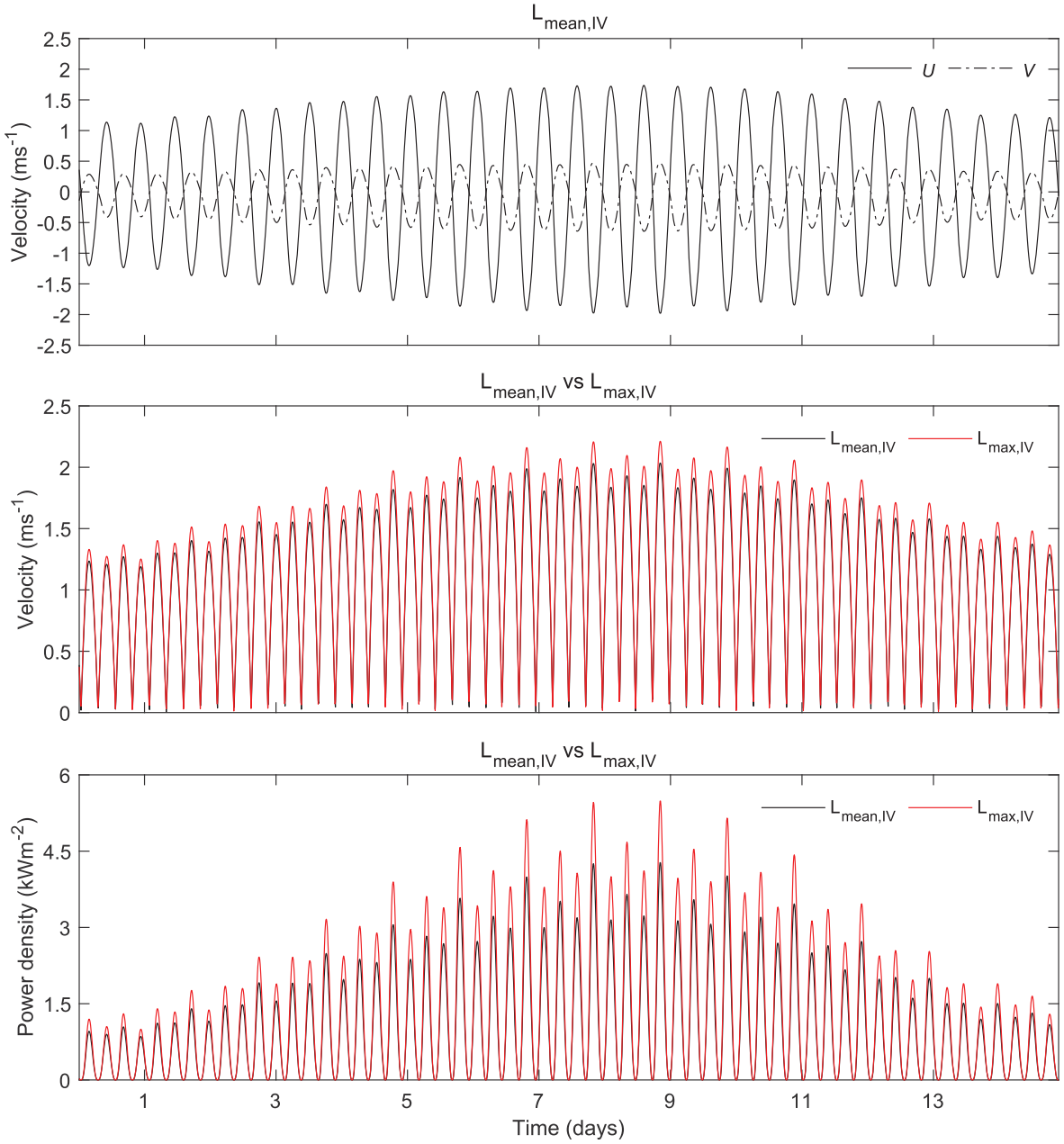


**Fig. 12.** High-resolution analysis in Area IV showing the time distribution of the current velocity components, *U* and *V*, at $L_{mean,IV}$ (above), the magnitude of current velocity at $L_{mean,IV}$ and $L_{max,IV}$ (intermediate), and the power density at $L_{mean,IV}$ and $L_{max,IV}$ (bottom).

through state-of-the-art numerical modelling. The model is validated against field measurements.

The hydrodynamics of the estuary are characterized in cases CS1 to CS4 which found freshwater inflows to have little influence —the Shannon Estuary is indeed tide-dominated, as a result of its large tidal range and tidal prism. In terms of hydrokinetic energy availability, the intra-annual variability that might arise from variations in freshwater discharges is all but negligible— a positive effect insofar as it would ensure seasonally stable energy production throughout the year.

The strongest current velocities are found in the Tarbert area, with peaks of up to 2.3 $ms^{-1}$ during the ebb tide. Other hotspots are: the area surrounding Kilcredaun and the strait between Scattery Island and Carrig Island, with speeds of up to ~2 $ms^{-1}$. Other areas with a somewhat lower resource may be of interest given their proximity to port facilities, such as: the areas around Moneypoint and close to the Port of Foynes, and Aughinish, where speeds are ~1.4 $ms^{-1}$.

In Case Study CS5 an accurate estimation of the total available energy is computed by simulating a complete year under real conditions. The areas with the highest power density correspond to the strongest flows, especially, the Tarbert area, with ~2 $kWm^{-2}$, followed by the other hotspots, with ~1.2 $kWm^{-2}$ to ~0.5 $kWm^{-2}$.

Despite the importance of the resource, the selection of hotspots for hydrokinetic energy conversion should also consider other aspects, such as the water depth, which may have an important role in the Shannon Estuary, not only because of its large areas of shallow and intermediate depths, but also deep areas. With this in

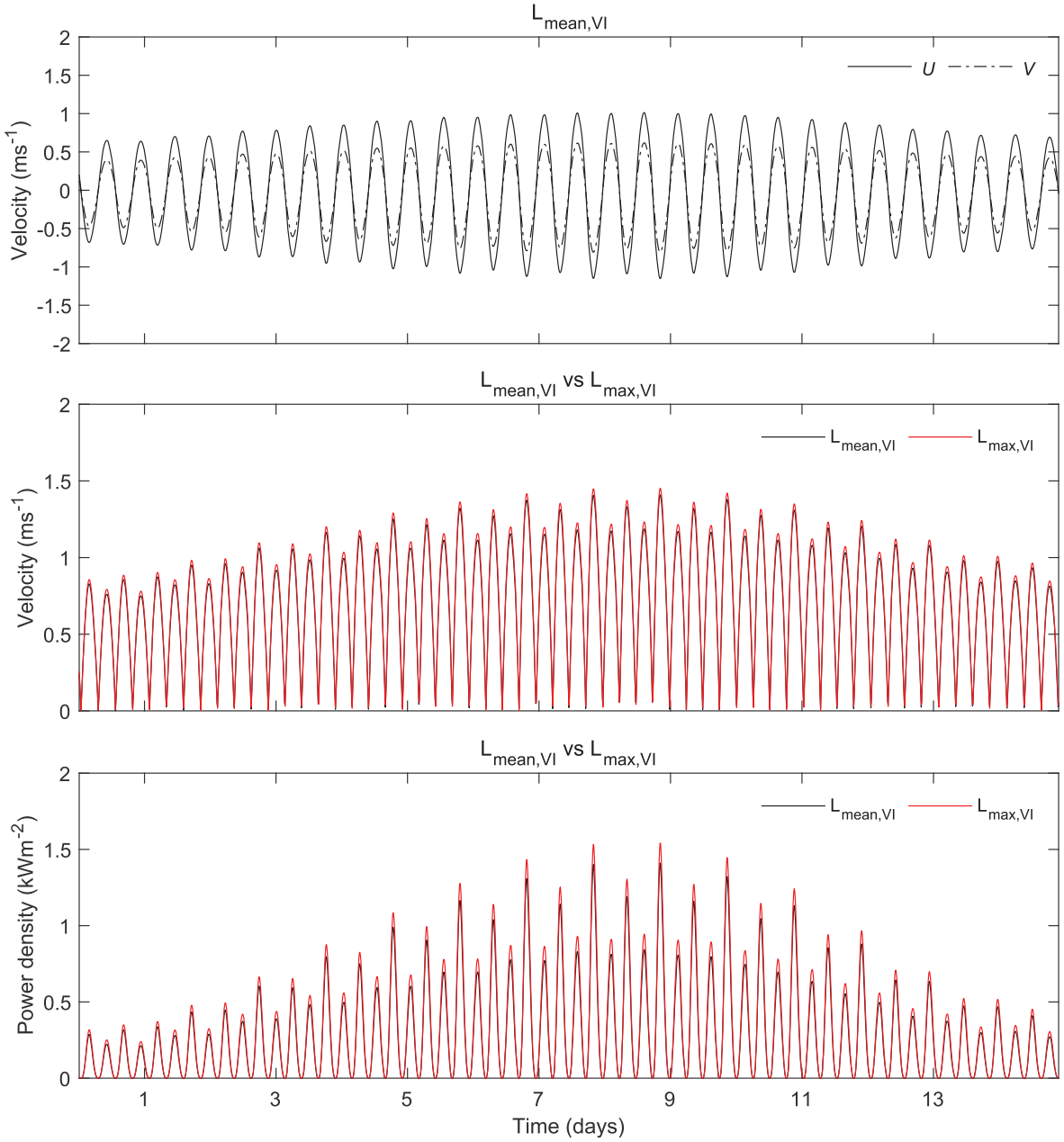


**Fig. 13.** High-resolution analysis in Area VI showing the time distribution of the current velocity components, *U* and *V*, at $L_{mean,VI}$ (above), the magnitude of current velocity at $L_{mean,VI}$ and $L_{max,VI}$ (intermediate), and the power density at $L_{mean,VI}$ and $L_{max,VI}$ (bottom).

view, a new version of the Tidal Stream Exploitability (TSE) index adapted to non-depth-limited areas, the $TSE_{ndl}$ index, is proposed and implemented in Case Study CS6. A new penalty-limiting function, $\xi_{ndl}$, is defined for this to avoid overestimating the available tidal stream power in areas where water depths exceed than those required for operating most commercial TECs.

Seven suitable areas (I to VII) are delimited by considering specific thresholds of the $TSE_{ndl}$ index, based on its physical meaning, and applying spatial analysis. With a view to supplying energy to the port facilities in the estuary, the distance to these facilities is also considered, resulting in the selection of four areas: III, IV, VI and VII.

Finally, a high-resolution analysis of the resource in these four areas is carried out in Case Study CS7. Two representative locations were selected in each area, corresponding to the mean and maximum $TSE_{ndl}$ in the area. The available resource is found to differ greatly amongst areas, depending on their location within the estuary. In all four areas, there is little spatial variations in the resource, except for Area IV (Tarbert), where the $TSE_{ndl}$ index varies from 2 to 9.36 —the reason being its large surface area.

Summarizing, the most suitable areas for tidal stream energy conversion in the Shannon Estuary were identified, and their resource characterized. The procedure implemented in this study, and in particular, the new $TSE_{ndl}$ index, could be applied to any other coastal region of interest, including deep-water areas. The final decision regarding the installation of a hydrokinetic energy farm should consider not only the resource, but also Marine Spatial Planning, environmental and socioeconomic factors (including the

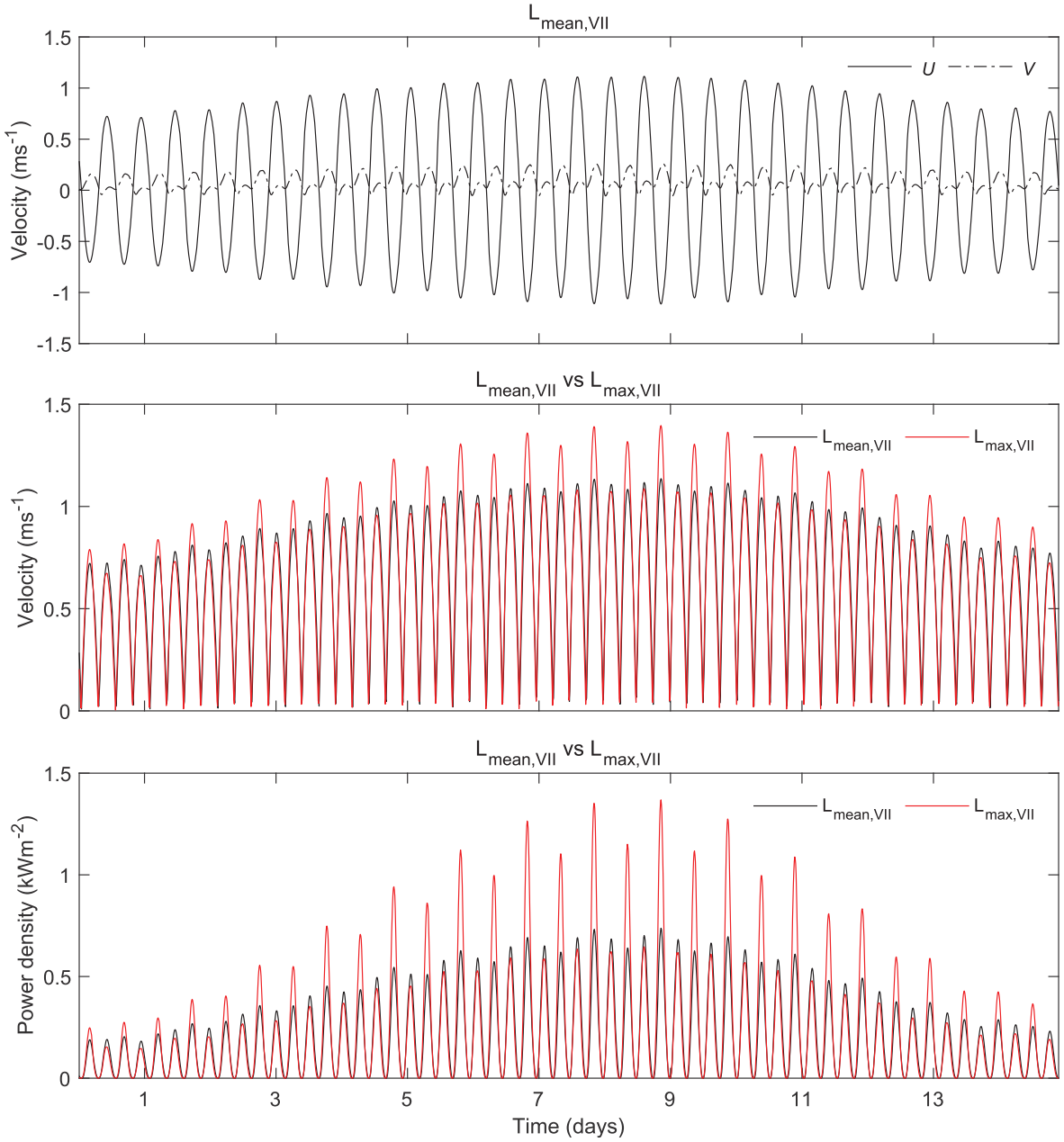


**Fig. 14.** High-resolution analysis in Area VII showing the time distribution of the current velocity components, *U* and *V*, at $L_{mean,VII}$ (above), the magnitude of current velocity at $L_{mean,VII}$ and $L_{max,VII}$ (intermediate), and the power density at $L_{mean,VII}$ and $L_{max,VII}$ (bottom).

**Table 4**
Mean and peak velocities and power density at the selected locations (CS7).

| Locations | Mean velocity ($ms^{-1}$) | Peak velocity ($ms^{-1}$) | Mean power density ($kWm^{-2}$) | Peak power density ($kWm^{-2}$) |
|---|---|---|---|---|
| **$L_{mean,III}$** | 0.61 | 1.17 | 0.20 | 0.82 |
| **$L_{max,III}$** | 0.71 | 1.37 | 0.31 | 1.30 |
| **$L_{mean,IV}$** | 1.06 | 2.04 | 1.03 | 1.28 |
| **$L_{max,IV}$** | 1.14 | 2.21 | 4.28 | 5.49 |
| **$L_{mean,VI}$** | 0.69 | 0.71 | 0.28 | 0.32 |
| **$L_{max,VI}$** | 1.41 | 1.45 | 1.41 | 1.54 |
| **$L_{mean,VII}$** | 0.62 | 0.64 | 0.20 | 0.24 |
| **$L_{max,VII}$** | 1.13 | 1.39 | 0.74 | 1.37 |

computation of capital and operational expenditures), which will be addressed in future research.

## CRediT authorship contribution statement

**D.M. Fouz:** Conceptualization, Methodology, Investigation, Formal analysis, Visualization, Writing – original draft. **R. Carballo:** Conceptualization, Methodology, Writing – review & editing, Supervision, Project administration, Funding acquisition. **I. López:** Formal analysis, Visualization, Writing – review & editing, Supervision. **G. Iglesias:** Conceptualization, Methodology, Writing – review & editing, Supervision.

## Declaration of competing interest

The authors declare that they have no known competing financial interests or personal relationships that could have appeared to influence the work reported in this paper.

## Acknowledgements

This work was funded by the PORTOS project co-financed by the Interreg Atlantic Area Programme through the European Regional Development Fund [grant number EAPA_784/2018] and 'Axudas para a consolidación e estruturación de unidades de investigación competitivas nas universidades do Sistema Universitario Galego (2020-22)' with reference number ED341B 2020/25.

The authors are also grateful for the support of Science Foundation Ireland and MaREI, the Marine Renewable Energy Centre of Ireland, grant SFI MAREI2_12/RC/2302/P2 Platform RA1b.

During this work I. López was supported by a postdoctoral grant of the 'Programa de Axudas á etapa posdoutoral da Xunta de Galicia' with reference number ED481D 2019/019.

## References

[1] G. Agrawal, D. Mohan, H. Rahman, Ambient Air Pollution in Selected Small Cities in India: Observed Trends and Future Challenges, IATSS Research, 2021.
[2] Y. Kazancoglu, M. Ozbiltekin-Pala, Y.D. Ozkan-Ozen, Prediction and evaluation of greenhouse gas emissions for sustainable road transport within Europe, Sustainable Cities and Society 70 (2021) 102924.
[3] A.J. Njoh, Renewable energy as a determinant of inter-country differentials in CO2 emissions in Africa, Renewable Energy 172 (2021) 1225–1232.
[4] M. Zhai, G. Huang, L. Liu, B. Zheng, Y. Li, Economic modeling of national energy, water and air pollution nexus in China under changing climate conditions, Renewable Energy 170 (2021) 375–386.
[5] G. Lonati, S. Cernuschi, S. Sidi, Air quality impact assessment of at-berth ship emissions: case-study for the project of a new freight port, Sci Total Environ 409 (2010) 192–200.
[6] D. Bailey, G. Solomon, Pollution prevention at ports: clearing the air, Environ Impact Assess Rev 24 (2004) 749–774.
[7] E. Bachvarova, T. Spasova, J. Marinski, Air pollution and specific meteorological conditions at the adjacent areas of sea ports, IFAC-PapersOnLine 51 (2018) 378–383.
[8] A.M. Kotrikla, T. Lilas, N. Nikitakos, Abatement of air pollution at an aegean island port utilizing shore side electricity and renewable energy, Mar Policy 75 (2017) 238–248.
[9] T. Cabral, D. Clemente, P. Rosa-Santos, F. Taveira-Pinto, T. Morais, F. Belga, et al., Performance assessment of a hybrid wave energy converter integrated into a harbor breakwater, Energies 13 (2020).
[10] I. López, R. Carballo, D.M. Fouz, G. Iglesias, Design selection and geometry in OWC wave energy converters for performance, Energies 14 (2021).
[11] F. Taveira-Pinto, P. Rosa-Santos, T. Fazeres-Ferradosa, Marine renewable energy, Renewable Energy 150 (2020) 1160–1164.
[12] P. Rosa-Santos, F. Taveira-Pinto, C.A. Rodríguez, V. Ramos, M. López, The CECO wave energy converter: recent developments, Renewable Energy 139 (2019) 368–384.
[13] E. Dallavalle, M. Cipolletta, V.C. Moreno, V. Cozzani, B. Zanuttigh, Towards Green Transition of Touristic Islands through Hybrid Renewable Energy Systems. A Case Study in Tenerife, Canary Islands, Renewable Energy, 2021.
[14] M. López, N. Rodríguez, G. Iglesias, Combined floating offshore wind and solar PV, Journal of Marine Science and Engineering 8 (2020).
[15] C. Perez-Collazo, R. Pemberton, D. Greaves, G. Iglesias, Monopile-mounted wave energy converter for a hybrid wind-wave system, Energy Conversion and Management 199 (2019) 111971.
[16] I. Iglesias, A. Bio, L. Bastos, P. Avilez-Valente, Estuarine hydrodynamic patterns and hydrokinetic energy production: the Douro estuary case study, Energy 222 (2021) 119972.
[17] D.M. Fouz, R. Carballo, V. Ramos, G. Iglesias, Hydrokinetic energy exploitation under combined river and tidal flow, Renewable Energy 143 (2019) 558–568.
[18] Z. Yang, T. Wang, R. Branch, Z. Xiao, M. Deb, Tidal stream energy resource characterization in the Salish Sea, Renewable Energy 172 (2021) 188–208.
[19] M. Lewis, R. O'Hara Murray, S. Fredriksson, J. Maskell, A. de Fockert, S.P. Neill, et al., A standardised tidal-stream power curve, optimised for the global resource, Renewable Energy 170 (2021) 1308–1323.
[20] M. Thiébaut, A. Sentchev, Tidal stream resource assessment in the Dover Strait (eastern English Channel), International Journal of Marine Energy 16 (2016) 262–278.
[21] G. Pinon, P. Mycek, G. Germain, E. Rivoalen, Numerical simulation of the wake of marine current turbines with a particle method, Renewable Energy 46 (2012) 111–126.
[22] D. Fallon, M. Hartnett, A. Olbert, S. Nash, The effects of array configuration on the hydro-environmental impacts of tidal turbines, Renewable Energy 64 (2014) 10–25.
[23] D.T. Pugh, Tides, Surges, and Mean Sea-Level/a Handbook for Engineers and Scientists, John Wiley & Sons Inc, 1996.
[24] T.L. Sheehan, M.G. Healy, Sub-recent changes in annual average water level in the Shannon estuary, Western Ireland, J Coast Res (2006) 193–197.
[25] M. Álvarez, R. Carballo, V. Ramos, G. Iglesias, An integrated approach for the planning of dredging operations in estuaries, Ocean Engineering 140 (2017) 73–83.
[26] G. Iglesias, R. Carballo, Seasonality of the circulation in the Ría de Muros (NW Spain), J Mar Syst 78 (2009) 94–108.
[27] G. Iglesias, M. Sánchez, R. Carballo, H. Fernández, The TSE index – a new tool for selecting tidal stream sites in depth-limited regions, Renewable Energy 48 (2012) 350–357.
[28] R. Carballo, G. Iglesias, A. Castro, Residual circulation in the Ría de Muros (NW Spain): a 3D numerical model study, J Mar Syst 75 (2009) 130.
[29] G. Iglesias, R. Carballo, Effects of high winds on the circulation of the using a mixed open boundary condition: the Ría de Muros, Spain, Environmental Modelling & Software 25 (2010) 455–466.
[30] L.S. Blunden, A.S. Bahaj, Initial evaluation of tidal stream energy resources at Portland Bill, UK, Renewable Energy 31 (2006) 121–132.
[31] R. Carballo, G. Iglesias, A. Castro, Numerical model evaluation of tidal stream energy resources in the Ría de Muros (NW Spain), Renewable Energy 34 (2009) 1517–1524.
[32] V. Ramos, G. Iglesias, Performance assessment of tidal stream turbines: a parametric approach, Energy Conversion and Management 69 (2013) 49–57.
[33] C.J. Mejia-Olivares, I.D. Haigh, N.C. Wells, D.S. Coles, M.J. Lewis, S.P. Neill, Tidal-stream energy resource characterization for the Gulf of California, México. Energy 156 (2018) 481–491.
[34] Deltares User, Manual Delft3D-FLOW, Deltares ed., 2010. Delft, The Netherlands.
[35] R. O'Toole, M. Judge, F. Sacchetti, T. Furey, E. Mac Craith, K. Sheehan, et al., Mapping Ireland's coastal, shelf and deep-water environments using illustrative case studies to highlight the impact of seabed mapping on the generation of blue knowledge, Geological Society, London, Special Publications 505 (2020) SP505–2019-2207.
[36] C. Souto, M. Gilcoto, L. Fariña-Busto, F.F. Pérez, Modeling the residual circulation of a coastal embayment affected by wind-driven upwelling: circulation of the Ría de Vigo (NW Spain), Journal of Geophysical Research 108 (4–1) (2003) 4–18.
[37] S. Torres López, R.A. Varela, E. Delhez, Residual circulation and thermohaline distribution of the Ría de Vigo: a 3-D hydrodynamic model, Scientia Marina 65 (2001) 277–289.
[38] C. Le Provost, A.F. Bennett, D.E. Cartwright, Ocean tides for and from topex/poseidon, Science 267 (1995) 639–647.
[39] G.D. Egbert, A.F. Bennett, M.G.G. Foreman, Topex/Poseidon tides estimated using a global inverse model, Journal of Geophysical Research 99 (1994) 24821–24852.
[40] G. Iglesias, R. Carballo, A. Castro, Baroclinic modelling and analysis of tide- and wind-induced circulation in the Ría de Muros (NW Spain), J Mar Syst 74 (2008) 475–484.
[41] J.P. Sánchez-Úbeda, M.L. Calvache, C. Duque, M. López-Chicano, Filtering methods in tidal-affected groundwater head measurements: application of harmonic analysis and continuous wavelet transform, Advances in Water Resources 97 (2016) 52–72.
[42] V. Ramos, R. Carballo, M. Álvarez, M. Sánchez, G. Iglesias, A port towards energy self-sufficiency using tidal stream power, Energy 71 (2014) 432–444.
[43] V. Ramos, R. Carballo, M. Álvarez, M. Sánchez, G. Iglesias, Assessment of the impacts of tidal stream energy through high-resolution numerical modeling, Energy 61 (2013) 541–554.
[44] O'Carroll JPJ, R.M. Kennedy, A. Creech, G. Savidge, Tidal Energy: the benthic effects of an operational tidal stream turbine, Mar Environ Res 129 (2017) 277–290.
[45] R. Joy, J.D. Wood, C.E. Sparling, D.J. Tollit, A.E. Copping, B.J. McConnell, Empirical measures of harbor seal behavior and avoidance of an operational tidal turbine, Mar Pollut Bull 136 (2018) 92–106.
[46] P. Qian, B. Feng, H. Liu, X. Tian, Y. Si, D. Zhang, Review on configuration and

control methods of tidal current turbines, Renewable and Sustainable Energy Reviews 108 (2019) 125–139.
[47] L. Castro-Santos, M.I. Lamas-Galdo, A. Filgueira-Vizoso, Managing the oceans: site selection of a floating offshore wind farm based on GIS spatial analysis, Marine Policy 113 (2020) 103803.
[48] L. Castro-Santos, G.P. Garcia, T. Simões, A. Estanqueiro, Planning of the Installation of Offshore Renewable Energies: a GIS Approach of the Portuguese Roadmap, Renewable Energy, 2018.
[49] European Comission, The Exploitation of Tidal Marine Currents, Report EUR16683EN, 1996.
[50] I.P.L. Technomare SpA, Non Nuclear Energy – JOULE II. Wave Energy Project Results. The Exploitation of Tidal Marine Currents, EU JOULE contract JOU2-CT94-0355, 1996.
[51] K.E. Dyer, Estuaries: A Physical Introduction, John Wiley, New York, 1997.

# 5 A HOLISTIC METHODOLOGY FOR HYDROKINETIC ENERGY SITE SELECTION

This chapter corresponds with the following research article:


- **Tittle:** A holistic methodology for hydrokinetic energy site selection
- **Journal:** Applied Energy, Volume 317, 1 July 2022, 119155
- **Editorial:** Elsevier
- **ISSN:** 1872-9118
- **DOI:** https://doi.org/10.1016/j.apenergy.2022.119155


- **Authors:** D.M. Fouz[a], R. Carballo[a], I. López[a], G. Iglesias [b, c]
- **Institutions:**
  - [a]Departamento de Enxeñaría Agroforestal, Universidade de Santiago de Compostela, EPSE, Rúa Benigno Ledo s/n, 27002, Lugo, Spain
  - [b]School of Engineering and Architecture & MaREI, Environmental Research Institute, University College Cork, Ireland
  - [c]School of Engineering, Computing and Mathematics, University of Plymouth, UK

- **CRediT authorship contribution statement:**
  - **D.M. Fouz:** Conceptualization, Methodology, Investigation, Formal analysis, Visualization, Writing - Original draft
  - **R. Carballo:** Conceptualization, Methodology, Writing - Review and editing, Supervision, Project Administration, Funding acquisition
  - **I. López:** Methodology, Formal analysis, Writing - Review and editing, Supervision
  - **G. Iglesias:** Conceptualization, Methodology, Writing - Review and editing, Supervision
- **Indicators (2022):** Impact factor, IF = 11.200; First quartile (Q1; 15/119) of this category (*Energy & Fuels*)

Applied Energy 317 (2022) 119155

Contents lists available at ScienceDirect

Applied Energy

journal homepage: www.elsevier.com/locate/apenergy

# A holistic methodology for hydrokinetic energy site selection

D.M. Fouz [a], R. Carballo [a,*], I. López [a], G. Iglesias [b,c]

[a] Departamento de Enxeñaría Agroforestal, Universidade de Santiago de Compostela, EPSE, Rúa Benigno Ledo s/n, 27002 Lugo, Spain
[b] School of Engineering and Architecture & MaREI, Environmental Research Institute, University College Cork, Ireland
[c] School of Engineering, Computing and Mathematics, University of Plymouth, UK

## HIGHLIGHTS

- A holistic methodology for hydrokinetic energy exploitation site selection is proposed.
- The novel Integrated Hydrokinetic Energy (IHE) index is developed.
- The IHE index is applied to the Shannon Estuary.
- The optimum areas for hydrokinetic energy exploitation are identified.

## ARTICLE INFO

*Keywords:*
Hydrokinetic energy
Tidal power
Numerical modelling
Socioeconomic impact
CAPEX

## ABSTRACT

Hydrokinetic energy can contribute to diversify and decarbonise the energy mix in many coastal regions, in particular estuaries. These are typically areas of high environmental value and with intense socioeconomic activity. The aim of this work is to provide a comprehensive methodology for selecting the optimum locations for hydrokinetic energy exploitation, by considering all the relevant aspects which affect the decision-making process, and improve the current available procedures. The methodology is centred around a novel holistic index, the Integrated Hydrokinetic Energy (IHE) index, which considers: (i) the exploitable resource, (ii) the costs of installation, and (iii) the socioeconomic and environmental aspects. The approach is illustrated through a case study in the Shannon Estuary, on the west coast of Ireland. It is shown that the application of this methodology facilitates the planning and reduces the uncertainties in the development of a hydrokinetic farm project.

## 1. Introduction

Marine renewable energies (MREs) have been recognised as a significant source of green energy, with potential to contribute to reducing greenhouse gases emissions and thus combat climate change [1–4]. Within MREs, hydropower is highlighted as a feasible alternative renewable energy source, which may be used to diversify and decarbonise the energy mix in many regions [5–9]. Focusing on coastal areas, a specific type of hydropower, hydrokinetic energy, stands out because of its predictability, electricity quality and low environmental impact [10–12]. In this regard, estuaries are promising areas for the exploitation of hydrokinetic energy thanks to their strong tidal currents and, in some cases, large fluvial discharges [13–15], or sea level rise [16].

Over the last years, considerable efforts have been made to develop hydrokinetic energy converters (HECs), with emphasis on hydrokinetic turbines [17,18], and to identify the best areas for their operation [10,14,19–25]. For all their interest, these studies were carried out from the perspective of the energy yield, disregarding economic and environmental aspects; therefore, more comprehensive studies are required for an informed decision–making process in developing a hydrokinetic farm project [26]. This is of great importance in the case of estuaries, where different areas for installing HECs may be of interest. In effect, the costs of installation and operation of a hydrokinetic farm, along with the restrictions that would be imposed by the existing or potential socioeconomic activities and environmental aspects, may greatly differ among locations within the same coastal area [27].

In this research, a novel comprehensive methodology is developed for selecting the most suitable location for hydrokinetic energy exploitation in a coastal region, irrespective of the conversion technology or farm layout, and therefore significantly improving the current available procedures, by considering the key aspects affecting the decision-making process. The application of this methodology to a coastal

* Corresponding author.
*E-mail address:* rodrigo.carballo@usc.es (R. Carballo).

https://doi.org/10.1016/j.apenergy.2022.119155
Received 10 February 2022; Received in revised form 1 April 2022; Accepted 15 April 2022
Available online 25 April 2022

region will allow the reduction of the uncertainties in the early stages of planning the installation of a hydrokinetic farm [28]. The final design of the farm configuration in subsequent stages would require a detailed cost analysis [29,30].

The proposed integrated site selection is conducted by means of the novel Integrated Hydrokinetic Energy (IHE) index. Based on a holistic approach, the IHE index integrates the three main aspects affecting the installation of hydrokinetic energy farms: (i) the exploitable resource, which is computed by high–resolution numerical modelling; (ii) the geomorphological configuration, for which the main Capital Expenditures (CAPEX) of a hydrokinetic farm are parameterised according to water depth and shoreline distance; (iii) the socioeconomic activities (aquaculture, shellfish, and shipping) and environmental uses (Special Areas of Conservation, SACs, Spatial Protection Areas, SPAs) which are considered by analysing and parameterising a large amount of geospatial data.

In this work, the IHE index is defined and applied to a case study: the Shannon Estuary, on the west coast of Ireland (Fig. 1). The Shannon Estuary is a macrotidal coastal area characterised, from a hydrodynamic perspective, by a semidiurnal tidal regime and large riverine inputs from several tributaries subject to a marked seasonality. A number of areas of interest for hydrokinetic energy conversion were identified in preliminary studies, in particular the Strategic Integrated Framework Plan for the Shannon Estuary (SIFP) [31]. Likewise, in recent studies based on the Tidal Stream Exploitability index adapted to non-depth-limited areas, $TSE_{ndl}$ index, a number of areas were identified as of potential interest [13]: Kilcredaun (Area I), the constriction between Scattery Island and Carrig Island (Area II), the area close to Moneypoint (Area III), Tarbert (Area IV), the surroundings of Glin (Area V), the approaches to Port of Foynes (area VI), the area close to Aughinish (Area VII). However, a comprehensive analysis of these areas encompassing not only the resource itself but also the socioeconomic and environmental aspects is lacking to the best of the authors' knowledge.

Regarding its geomorphologic configuration, the Shannon Estuary has extensive deep (over 20 m) areas (main channel), areas of intermediate water depths, and intertidal areas. The average water depth is approximately 16 m. With much of its area sheltered from wave action and a wide and deep main channel, the Shannon Estuary is an excellent location for a port. Indeed, with its six commercial maritime terminals, the Shannon Foynes port is the second largest in Ireland, after Dublin, in terms of commercial traffic. These activities must naturally be accounted for in developing hydrokinetic energy. More generally, a thorough investigation of the costs, socioeconomic activity and environmental aspects of the areas of interest is required for the definition of a plan for developing hydrokinetic energy in the Shannon Estuary.

This paper is structured as follows. In Section 2, a general overview of the IHE index is presented. Next, in Sections 3 to 5, the different aspects considered in the index are defined: the energy resource (Section 3), costs (Section 4), and socioeconomic and environmental uses (Section 5). In Section 6, the results are presented. Finally, conclusions are drawn in Section 7.

## 2. General description of the procedure

The objective of this research is to define and apply a comprehensive methodology, leading to the identification of the most suitable area for hydrokinetic energy exploitation in a coastal region, independently of the type of energy converter or farm layout. To this end, the IHE index is developed, based on a holistic procedure, while considering: (i) the exploitable resource, (ii) the costs of installation and operation, and (iii) the socioeconomic and environmental activities.

This procedure is carried out by considering four different steps: (i) a thorough characterisation of the energy resource, based on high–resolution spatiotemporal numerical modelling, (Section 3); (ii) the development of a geospatial penalty function while considering the relation between the main drivers of the CAPEX and the coastal configuration (depth and distance to coast), leading to a penalisation of those areas where the costs of hydrokinetic energy exploitation are higher (Section 4); (iii) an accurate geospatial analysis of socioeconomic and environmental uses, assessing the suitability of their coexistence with hydrokinetic energy exploitation, leading to an additional penalty function (Section 5); and finally, (iv) the integration of previous results (i to iii) in order to provide a reliable indicator that shows the viability of the hydrokinetic energy exploitation throughout a coastal region (Section 6).

Each one of the aforementioned steps is reflected in the corresponding term that constitutes the IHE index, which is computed as follows:

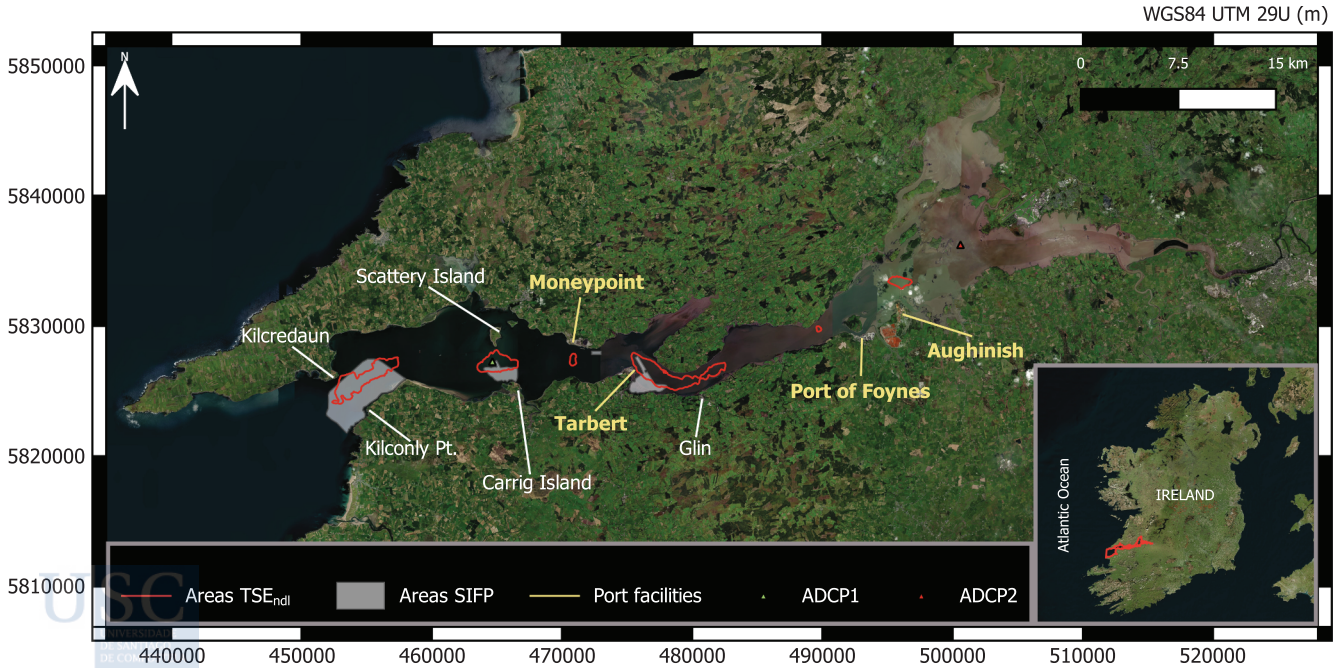


**Fig. 1.** Location of the Shannon Estuary.

$$\mathrm{IHE} = \mathrm{HE} C_{gp} U_{gp}, \tag{1}$$

where HE is the hydrokinetic energy resource index (step i), according to which values equal to or higher than 1 indicate suitability for energy exploitation; $C_{gp}$ is a geospatial cost penalty function (values ranging from 1 to 0) (step ii), meaning that a location with $C_{gp} = 1$ is not penalised by the costs that are associated to the operation and maintenance of a hydrokinetic farm, and where $C_{gp} = 0$ has the largest penalisation (in the latter case, IHE = 0); finally, $U_{gp}$ stands for the geospatial water use penalty function (values ranging from 0 to 1) (step iii), having the same interpretation as $C_{gp}$. As a result, the physical interpretation of the IHE index is straightforward. The higher the IHE index, the better the site for hydrokinetic energy exploitation, with values above 1 indicating suitability for hydrokinetic energy exploitation, which would correspond with a site with IHE = 1 (minimum value for suitability), and without any penalisation ($C_{gp} = 1$ and $U_{gp} = 1$).

## 3. Hydrokinetic energy resource (HE) index

The first step of the proposed methodology is to define an index which accurately reflects the suitability of a given coastal area, by considering not only its total available energy, but its exploitable resource. To this end, the hydrokinetic energy (HE) resource index is defined as:

$$\mathrm{HE} = \frac{E_e}{E_{ref}}, \tag{2}$$

where $E_e$ is the exploitable energy resource at a given location, i.e., the resource resulting from current velocity magnitudes that allow a tidal turbine to operate (Section 3.2), and $E_{ref}$ is a reference level of energy resource representing the minimum annual energy that is required for hydrokinetic energy exploitation. In the following subsections the development of HE is presented, along with its application to the Shannon Estuary.

### 3.1. Numerical modelling

An accurate characterisation of the hydrokinetic energy potential in a coastal region, requires a thorough description of its hydrodynamics during a long period of time, ideally a complete year [19], for which high-resolution spatiotemporal numerical modelling constitutes a powerful tool [32]. To this end, the state-of-the-art model Delft3D-FLOW is applied, which has been widely used to analyse the hydrodynamics of estuarine areas [33–38]. This model approximates the Navier–Stokes equations under the Shallow Water and Boussinesq's assumptions by means of a finite–difference scheme. The results are coupled with the transport equation (in terms of water temperature and salinity), leading to the computation of the density spatial distribution and thus the baroclinic flows, which in turn may be of importance in coastal areas that are subject to large river discharges, or where two different types of water masses meet [39,40]. The Delft3D–FLOW model can be implemented in its 3D or 2DH form (i.e., vertically averaged). The usual dominance of the tide in the coastal areas of interest for hydrokinetic energy exploitation leads to 2DH models, being those that are most used in energy resource assessments [10,13,14,32,41]. For further details about the Delft3D–FLOW model, the reader is referred to [42].

In the present work, a high-resolution 2DH application of the Delft3D–FLOW model is conducted for the Shannon Estuary and the adjacent continental shelf, up to 100 m water depth, approximately. To this end, a varying–size numerical grid (Fig. 2) is used, covering the whole estuary and extending over the Atlantic Ocean, approximately 30 km offshore. From the inner estuary to the mouth, the grid resolution is set to 100 × 100 m, progressively decreasing up to 100 × 300 m, towards the westernmost oceanic open boundary. The bathymetric data is obtained from the INFOMAR programme (Integrated Mapping for the Sustainable Development of Ireland's Marine Resource) [43]. The numerical model is validated against ADCP (Acoustic Doppler Current Profiler) field measurements of flow velocity, gathered at two different locations in the inner and middle estuary (Fig. 1), ADCP1 (25/06/2017 to 29/07/2017) and ADCP2 (24/03/2006 to 28/03/2006). Fig. 3 shows the linear regression fit of the magnitude of computed and observed velocities at ADCP1 and ADCP2, and Table 1 provides the statistical parameters obtained. The results show an excellent agreement between both time series, and, therefore, the capability of the model to accurately reproduce the hydrodynamics of this coastal area.

Once the numerical model is validated, it can be used to accurately characterise the available energy resource. With this aim, a complete annual scenario is computed by using the following forcing factors: main tidal harmonics (TOPEX/Poseidon database) [44,45], average monthly river discharges (Irish Office of Public Works, OPW), and thermohaline conditions at open boundaries (Irish Marine Institute, MI).

### 3.2. Available and exploitable energy resource

The available time-dependent hydrokinetic energy resource is computed in terms of power density, $E_a(t)$ ($\mathrm{Wm}^{-2}$), as [10]:

$$E_a(t) = \frac{\rho}{2}[V(t)]^3, \tag{3}$$

where $\rho$ ($\mathrm{kgm}^{-3}$) is the seawater density and $V(t)$ ($\mathrm{ms}^{-1}$) stands for the time–dependent flow velocity. In Fig. 4 the spatial distribution of the mean flow velocity, $V_m$, during a complete annual scenario is plotted.

However, all of the available resource cannot be harnessed. In effect, HECs usually work within a range of velocities, defined by lower and upper thresholds [41]: the so–called cut-in velocity, $V_{ci}$ ($\mathrm{ms}^{-1}$), which indicates the minimum velocity that is required for their operation, and the cut-off velocity, $V_{co}$ ($\mathrm{ms}^{-1}$), or the maximum velocity at which HECs can operate, due to safety reasons.

In view of the aforementioned aspects, the exploitable time-dependent energy resource in terms of power density, $E_e(t)$ ($\mathrm{Wm}^{-2}$) is

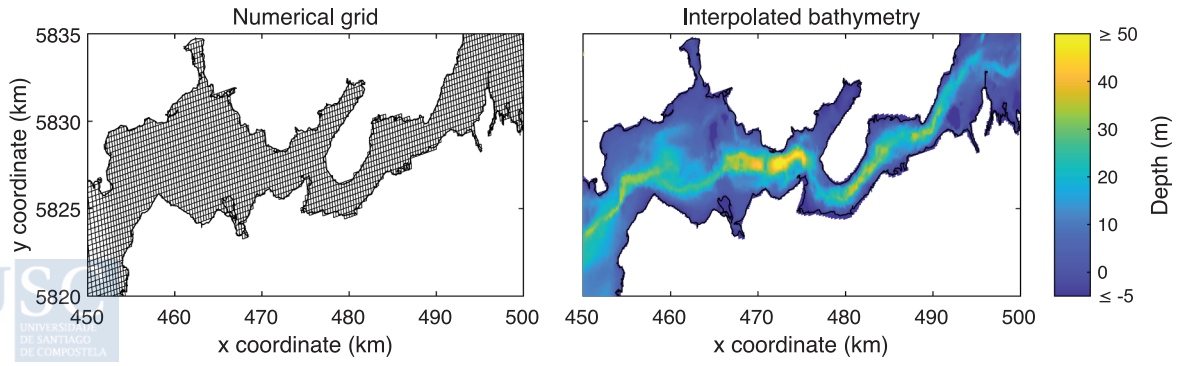


**Fig. 2.** Numerical grid (left) and its interpolation to the bathymetric data (right).

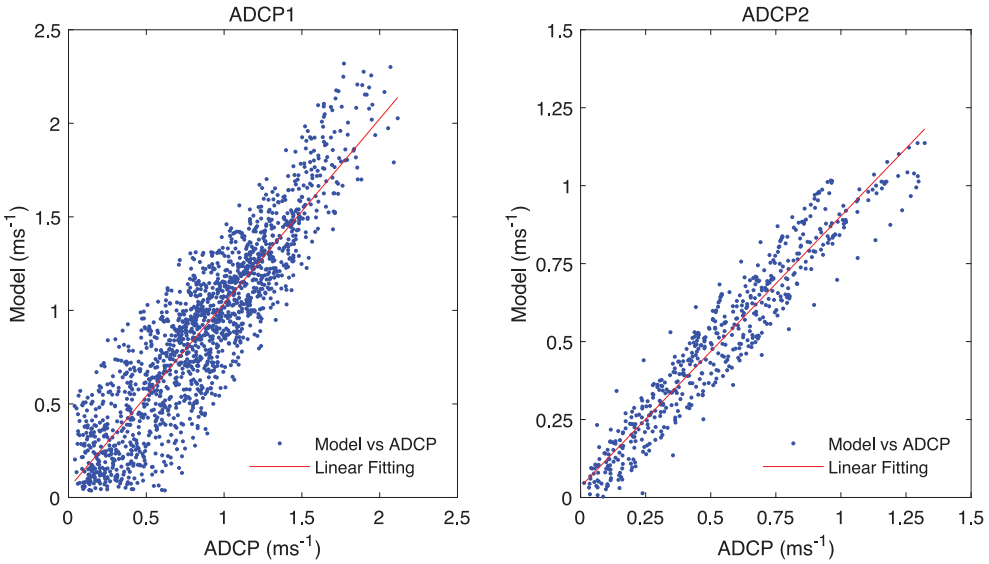


**Fig. 3.** Numerical model validation against ADCP measurements at ADCP1 (left) and ADCP2 (right) sites.

**Table 1**
Validation: statistical parameters.

| Parameter | ADCP1 | ADCP2 |
|---|---|---|
| R | 0.900 | 0.959 |
| NRMSE (%) | 10.162 | 6.038 |
| BIAS ($ms^{-1}$) | 0.038 | −0.037 |
| SI | 0.245 | 0.146 |

defined as [41]:

$$E_e(t) = \begin{cases} 0, V(t) < V_{ci} \\ \frac{\rho}{2}[V(t)]^3, V_{ci} \le V(t) \langle V_{co} \\ 0, V(t) \ge V_{co} \end{cases}, \quad (4)$$

and therefore the mean non-exploitable power density, $E_{ne}$ ($Wm^{-2}$) can be computed as:

$$E_{ne} = E_a - E_e \quad (5)$$

where $E_a$ and $E_e$ are the mean available and mean exploitable power density, respectively, over a given period of interest.

As previously stated, the objective of this work is to provide a methodology, which can be applied with independence of the energy conversion technology and farm layout. Thus, in the present application, and on the basis of the characteristics of the current available HECs, $V_{ci}$ and $V_{co}$ are set to 0.7 and 3.1 $ms^{-1}$, respectively [14,28,46,47]. These values can be adapted, if required, in forthcoming applications of the IHE index, based on future technological developments.

Fig. 5 shows the spatial distribution of $E_e$ (top) and $E_{ne}$ (bottom) in the Shannon Estuary. In Table 2, the mean and maximum figures of the exploitable resource in the areas identified as being of potential interest according to their available power (Areas I to VII), $E_{e,mean}$ and $E_{e,max}$, respectively, are provided. As can be observed, the largest part of the available hydrokinetic energy in this estuary could be harnessed, as it emerges from the overall much larger figures of the exploitable rather than the non-exploitable resource. However, the difference between exploitable and non-exploitable resource largely varies throughout the estuary, being the areas with the largest exploitable energy those that present the lowest non-exploitable resource. In effect, the non-exploitable energy density in Areas I to VII is very low (<0.03 $kWm^{-2}$), resulting from their current velocities being higher than the cut-in of the turbines ($V_{ci} = 0.7$ $ms^{-1}$), throughout virtually the complete tidal cycle.

### 3.3. Reference energy resource and categorisation

In order to non-dimensionalise Eq. (2), and also to provide a straightforward categorisation, thus allowing simple comparisons among coastal areas and regions, the $E_{ref}$ term is introduced in the definition of the IHE index. This term should be interpreted as a threshold value of the exploitable hydrokinetic energy resource, which is required for a feasible energy exploitation.

As a result, the dimensionless HE index constitutes a reliable metric for the quantification of the exploitable hydrokinetic energy resource at a coastal location, and it can be used as a simple way for the categorisation of its potential. Based on a thorough review of previous research on the potential of the hydrokinetic energy throughout a large number

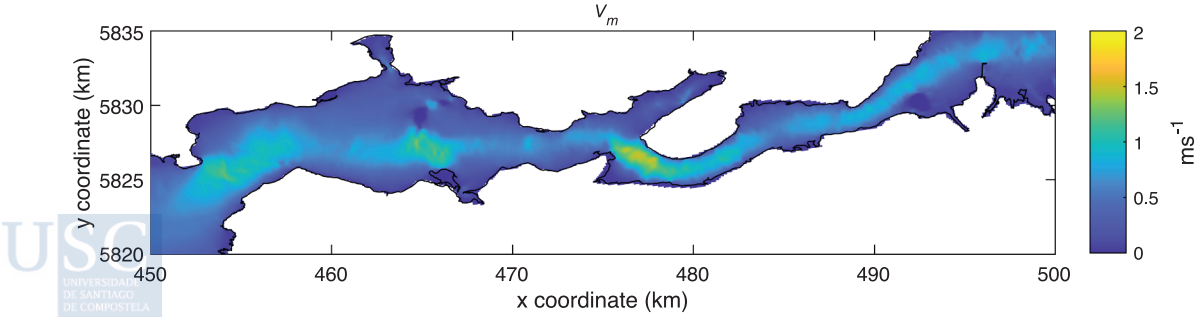


**Fig. 4.** Spatial distribution of $V_m$ throughout the Shannon Estuary.

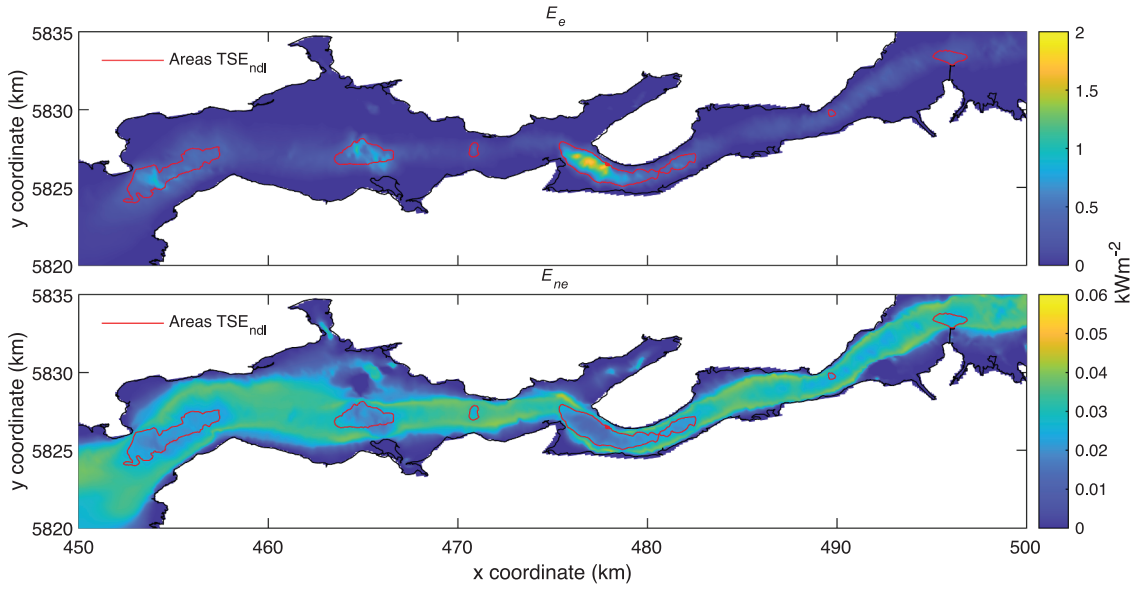


**Fig. 5.** Spatial distribution of $E_e$ (top) and $E_{ne}$ (bottom) throughout the Shannon Estuary.

**Table 2**
$E_{e,mean}$ and $E_{e,\max}$ in the areas of potential interest.

| Area | $E_{e,mean}$ (kWm$^{-2}$) | $E_{e,\max}$ (kWm$^{-2}$) |
|---|---|---|
| I | 0.47 | 1.02 |
| II | 0.56 | 1.22 |
| III | 0.21 | 0.41 |
| IV | 0.82 | 1.83 |
| V | 0.41 | 0.61 |
| VI | 0.37 | 0.44 |
| VII | 0.24 | 0.34 |

of coastal regions [10,13–15,19,20,22,25,48–53], in which current velocity data obtained by high-resolution numerical modelling and in situ measurements are analysed, the value of $E_{ref}$ is set to 0.2 kWm$^{-2}$, and a total of five different categories defining the hydrokinetic energy potential are established: Zones I to V, from lower to higher potential (Table 3).

The aforementioned values can be used as a reference for any coastal region of interest, leading to a straightforward comparison with other areas; however, they could be adapted based on future technological developments. In Fig. 6, the results of the spatial distribution of the HE index throughout the Shannon Estuary are shown. The resulting mean, HE$_{mean}$, and maximum values, HE$_{max}$, of previously defined areas of interest, along with their resulting categorisation are provided in Table 4. The area with the largest exploitable resource is Area IV (HE$_{mean}$ = 3.78, category III), followed by Area II (HE$_{mean}$ = 2.58, category III) and Area I (HE$_{mean}$ = 2.16, category III) with somewhat lower resource, Area V (HE$_{mean}$ = 1.89, category II) and Area VI (HE$_{mean}$ = 1.70, category II) with significantly lower energy, and finally, Area VII (HE$_{mean}$ = 1.11, category II) and Area III (HE$_{mean}$ = 0.97, category I), which are close to the threshold of viability from a resource standpoint.

**Table 3**
Hydrokinetic energy resource categorization based on the HE index.

| Category | HE |
|---|---|
| I | $< 1$ |
| II | $1 \leq$ HE $< 2$ |
| III | $2 \leq$ HE $< 4$ |
| IV | $4 \leq$ HE $< 8$ |
| V | $\geq 8$ |

However, these areas are extensive, presenting locations with larger values of exploitable resource and, therefore, more reduced areas could be defined for establishing a plan for hydrokinetic energy conversion.

## 4. Cost penalty function ($C_{gp}$)

The next step of the methodology to implement the IHE index is the definition of a geospatial cost penalty function and its application to the Shannon Estuary. This function should relate the main drivers of CAPEX with the coastal configuration of a region, penalising the areas in which the energy exploitation will incur higher expenses, as a result of their depth and distance to the coast, but without considering a specific energy conversion technology or farm layout.

### 4.1. Identification of the main CAPEX drivers

CAPEX refers to the costs incurred prior to the operation of an energy installation, i.e., all the construction expenses, including the deployment and grid connection. CAPEX are usually broken down as [27,54]: (i) device costs, (ii) cable costs, (iii) foundations or mooring system costs, (iv) installation costs (e.g., transporting and deployment costs), and (v) grid connection costs. As a reference value, it can be considered that cost categories (i) to (iii) represent approx. 80% of the total CAPEX [27,55].

Device and grid connection costs are, *a priori*, independent of the geomorphology of the study area, and depend on a specific type of technology. Notwithstanding, cable and foundations, or mooring systems costs, are clearly dependent on the main geomorphological aspects, i.e., shoreline distance and water depth, respectively. Consequently, they are retained for a detailed analysis. Finally, installation costs also depend on a wide range of parameters (e.g., nautical and terrestrial transport distance, type of vessel required, climate conditions, etc.), which are difficult to evaluate accurately and, therefore, are out of the scope of this work [29].

The total (per plant) cable costs, $c_c$ (€), can be assessed on the basis of the exporting cable cost, which allows the transport of the electric energy that is produced to a land–based electrical substation, by means of an underwater cable. As a consequence, the costs are highly influenced by the cable length and directly related to the distance to the shoreline as [27]:

$$c_c = a_2 l, \tag{7}$$

where $a_2$ (€m$^{-1}$) is an empirical coefficient which, based on [27], is

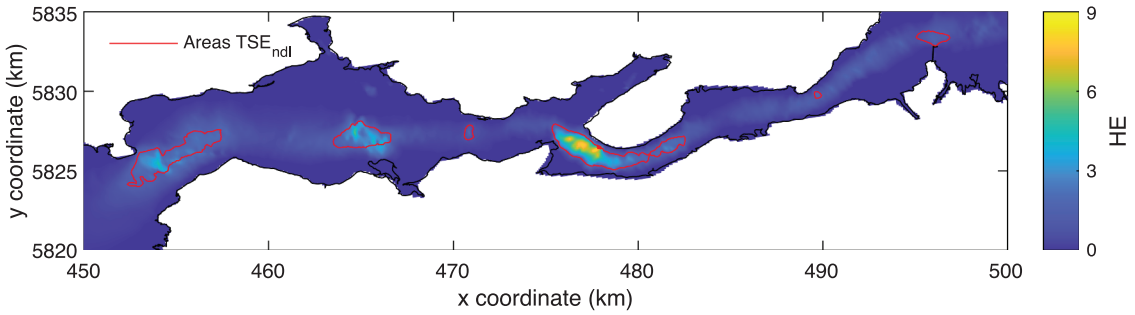


**Fig. 6.** Spatial distribution of the HE index throughout the Shannon Estuary.

**Table 4**
Categorization of areas of potential interest based on the HE index.

| Area | $HE_{mean}$ | $HE_{max}$ | Category |
|---|---|---|---|
| I | 2.16 | 4.70 | III |
| II | 2.58 | 5.62 | III |
| III | 0.97 | 1.89 | I |
| IV | 3.78 | 8.43 | III |
| V | 1.89 | 2.81 | II |
| VI | 1.70 | 2.03 | II |
| VII | 1.11 | 1.57 | II |

set as 196.96, and $l$ (m) is the shoreline distance or, in other words, the cable length from the central hub of the hydrokinetic farm to the shoreline.

As regards the foundations, the most habitual constructive solutions are monopile gravity foundations, which are usually prescribed up to water depths of 20–30 m. Their costs, $c_f$ (M€MW$^{-1}$), can be computed (per unit of converter) as a function of the water depth, $h$ (m) as follows [27,56]:

$$c_f = 0.15 + 10^{-5}h^3. \tag{8}$$

Finally, with respect to the cost of mooring systems, $c_m$ (€), they depend on the type of mooring solution that is used. The most habitual system is the so-called CALM (Catenary Anchor Leg Mooring) system, whose cost per energy converter is related with the mass of each mooring line, $w_{CALM}$ (kg), by 300 € ton$^{-1}$ as [57]:

$$c_m = 300 n_c w_{CALM}, \tag{9}$$

$$w_{CALM} = l_c d_c^2 k, \tag{10}$$

where $n_c$ represents the number of mooring lines, $l_c$ (m) is the length of the catenary, $d_c$ (mm) stands for the diameter of the mooring line, which is usually set to 45 mm in the case of hydrokinetic energy devices [29]; and $k$ (kgm$^{-1}$mm$^{-2}$) represents a constant that can be estimated as 0.02 or 0.0219 for studless and stud-link chains, respectively. Based on [57], a CALM system, which is composed by three stud–link chain lines with a total length of four times the water depth is retained. Thus, Eq. (9) can be rewritten, per unit of energy converter as:

$$c_m = 159.651h. \tag{11}$$

Regarding foundations and mooring systems, it is necessary to note that the choice between both solutions strongly depends on the specific characteristics of each energy conversion technology and, mainly, on its working principle. However, as a general rule, bottom–fixed devices usually use monopile gravity foundations when they operate up to the abovementioned water depth limit (i.e., 20–30 m); above this limit, floating devices that are anchored to the sea bottom by means of mooring lines are the most common solution [47].

What emerges from Eqs. (7) to (11), are other aspects that should be considered when assessing the influence of the coastal configuration on CAPEX, even with independence of the energy conversion technology and layout: the total plant power (Eq. (8)) and the number of devices that will compose the hydrokinetic farm so as to achieve this plant power (Eqs. (8) and (11)). For further details about these two aspects, the reader is referred to Section 4.2.

### 4.2. *Pre-sizing towards generalisation: Total plant power and number of devices*

The consideration of the coastal configuration in a site-selection cost-effective analysis requires, even in early project stages, a pre-sizing of a "standard" hydrokinetic farm including: (i) total power plant, and (ii) number of HECs.

There are many variables involved in defining the total plant power which may be not clear in the preliminary project stages. After a thorough analysis of the current trends and prospects of hydrokinetic technology [46] and, focusing on the hydrokinetic energy conversion in coastal regions by installing second- or third-generation converters [47], a plant with total power of 1 MW is retained.

Regarding the number of devices composing the hydrokinetic farm, the situation is similar to that in the case of the plant power; there is a vast gamut of requirements and limitations that should be considered in order to conduct a cost analysis with independence of the final layout and energy conversion technology [28,29]: available surface, area per device, security margins, etc. Similarly, there is a marked heterogeneity within hydropower projects, ranging from small-scale applications with small-sized turbines to large–scale farms, covering entire coastal regions with large-diameter turbines. Therefore, a wide range of energy conversion devices must be covered in order to generalise the results that are obtained.

Based on a thorough analysis of the current available technologies that are considered in real hydrokinetic projects [14,41,58–63], eight different types of energy converters, ranging from floating micro-turbines (Ø 1 m) to large-diameter bottom–fixed turbines (Ø 16 m), and considering representative designs, are retained (Table 5): (i) Darrieus Turbine (DT), (ii) Darrieus Ducted Turbine (DDT), (iii) Evopod Turbine (ET), (iv) Gorlov Helicoidal Turbine (GHT), (v) Smart Freestream Turbine (SFT), (vi) Smart Monofloat Turbine (SMT), (vii) SeaGen Turbine (SGT), and (viii) Savonius Turbine (ST).

The analysis of the CAPEX of a 1 MW farm, that is composed by each of these representative types of HECs, can lead to the definition of a

**Table 5**
Main characteristics of the HECs considered.

| HEC | Diameter (m) | $V_{ci}$ (ms$^{-1}$) | Rated power (kW) | Swept area (m$^2$) |
|---|---|---|---|---|
| DT | 1.50 | 0.80 | 1.50 | 2.25 |
| DDT | 1.50 | 0.80 | 2.70 | 3.80 |
| ET | 3.00 | 0.70 | 30.00 | 7.10 |
| GHT | 1.00 | 0.50 | 6.30 | 2.50 |
| SFT | 1.00 | 0.70 | 5.00 | 0.80 |
| SMT | 1.00 | 0.70 | 5.00 | 0.80 |
| SGT | 16.00 | 1.00 | 1200.00 | 400.00 |
| ST | 2.00 | 1.00 | 2.50 | 4.00 |

penalty function, $C_{gp}$, relating the costs and the characteristics of a given location (depth and distance to coast). The details of the development and application of this cost penalty function are presented in Section 4.3.

### 4.3. Development and application of the cost penalty function

The total CAPEX of a pre-sized hydrokinetic farm, as defined in Section 4.2, can be assessed by means of its total cost function, $c_{farm}$ (€), built using Eqs. (7), 8 and 11 as:

$$c_{farm} = \begin{cases} c_c + 10^6 P n_c c_f \\ c_c + n_c c_m \end{cases} \quad (12)$$

where $P$ (MW) represents the total plant power, and $n_c$ is the number of converters that are required, which vary depending on the converter that is analysed. Note that the terms $c_f$ and $c_m$ (Eqs. (8) and (11), respectively) cannot be computed simultaneously for a given HEC, being computed based on the technical requirements of the energy converters.

Substituting each term by its value in Eq. (12), it can be rearranged as:

$$c_{farm} = \begin{cases} 196.96l + 10^6 P n_c \left[0.15 + 10^{-5} h^3\right] \\ 196.96l + n_c [159.65h] \end{cases} \quad (13)$$

This function clearly shows the relation between the estuarine coastal configuration (i.e., water depth and shoreline distance, $h$ and $l$, respectively) and the total CAPEX. However, as previously stated, Eq. (13) cannot be used to represent the whole available farm configurations because of its constant coefficients ($P$ and $n_c$), which must be defined. In order to generalise this function to make it representative for any hydrokinetic project, as discussed in Section 4.2, the total power plant is set to 1 MW.

However, the generalisation of this function, when considering all the different types of energy converters, is not straightforward. To this end, the values of $c_{farm}$ for plants that are composed by the devices (i) to (viii), defined in Section 4.2, are computed and averaged. After operating and rearranging, the generalised total cost function, $c_{farm,g}$ reads:

$$c_{farm,g} = 1.5d^3 + 34624.31d + 196.96l + 22500. \quad (14)$$

Eq. (14) constitutes a generalised expression, which can be applied to any coastal area, so as to obtain an estimated assessment of CAPEX, based on the water depth and shoreline distance of a specific location. The geospatial cost penalty function, $C_{gp}$, can be easily obtained as:

$$C_{gp} = 1 - \frac{c_{farm,g}}{c_{farm,g,ref}}, \quad (15)$$

where $c_{farm,g,ref}$ stands for a reference value (Eq. (14)) within the coastal area of interest, or a threshold value beyond which hydrokinetic energy conversion is not feasible (corresponding to a limiting values of $h$ and $l$). Based on previous analyses of hydrokinetic energy projects in coastal areas [64], $c_{farm,g,ref}$ is defined for $h = 50$ m and $l = 7.5$ km.

The representation of Eq. (15) for a generic domain up to 7.5 km distance from shoreline and 50 m water depth ($c_{farm,g,ref}$) is shown in Fig. 7. As can be observed, water depth has a more important role as CAPEX driver than shoreline distance resulting from the cubic term in Eq. (14).

The results of application of the cost penalty function, $C_{gp}$, to the Shannon Estuary is plotted in Fig. 8. As is apparent, the results show an excellent correlation with the coastal configuration of the estuary. In effect, values of roughly 0.4–0.6 within the central channel of the inner and middle estuary are found, approx. 0.9 in the nearest shoreline areas (virtually not penalised due to their reduced depth and distance to the coast) and plummeting to a mere 0.2 in the surroundings of the mouth (larger water depths and distance to coast). The resulting mean and maximum values of the cost penalty function, $C_{gp,mean}$, $C_{gp,\max}$, respectively, in the areas of interest (Areas I to VII) are provided in Table 6.

The area with the highest costs is Area V ($C_{gp,mean} = 0.64$), closely followed by Area I ($C_{gp,mean} = 0.67$) and Area III ($C_{gp,mean} = 0.68$), at some distance by Area II ($C_{gp,mean} = 0.71$), Area VI ($C_{gp,mean} = 0.71$) and Area IV ($C_{gp,mean} = 0.76$), and finally by Area VII ($C_{gp,mean} = 0.82$) with the lowest costs. However, as in the case of the exploitable resource analysis, and resulting from the large extension of these areas, the costs of the installation of a hydrokinetic farm significantly differ within each them, with a mean variation (mean variation between $C_{gp,mean}$ and $C_{gp,\max}$) of 24%, which in the case of Area V and Area I attains 39% and 33%, respectively. These variations may significantly alter the delimitation of the best areas for installing a hydrokinetic farm, and they have to be considered in the decision-making process.

## 5. Water use penalty function ($U_{gp}$)

Coastal regions and, in particular, estuaries are usually areas of a high environmental value, which in turn produce an intense socioeconomic activity. Thus, the following step for the application of the IHE index is to assess the compatibility between hydrokinetic energy exploitation and the marine uses with which it may coexist. To this end, a water use penalty function, $U_{gp}$, is defined and applied to the Shannon Estuary. This function is developed as followed.

First, the marine uses and their characteristics (area occupied, intensity of the activity, etc.), taking place in a coastal region, must be identified. As was previously introduced, they can be categorised into: (i) socioeconomic activities and (ii) environmental uses. Socioeconomic

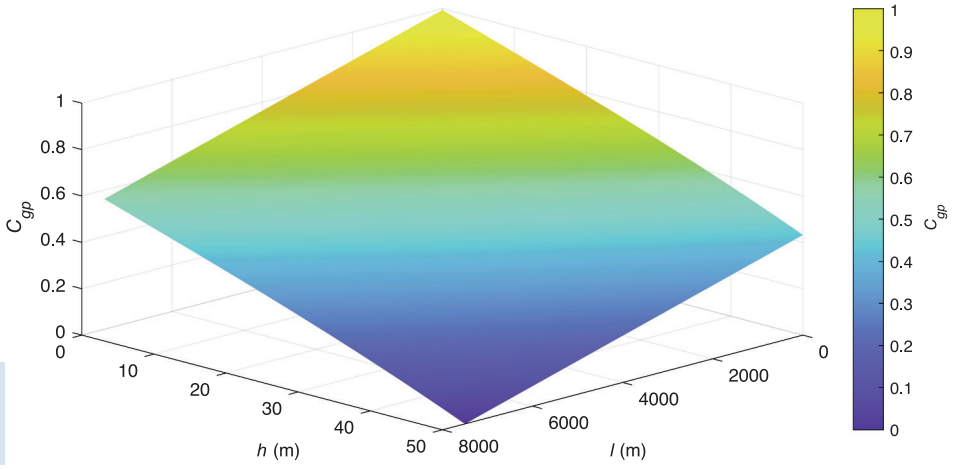


**Fig. 7.** Graphical representation of the geospatial cost penalty function, $C_{gp}$ (Eq. (15)) as function of water depth, $h$, and shoreline distance, $l$.

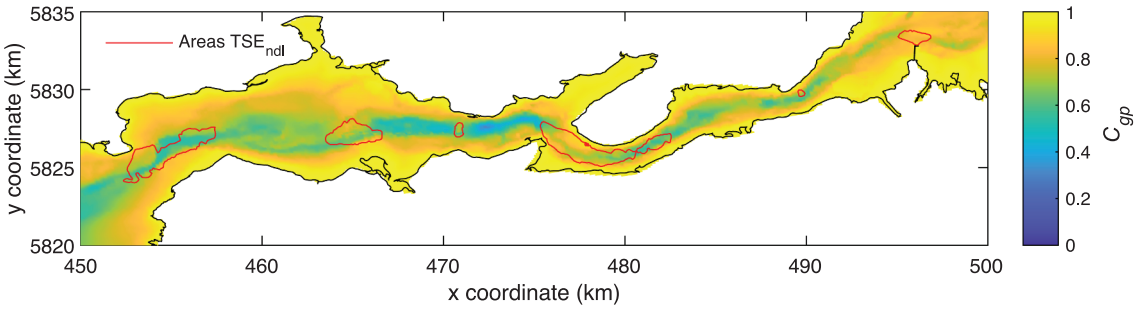


**Fig. 8.** Spatial distribution of $C_{gp}$ throughout the Shannon Estuary.

**Table 6**
Characteristic values of $C_{gp}$ in the areas of potential interest.

| Area | $C_{gp,mean}$ | $C_{gp,max}$ |
|---|---|---|
| I | 0.67 | 0.89 |
| II | 0.71 | 0.90 |
| III | 0.68 | 0.73 |
| IV | 0.76 | 0.96 |
| V | 0.64 | 0.89 |
| VI | 0.71 | 0.81 |
| VII | 0.82 | 0.98 |

activities can be defined as those leading to a straightforward economic or social profit. On the other hand, environmental uses correspond with areas with specific characteristics that constitute the natural habitat for many different wildlife. The socioeconomic marine activities that are considered in this work are aquaculture, shellfish, and navigation. Regarding environmental uses, Special Areas of Conservation (SACs) and Special Protection Areas (SPAs) are analysed.

Next, a quantitative approach to assessing the coexistence of these marine uses, either socioeconomic or environmental, and hydrokinetic energy exploitation is proposed. The method resorts to the definition of the penalty function $U_{gp}$ whose values range between 0 (totally restricted i.e., no coexistence) and 1 (no restrictions, i.e., full coexistence), with intermediate values that are adapted to the specific characteristics of each marine use [65], meaning a lower value of $U_{gp}$ and a higher restriction. The values for the different types of marine uses are defined as follows.

Aquaculture farming is subclassified into extensive or intensive areas. Extensive areas represent large zones that are suitable for the installation of aquaculture farms, whereas intensive areas stand for specific existing facilities, or areas that are legally delimited for this use. Values of $U_{gp} = 0.3$ (high restriction) and $U_{gp} = 0.6$ (medium restriction) are set for intensive and extensive aquaculture farming, respectively. In the case of shellfish exploitation, it constitutes an intensive activity by definition, and therefore a value of 0.3 (high restriction) is retained with some exceptions, such as areas that are legally delimited for this use and that are, considering their particular characteristics, unsuitable for energy exploitation ($U_{gp} = 0$).

As regards navigation, it is necessary to distinguish between the presence of marine traffic of a given intensity and the delimitation of navigation channels. Both aspects are considered in this work. For the analysis of the intensity of the marine traffic, the vessel density concept, $v_d$, is used, which is computed in terms of annual hours per square kilometre of water surface occupied by vessels, based on EMODnet Human Activities data [66]. After a thorough data analysis of representative European ports [67–69], a vessel density threshold of 50 hkm$^{-2}$ is defined, meaning that areas with traffic density over this value are considered as non-suitable for energy exploitation and, therefore, penalised with a value of $U_{gp} = 0$ (totally restricted, i.e., no coexistence). Areas with traffic density figures under this threshold are considered as appropriate, but with a restriction. This restriction is computed by linearly interpolating the limits of the function ($U_{gp} = 0$ for $v_d = 50$ hkm$^{-2}$ and $U_{gp} = 1$ for $v_d = 0$ hkm$^{-2}$), according to the geospatial distribution of $v_d$ figures. Finally, the water surface that is occupied by a navigation channel, which is legally defined, is considered as totally restricted ($U_{gp} = 0$). In the case of oversized navigation channels, these areas could be considered as partially restricted, by defining new limits according to the specific characteristics of each coastal region. With respect to the environmental uses, SACs and SPAs are assumed to be extensive areas. However, these areas occupy the whole estuary and, overall, impose a more limited restriction than in the case of an extensive economic activity (e.g., aquaculture). In these areas a value of $U_{gp} = 0.9$ (low restriction) is considered. In the case of areas with a special environmental value, in addition to SACs or SPAs, other values of $U_{gp}$ should be considered, while attending to their specific characteristics and the resulting restrictions (medium, high, or total restriction).

Finally, in the case of the presence of various marine uses in the same area, the most restrictive value of $U_{gp}$ is retained. Please note that the analysis of the specific impacts of hydrokinetic energy operation on the flow regime and its interactions with the surrounding water uses are out of the scope of this work, and should be analysed for each specific hydrokinetic energy project.

Fig. 9 shows the spatial distribution of the different abovementioned marine uses within the Shannon Estuary. It can be observed that extensive areas are occupied by aquaculture farming, or they are appropriate for this purpose. In addition, virtually all the extension of this estuary is used for navigation, with a legally delimited navigation area, occupying the whole main channel and various approaches to the nearby coast. Finally, environmental uses correspond, as previously stated, with areas occupying a much larger extension than the socioeconomic activity and, overall, not imposing a significant restriction for hydrokinetic energy operation. The combination of all the aforementioned uses provides a global picture of the potential available areas, and their socioeconomic and environmental restrictions for hydrokinetic energy conversion in this estuary.

A clearer understanding of the most suited areas from a socioeconomic and environmental standpoint is provided by computing the previously defined water use penalty function, $U_{gp}$, for the different socioeconomic and environmental uses (Fig. 10), and their combination, to obtain an overall value of $U_{gp}$ (Fig. 11). Based on the results obtained, the extension of the areas that are identified as of interest can be significantly reduced by considering only the surface without total restriction ($U_{gp} > 0$). The resulting mean and maximum values of the

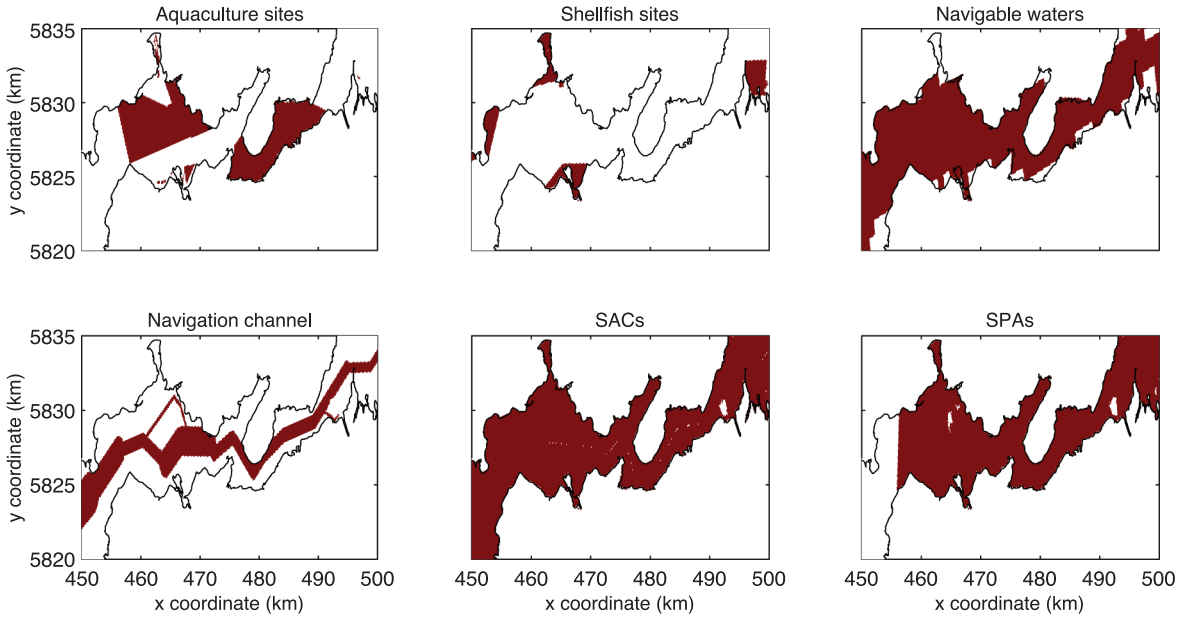


**Fig. 9.** Spatial distribution of marine uses (in red) within the Shannon Estuary.

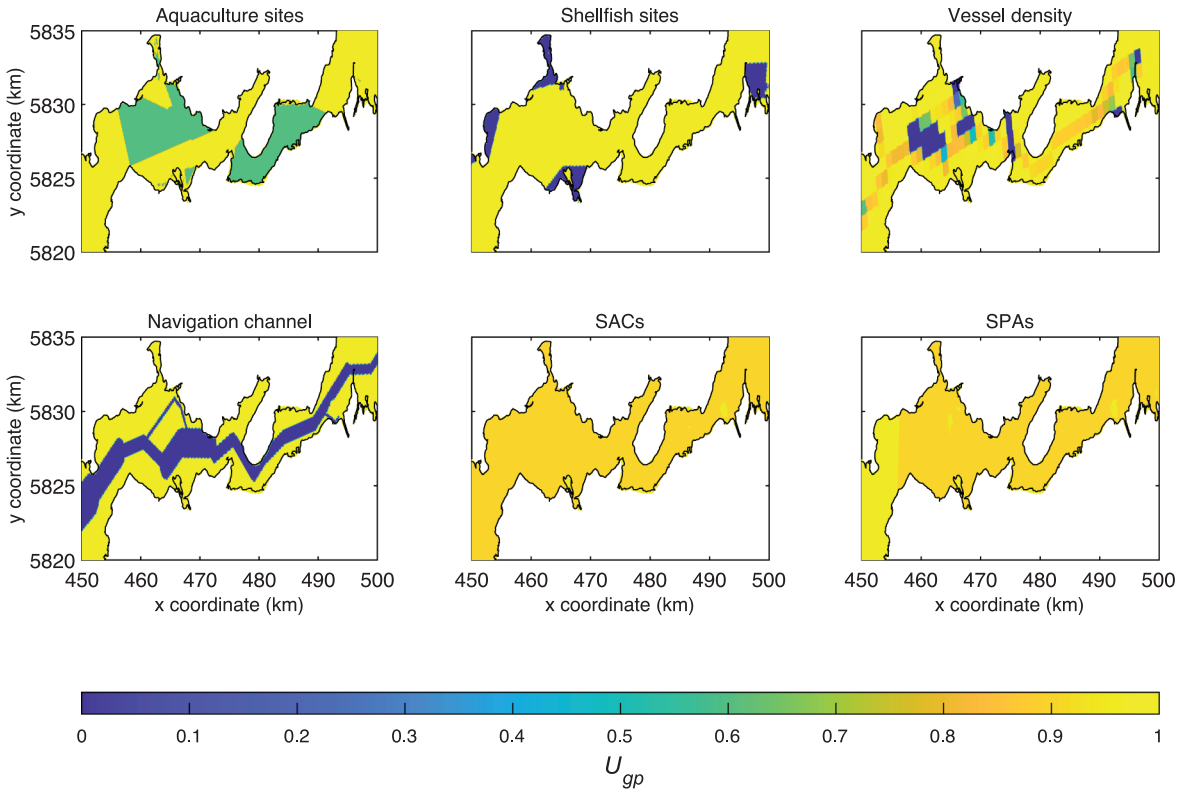


**Fig. 10.** Representation of $U_{gp}$ for the different marine uses throughout the Shannon Estuary.

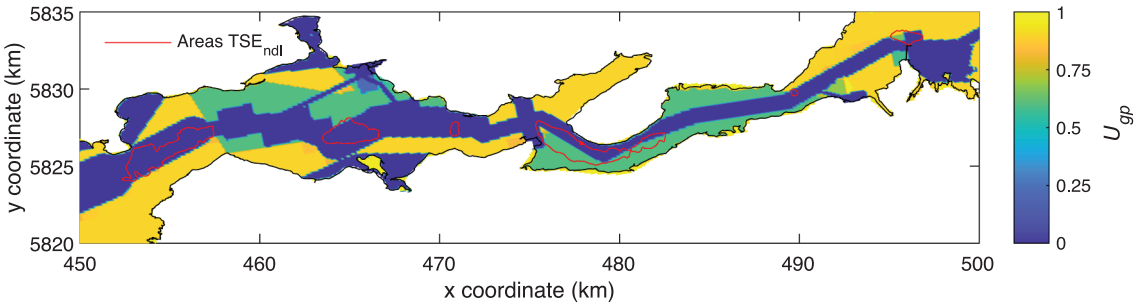


**Fig. 11.** Spatial distribution of $U_{gp}$ throughout the Shannon Estuary.

**Table 7**
Characteristic values of $U_{gp}$ in areas of potential interest.

| Area | $U_{gp,mean}$ | $U_{gp,\max}$ |
|---|---|---|
| I ($U_{gp} > 0$) | 0.88 | 0.90 |
| II ($U_{gp} > 0$) | 0.60 | 0.60 |
| IV ($U_{gp} > 0$) | 0.61 | 0.90 |
| V ($U_{gp} > 0$) | 0.60 | 0.60 |
| VII ($U_{gp} > 0$) | 0.74 | 0.90 |

penalty function, $U_{gp,mean}$ and $U_{gp,\max}$, respectively, for the new delimited surface (i.e., the surface delimited by $U_{gp} > 0$) of Areas I to VII is provided in Table 7.

The area that is compatible with hydrokinetic energy operation and presents fewer socioeconomic and environmental restrictions is Area I ($U_{gp,mean} = 0.88$), followed by Area VII ($U_{gp,mean} = 0.74$) and finally, with similar values, Area IV ($U_{gp,mean} = 0.61$), Area V ($U_{gp,mean} = 0.60$) and Area II ($U_{gp,mean} = 0.60$). Areas III and VI are not suitable for energy conversion. In contrast with the resource and costs results, the variations of $U_{gp}$ within each area are less pronounced, with the exception of Area IV.

## 6. Integration of the results

The integration of the different terms considered in the proposed index leads to the geospatial distribution of the IHE index in the study region (Eq. (1)). Its physical interpretation, as was previously introduced, is straightforward: the higher the IHE index, the better the site for hydrokinetic energy exploitation, with figures above 1 indicating suitability for hydrokinetic energy exploitation. Therefore, IHE = 1 would represent a suitability threshold indicating a site with the bare minimum amount of exploitable energy (HE = 1), and without any penalisation in terms of costs derived from its coastal configuration ($C_{gp} = 1$) or from the surrounding socioeconomic or environmental uses ($U_{gp} = 1$).

Fig. 12 shows the spatial distribution of the IHE index throughout the Shannon Estuary. The areas with IHE>1 are delimited along, with the areas that are identified as of interest in previous studies (and analysed in the preceding sections). The mean and maximum values of the IHE index, IHE$_{mean}$, and IHE$_{max}$, respectively, for the new delimited areas are provided in Table 8, along with their main characteristics.

The computation of the IHE index for the Shannon Estuary allows the identification of six areas for hydrokinetic energy exploitation (Area I$_{IHE}$ to Area VI$_{IHE}$) which significantly differ from previous analyses. The most suited area is Area IV$_{IHE}$, close to Tarbert, as in the case of previous studies, but now occupying a smaller area within the previously identified Area IV, with lower available resource, and lower costs and fewer restrictions for hydrokinetic energy operation. The other newly identified areas do not correspond with those that were previously identified. Instead, the new areas are close to the previous areas, occupying a more limited surface with, again, somewhat of a lower resource, but with lower costs and fewer restrictions for energy conversion.

The results of IHE index show that Area IV$_{IHE}$ is of high interest for energy operation (IHE$_{mean}$ of category III with locations in category IV), whereas Area I$_{IHE}$, and Area III$_{IHE}$, although with less potential, are also of significant interest (IHE$_{mean}$ of category II with locations in category III). Finally, the remaining areas, Area II$_{IHE}$, Area V$_{IHE}$, and Area VI$_{IHE}$, could be of interest, but with a more limited potential (IHE$_{mean}$ close to 1).

**Table 8**
Characteristic values of the IHE index in new areas of interest and their main characteristics.

| Area | IHE$_{mean}$ | IHE$_{max}$ | Surface (km$^2$) | Mean depth (m) | Seabed type |
|---|---|---|---|---|---|
| I$_{IHE}$ | 1.31 | 2.28 | 1.64 | 7.40 | Rock |
| II$_{IHE,N}$ | 1.19 | 1.67 | 0.21 | 7.65 | Rock |
| II$_{IHE,S}$ | 1.66 | 2.74 | 0.35 | 5.43 | Rock |
| IV$_{IHE}$ | 2.10 | 4.15 | 2.99 | 16.83 | Mixed sediment |
| V$_{IHE}$ | 1.04 | 1.28 | 0.28 | 22.73 | Mixed sediment |
| VI$_{IHE}$ | 1.03 | 1.16 | 0.47 | 17.75 | Sand |

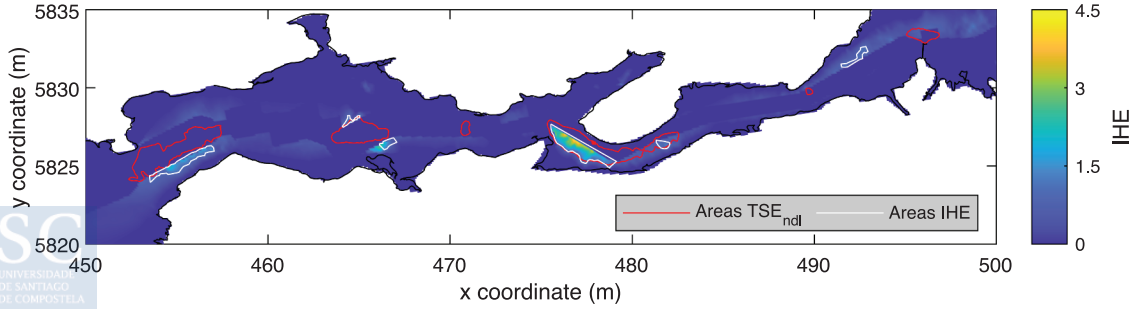


**Fig. 12.** Spatial distribution of the IHE index and the resulting areas of interest (Areas IHE), along with the previously identified areas (Areas TSE$_{ndl}$).

## 7. Conclusions

A comprehensive methodology was developed for identifying the best locations for hydrokinetic energy operation in a coastal region, The proposed methodology considers not only the resource, but also the costs of installation, along with the socioeconomic activities and environmental aspects. The combination of these aspects leads to the definition of the novel IHE index.

The methodology is composed of four steps. First, the distribution of the energy resource is investigated through the hydrokinetic energy resource index, HE index, which characterises the exploitable resource (rather than the total available resource) by considering the velocity ranges of operation of the current available HECs. Secondly, the geospatial cost penalty function, $C_{gp}$, is used to determine the costs of installation of a hydrokinetic farm, resulting from the coastal configuration, based on the water depth and shoreline distance. Then, the geospatial water use penalty function, $U_{gp}$, assesses the suitability of the coexistence of hydrokinetic energy operation with the socioeconomic activity and environmental aspects. From a resource standpoint, HE values higher than 1 indicate suitability for hydrokinetic energy operation (other restrictions are not considered at this point). Regarding the penalty functions, $C_{gp}$ and $U_{gp}$, they range from 1 (no restriction) to 0 (total restriction). In the final step, the geospatial distribution of the IHE index is obtained by integrating (multiplying) the aforementioned terms (HE, $C_{gp}$ and $U_{gp}$). As a result, the higher the IHE index, the better the site for hydrokinetic energy exploitation, with values above 1 indicating suitability for hydrokinetic energy exploitation. For a better interpretation of the results, different thresholds of the IHE index are established based on a thorough analysis of the available and exploitable resource in coastal regions of interest for hydrokinetic energy conversion throughout the world, leading to a total of five categories (category I to category V, from lower to higher interest).

The IHE index is applied to the Shannon Estuary to assess the potential of the areas identified in previous studies as of interest for energy conversion. A total of six areas (Area $I_{IHE}$ to Area $VI_{IHE}$) are identified with an IHE index higher than 1 and, therefore, of interest for energy conversion, which differ from those selected in previous studies. The most suitable is Area $IV_{IHE}$ (a mean IHE of category III with locations in category IV), close to Tarbert, as in the case of previous studies, but now occupying a smaller surface with somewhat lower resource and fewer restrictions for energy conversion. The remaining delimited areas do not correspond with those in previous studies.

The results show the capability of the IHE index for selecting the most appropriate locations for energy conversion in a coastal region, reducing the uncertainties in the early stages of the planning of MRE conversion. The final design of the farm configuration in subsequent stages would require a detailed cost analysis of the selected HEC-site combinations.

## Declaration of Competing Interest

The authors declare that they have no known competing financial interests or personal relationships that could have appeared to influence the work reported in this paper.

*Acknowledgements*

This work was supported by the PORTOS project, which is co-financed by the Interreg Atlantic Area Programme, through the European Regional Development Fund [grant number EAPA_784/2018] and 'Axudas para a consolidación e estruturación de unidades de investigación competitivas nas universidades do Sistema Universitario Galego (2020-22)' with reference number ED341B 2020/25.

The authors are also grateful for the support of Science Foundation Ireland and MaREI, the Marine Renewable Energy Centre of Ireland, grant SFI MAREI2_12/RC/2302/P2 Platform RA1b.

During this work I. López was supported by a postdoctoral grant of the 'Programa de Axudas á etapa posdoutoral da Xunta de Galicia' with reference number ED481D 2019/019.

## References

[1] Bhattacharya S, Pennock S, Robertson B, Hanif S, Alam MJE, Bhatnagar D, et al. Timing value of marine renewable energy resources for potential grid applications. Appl Energy 2021;299:117281.
[2] Lange M, Cummins V. Managing stakeholder perception and engagement for marine energy transitions in a decarbonising world. Renew Sustain Energy Rev 2021;152:111740.
[3] Akbari N, Jones D, Arabikhan F. Goal programming models with interval coefficients for the sustainable selection of marine renewable energy projects in the UK. Eur J Oper Res 2021;293(2):748–60.
[4] Penalba M, Aizpurua JI, Martinez-Perurena A. On the definition of a risk index based on long-term metocean data to assist in the design of Marine Renewable Energy systems. Ocean Eng 2021;242:110080.
[5] Alsaleh M, Abdul-Rahim AS. The pathway toward pollution mitigation in EU28 region: Does hydropower growth make a difference? Renewable Energy 2022;185:291–301.
[6] Zhao Y, Xu K, Dong N, Wang H. Projection of climate change impacts on hydropower in the source region of the Yangtze River based on CMIP6. J Hydrol 2022;606:127453.
[7] Sibtain M, Li X, Bashir H, Azam MI. Hydropower exploitation for Pakistan's sustainable development: A SWOT analysis considering current situation, challenges, and prospects. Energy Strategy Reviews 2021;38:100728.
[8] Hunt JD, Nascimento A, Caten CST, Tomé FMC, Schneider PS, Thomazoni ALR, et al. Energy crisis in Brazil: Impact of hydropower reservoir level on the river flow. Energy 2022;239:121927.
[9] Zhang J, Cheng C, Yu S, Wu H, Gao M. Sharing hydropower flexibility in interconnected power systems: A case study for the China Southern power grid. Appl Energy 2021;288:116645.
[10] Carballo R, Iglesias G, Castro A. Numerical model evaluation of tidal stream energy resources in the Ría de Muros (NW Spain). Renewable Energy 2009;34(6):1517–24.
[11] Brooks DA. The hydrokinetic power resource in a tidal estuary: The Kennebec River of the central Maine coast. Renewable Energy 2011;36(5):1492–501.
[12] Lewis M, McNaughton J, Márquez-Dominguez C, Todeschini G, Togneri M, Masters I, et al. Power variability of tidal-stream energy and implications for electricity supply. Energy 2019;183:1061–74.
[13] Fouz DM, Carballo R, López I, Iglesias G. Tidal stream energy potential in the Shannon Estuary. Renewable Energy 2022;185:61–74.
[14] Fouz DM, Carballo R, Ramos V, Iglesias G. Hydrokinetic energy exploitation under combined river and tidal flow. Renewable Energy 2019;143:558–68.
[15] Iglesias I, Bio A, Bastos L, Avilez-Valente P. Estuarine hydrodynamic patterns and hydrokinetic energy production: The Douro estuary case study. Energy 2021;222:119972.
[16] Khojasteh D, Lewis M, Tavakoli S, Farzadkhoo M, Felder S, Iglesias G, et al. Sea level rise will change estuarine tidal energy: A review. Renew Sustain Energy Rev 2022;156:111855.
[17] Kamal MM, Saini RP. A review on modifications and performance assessment techniques in cross-flow hydrokinetic system. Sustainable Energy Technol Assess 2022;51:101933.
[18] Khan MJ, Bhuyan G, Iqbal MT, Quaicoe JE. Hydrokinetic energy conversion systems and assessment of horizontal and vertical axis turbines for river and tidal applications: A technology status review. Appl Energy 2009;86(10):1823–35.
[19] Sánchez M, Carballo R, Ramos V, Iglesias G. Energy production from tidal currents in an estuary: A comparative study of floating and bottom-fixed turbines. Energy 2014;77:802–11.
[20] Ramos V, Carballo R, Álvarez M, Sánchez M, Iglesias G. A port towards energy self-sufficiency using tidal stream power. Energy 2014;71:432–44.
[21] Iglesias G, Sánchez M, Carballo R, Fernández H. The TSE index – A new tool for selecting tidal stream sites in depth-limited regions. Renewable Energy 2012;48:350–7.
[22] Yang Z, Wang T, Branch R, Xiao Z, Deb M. Tidal stream energy resource characterization in the Salish Sea. Renewable Energy 2021;172:188–208.
[23] Alvarez EA, Rico-Secades M, Suárez DF, Gutiérrez-Trashorras AJ, Fernández-Francos J. Obtaining energy from tidal microturbines: A practical example in the Nalón River. Appl Energy 2016;183:100–12.
[24] Mejia-Olivares CJ, Haigh ID, Wells NC, Coles DS, Lewis MJ, Neill SP. Tidal-stream energy resource characterization for the Gulf of California. México Energy 2018;156:481–91.
[25] Robins PE, Neill SP, Lewis MJ, Ward SL. Characterising the spatial and temporal variability of the tidal-stream energy resource over the northwest European shelf seas. Appl Energy 2015;147:510–22.
[26] Vazquez A, Iglesias G. A holistic method for selecting tidal stream energy hotspots under technical, economic and functional constraints. Energy Convers Manage 2016;117:420–30.
[27] Vazquez A, Iglesias G. Capital costs in tidal stream energy projects – A spatial approach. Energy 2016;107:215–26.
[28] Lewis M, O'Hara Murray R, Fredriksson S, Maskell J, de Fockert A, Neill SP, et al. A standardised tidal-stream power curve, optimised for the global resource. Renewable Energy 2021;170:1308–23.

[29] López A, Morán JL, Núñez LR, Somolinos JA. Study of a cost model of tidal energy farms in early design phases with parametrization and numerical values. Application to a second-generation device. Renew Sustain Energy Rev 2020;117:109497.
[30] Goss ZL, Coles DS, Kramer SC, Piggott MD. Efficient economic optimisation of large-scale tidal stream arrays. Appl Energy 2021;295:116975.
[31] SIFP Steering Group. Strategic Integrated Framework Plan (SIFP) for the Shannon Estuary - An inter-jurisdictional land and marine based framework to guide the future developments and management of the Shannon Estuary. 2013.
[32] Blunden LS, Bahaj AS. Initial evaluation of tidal stream energy resources at Portland Bill. UK Renewable Energy 2006;31(2):121–32.
[33] Iglesias G, Carballo R. Effects of high winds on the circulation of the using a mixed open boundary condition: the Ría de Muros. Spain Environmental Modelling & Software 2010;25(4):455–66.
[34] Carballo R, Iglesias G, Castro A. Residual circulation in the Ría de Muros (NW Spain): A 3D numerical model study. J Mar Syst 2009;75(1-2):116–30.
[35] Iglesias G, Carballo R. Seasonality of the circulation in the Ría de Muros (NW Spain). J Mar Syst 2009;78(1):94–108.
[36] Álvarez M, Carballo R, Ramos V, Iglesias G. An integrated approach for the planning of dredging operations in estuaries. Ocean Eng 2017;140:73–83.
[37] Álvarez M, Ramos V, Carballo R, Arean N, Torres M, Iglesias G. The influence of dredging for locating a tidal stream energy farm. Renewable Energy 2020;146:242–53.
[38] Des M, deCastro M, Sousa MC, Dias JM, Gómez-Gesteira M. Hydrodynamics of river plume intrusion into an adjacent estuary: The Minho River and Ria de Vigo. J Mar Syst 2019;189:87–97.
[39] Iglesias G, Carballo R, Castro A. Baroclinic modelling and analysis of tide- and wind-induced circulation in the Ría de Muros (NW Spain). J Mar Syst 2008;74(1-2):475–84.
[40] González CJ, Reyes E, Álvarez Ó, Izquierdo A, Bruno M, Mañanes R. Surface currents and transport processes in the Strait of Gibraltar: Implications for modeling and management of pollutant spills. Ocean Coast Manage 2019;179:104869.
[41] Ramos V, Iglesias G. Performance assessment of Tidal Stream Turbines: A parametric approach. Energy Convers Manage 2013;69:49–57.
[42] Deltares. User Manual Delft3D-FLOW. Deltares ed. Delft, The Netherlands, 2010.
[43] O'Toole R, Judge M, Sacchetti F, Furey T, Mac Craith E, Sheehan K et al. Mapping Ireland's coastal, shelf and deep-water environments using illustrative case studies to highlight the impact of seabed mapping on the generation of blue knowledge. Geological Society, London, Special Publications 2020;505:SP505-2019-207.
[44] Le Provost C, Bennett AF, Cartwright DE. Ocean tides for and from Topex/Poseidon. Science 1995;267(5198):639–42.
[45] Egbert GD, Bennett AF, Foreman MGG. Topex/Poseidon tides estimated using a global inverse model. J Geophys Res 1994;99:24821–52.
[46] Chowdhury MS, Rahman KS, Selvanathan V, Nuthammachot N, Suklueng M, Mostafaeipour A, et al. Current trends and prospects of tidal energy technology. Environ Dev Sustainability 2021;23(6):8179–94.
[47] Segura E, Morales R, Somolinos JA, López A. Techno-economic challenges of tidal energy conversion systems: Current status and trends. Renew Sustain Energy Rev 2017;77:536–50.
[48] Ramos V, Ringwood JV. Implementation and evaluation of the International Electrotechnical Commission specification for tidal stream energy resource assessment: A case study. Energy Convers Manage 2016;127:66–79.
[49] Neill SP, Hashemi MR, Lewis MJ. The role of tidal asymmetry in characterizing the tidal energy resource of Orkney. Renewable Energy 2014;68:337–50.
[50] Thiébot J, Guillou S, Droniou E. Influence of the 18.6-year lunar nodal cycle on the tidal resource of the Alderney Race, France. Appl Ocean Res 2020;97:102107.
[51] O'Rourke F, Boyle F, Reynolds A. Ireland's tidal energy resource; An assessment of a site in the Bulls Mouth and the Shannon Estuary using measured data. Energy Convers Manage 2014;87:726–34.
[52] Marsh P, Penesis I, Nader JR, Cossu R, Auguste C, Osman P, et al. Tidal current resource assessment and study of turbine extraction effects in Banks Strait. Australia Renewable Energy 2021;180:1451–64.
[53] Liu X, Chen Z, Si Y, Qian P, Wu He, Cui L, et al. A review of tidal current energy resource assessment in China. Renew Sustain Energy Rev 2021;145:111012.
[54] Dalton G, Allan G, Beaumont N, Georgakaki A, Hacking N, Hooper T, et al. Economic and socio-economic assessment methods for ocean renewable energy: Public and private perspectives. Renew Sustain Energy Rev 2015;45:850–78.
[55] Allan G, Gilmartin M, McGregor P, Swales K. Levelised costs of Wave and Tidal energy in the UK: Cost competitiveness and the importance of "banded" Renewables Obligation Certificates. Energy Policy 2011;39(1):23–39.
[56] Serrano González J, Burgos Payán M, Riquelme Santos JM. An improved evolutive algorithm for large offshore wind farm optimum turbines layout. 2011 IEEE Trondheim PowerTech 2011:1–6.
[57] Astariz S, Iglesias G. Co-located wind and wave energy farms: Uniformly distributed arrays. Energy 2016;113:497–508.
[58] Tunio IA, Shah MA, Hussain T, Harijan K, Mirjat NH, Memon AH. Investigation of duct augmented system effect on the overall performance of straight blade Darrieus hydrokinetic turbine. Renewable Energy 2020;153:143–54.
[59] ed-Dín Fertahi S, Bouhal T, Rajad O, Kousksou T, Arid A, El Rhafiki T, et al. CFD performance enhancement of a low cut-in speed current Vertical Tidal Turbine through the nested hybridization of Savonius and Darrieus. Energy Convers Manage 2018;169:266–78.
[60] Marsh P, Penesis I, Nader JR, Cossu R, Auguste C, Osman P, et al. Tidal current resource assessment and study of turbine extraction effects in Banks Strait, Australia. Renewable Energy 2021;180:1451–64.
[61] Mestres M, Griñó M, Sierra JP, Mösso C. Analysis of the optimal deployment location for tidal energy converters in the mesotidal Ria de Vigo (NW Spain). Energy 2016;115:1179–87.
[62] Pudur R, Gao S. Performance Analysis of Savonius Rotor Based Hydropower Generation Scheme with Electronic Load Controller. Journal of Renewable Energy 2016;2016:1–7.
[63] Fraenkel P. Practical tidal turbine design considerations: a review of technical alternatives and key design decisions leading to the development of the SeaGen 12 MW tidal turbine 2010;19:1–19.
[64] Carballo R, López I, Areán N, Fouz DM. PORTOS Deliverable D5.6 - Technology-site selection based on high-resolution performance analysis. Universidade de Santiago de Compostela 2020.
[65] Galparsoro I, Korta M, Subirana I, Borja Á, Menchaca I, Solaun O, et al. A new framework and tool for ecological risk assessment of wave energy converters projects. Renew Sustain Energy Rev 2021;151:111539.
[66] Falco L, Pittito A, Adnams W, Earwaker N, Greidanus H. Eu Vessel density map. Detailed method 2019.
[67] Fiorini M, Capata A, Bloisi DD. AIS Data Visualization for Maritime Spatial Planning (MSP). International Journal of e-Navigation and Maritime Economy 2016;5:45–60.
[68] Vespe M, Gibin M, Alessandrini A, Natale F, Mazzarella F, Osio GC. Mapping EU fishing activities using ship tracking data. Mapping EU fishing activities using ship tracking data 2016;12(sup1):520–5.
[69] Pallotta G, Vespe M, Bryan K. Vessel Pattern Knowledge Discovery from AIS Data: A Framework for Anomaly Detection and Route Prediction. Entropy 2013;15(12):2218–45.

# 6 A METHODOLOGY FOR COST-EFFECTIVE ANALYSIS OF HYDROKINETIC ENERGY PROJECTS

This chapter corresponds with the following research article:


- **Tittle:** A methodology for cost-effective analysis of hydrokinetic energy projects
- **Journal:** Energy, Volume 282, 1 November 2023, 128373
- **Editorial:** Elsevier
- **ISSN:** 1873-6785
- **DOI:** https://doi.org/10.1016/j.energy.2023.128373


- **Authors:** D.M. Fouz[a], R. Carballo[a], I. López[a], X.P. González[a], G. Iglesias [b, c]
- **Institutions:**
  - [a]Departamento de Enxeñaría Agroforestal, Universidade de Santiago de Compostela, EPSE, Rúa Benigno Ledo s/n, 27002, Lugo, Spain
  - [b]School of Engineering and Architecture & MaREI, Environmental Research Institute, University College Cork, Ireland
  - [c]School of Engineering, Computing and Mathematics, University of Plymouth, UK

- **CRediT authorship contribution statement:**
  - **D.M. Fouz:** Conceptualization, Methodology, Investigation, Formal analysis, Visualization, Writing – original draft
  - **R. Carballo:** Conceptualization, Methodology, Writing – review & editing, Supervision, Project administration, Funding acquisition
  - **I. López:** Methodology, Formal analysis, Writing – review & editing, Supervision
  - **X.P. González:** Methodology, Formal analysis, Visualization, Supervision
  - **G. Iglesias:** Conceptualization, Methodology, Writing – review & editing, Supervision
- **Indicators (2023):** Impact factor, IF = 9.000; First quartile (Q1; 24/170) of this category (*Energy & Fuels*)

Energy 282 (2023) 128373

Contents lists available at ScienceDirect

Energy

journal homepage: www.elsevier.com/locate/energy

# A methodology for cost-effective analysis of hydrokinetic energy projects

D.M. Fouz [a], R. Carballo [a,*], I. López [a], X.P. González [a], G. Iglesias [b,c]

[a] Departamento de Enxeñaría Agroforestal, Universidade de Santiago de Compostela, EPSE, Rúa Benigno Ledo s/n, 27002, Lugo, Spain
[b] School of Engineering and Architecture & MaREI, Environmental Research Institute, University College Cork, Ireland
[c] School of Engineering, Computing and Mathematics, University of Plymouth, UK

ARTICLE INFO

Handling Editor: Soteris Kalogirou

*Keywords:*
Tidal stream
Tidal energy
Marine renewable energy
Offshore renewable energy
Cost model
Energy production model

ABSTRACT

The cost-effective analysis (CEA) of hydrokinetic farms is typically based on simplistic assumptions regarding the performance and cost structure of hydrokinetic energy converters (HECs) and, in consequence, may lead to ill-informed decision-making. In this work, a novel approach to selecting the most appropriate combination of HEC and site within a coastal area is developed, with the accurate computation of the CEA parameters as the cornerstone. The approach, which is illustrated through a case study in the Shannon Estuary (W Ireland), encompasses four models, namely: (i) HEC-site selection model, (ii) energy production model, (iii) CAPEX model, and (iv) OPEX model. By avoiding simplistic assumptions, the proposed approach improves on current procedures and enables developers to accurately compute any cost-effective parameter of interest. In particular, operation and maintenance costs are considered, along with economies of scale, which are typically disregarded in existing procedures. Beyond the interest of the results of the Shannon case study, the approach can be implemented in other regions with potential for hydrokinetic energy conversion.

## 1. Introduction

Coastal areas have supported human activity throughout history in many different ways. In the socioeconomic sphere, these areas have been traditionally used for transport and food supply [1,2]. As a result of the increased public awareness of environmental issues, protected or conservation areas (e.g., Natura 2000) have emerged alongside traditional socioeconomic activities, which have grown significantly (e.g., tourism or heritage) [3,4]. This is also the case of marine renewable energy exploitation, which is posited as a new, promising coastal use [5–12].

Within the different types of marine renewable energies, hydrokinetic energy, primarily resulting from the tide (e.g. Ref. [13]), reinforced in some coastal areas by river discharges and density gradients (e.g. Ref. [14]), is expected to attain a commercial stage in the forthcoming years [15]. The exploitation of this resource is carried out by means of hydrokinetic energy converters (HECs), of which different types exist with varying degrees of technological maturity. Turbine-based solutions, and in particular horizontal axis turbines, are considered to be approaching the commercial stage [16–18]. The state-of-the-art third-generation HECs are designed to operate with relatively low cut-in velocities (i.e., 0.7–1.0 m/s) [19,20].

As a consequence of this heterogeneity in technological maturity, reliable metrics should be developed to accurately assess the technical and economic viability of hydrokinetic energy projects in decision-making processes. As a first approach to technical viability, the Technology Readiness Level (TRL) is usually mentioned as a standard or a metric-based model with several applications in R&D activities, such as the development of HECs [21,22]. However, in order to reduce the uncertainties of hydrokinetic energy projects and ensure their economic viability, the TRL model should be complemented by a cost-effective analysis (CEA), which provides metrics (e.g., LCOE, NPV, IRR) describing the techno-economic performance of technologies under development or proposed projects [23].

The estimation of CEA parameters is usually based on simplified methods, considering either their spatial distribution or, in a simpler approach, delocalised approximations [24]. The main weakness of these approaches is their unrealistic cost structure, which may produce misleading results. In the case of tidal energy projects, the resulting figures typically lack accuracy, which may be seen as a direct consequence of the limitations of the procedure applied, namely [25]: (i) performance computation based on limited and non-reliable HEC data, (ii) consideration of the different economic aspects in terms of expected percentage over the total investment, or (iii) disregard for specific

* Corresponding author.
*E-mail address:* rodrigo.carballo@usc.es (R. Carballo).

https://doi.org/10.1016/j.energy.2023.128373
Received 1 February 2023; Received in revised form 11 May 2023; Accepted 7 July 2023
Available online 15 July 2023

aspects, which contributes significantly to real costs. Another aspect closely related to the computation of CEA parameters is the selection of the sites or areas to be subject to this analysis. This selection is typically based merely on the available energy resource [26–28]. In a few cases, a reduced number of geomorphological parameters (e.g., water depth) have also been taken into account [29,30]. Notwithstanding the interest of these methods for a preliminary selection of coastal areas, additional information (e.g., socioeconomic) needs to be considered in more advanced stages. In effect, an appropriate site-selection should also consider aspects such as the coexistence of the energy exploitation with other marine uses, or the site-specific costs of installation and operation [31,32].

In this context, it is important to remark that miscalculated CEA figures may result from not accurately considering specific aspects of cost analysis, such as the operation costs, or from neglecting potential cost reductions through economies of scale [33]. In the case of large coastal areas, the application of the current procedures could result in overly homogeneous CEA figures, as the spatial variability of the energy resource over short distances is not usually accounted for in the computation of these metrics (low to mid resolution energy resource models) [34].

In this research, a novel approach for accurately computing the CEA parameters of hydrokinetic energy projects is developed, leading to a significant improvement with respect to currently available methods. The proposed approach addresses the major difficulties and uncertainties when computing the main aspects affecting the CEA of hydrokinetic energy farms, avoiding simplistic and unreliable assumptions, and improving on current procedures. Thus, the implementation of this novel procedure will lead to the selection of the optimum HEC-site combination for installing a hydrokinetic farm in a coastal area.

The novelty of this work lies in the consideration of the following aspects: (i) the energy production, which is assessed by combining high-resolution numerical modelling results with spatial analysis algorithms; (ii) the installation costs, whose breakdown in terms of unitary costs is thoroughly analysed, including the effects of economies of scale; (iii) the operation costs, which are computed by means of an ad hoc Operation and Maintenance (O&M) model, including several operational parameters and strategies.

Other aspects dealing with the energy transmission or storage related to the specific characteristics of the electrical grid, or the integration with short-term energy storage to help balance the local demand with the varying supply typical of hydrokinetic and tidal farms, are outside the scope of the present work and require specific research [35–40].

The proposed procedure to develop the CEA of hydrokinetic energy projects is applied, for the first time, to a specific case study in the Shannon Estuary (W Ireland) (Fig. 1) and computed in terms of Levelized Cost of Energy (LCOE). Preliminary studies have recognised the potential of this area for hydrokinetic energy exploitation [41,42]. Previous works fully described the hydrokinetic energy resource in the Shannon Estuary, identifying a number of areas as of particular interest [30]. More recent studies highlighted the energy potential of Tarbert Area in the middle estuary (Figs. 1 and 2) by considering: (i) the exploitable resource, (ii) the costs of installation, and (iii) the socio-economic and environmental pre-existent activities [31,43,44]. The integration of these aspects led to the computation of the Integrated Hydrokinetic Energy (IHE) index and, on this basis, to the delimitation of a large area in the surroundings of Tarbert (≈3 $km^2$) (Fig. 2) with the highest potential, with a value of IHE = 4.15 (being IHE = 1 the suitability threshold for hydrokinetic energy exploitation). In the present work, this region is retained as a case study for defining the best HEC-site combination by applying the proposed procedure.

This paper is structured as follows. In Section 2, a brief overview of the proposed methodology used to compute the CEA is presented. Next, in Section 3, the tools for defining feasible HEC-site combinations are introduced and implemented to the area of interest. Afterwards, the main aspects considered for CEA computation are defined, and the results from its application summarized: (i) energy production (Section 4), (ii) capital expenditures, CAPEX (Section 5), and (iii) operational expenditures, OPEX (Section 6), In Section 7, the integration of results and CEA computation is conducted for the Tarbert Area, and the results compared with available state-of-the-art methodologies. Finally, the major conclusions to this work are depicted in Section 8.

## 2. General description of the procedure

The main objective of this work is to define and apply a new approach to accurately conduct a cost-effective analysis (CEA) of hydrokinetic energy farms, considering all the aspects involved in the process, and thus leading to the identification of the best HEC-site combination within a coastal area.

The proposed approach consists of five steps:

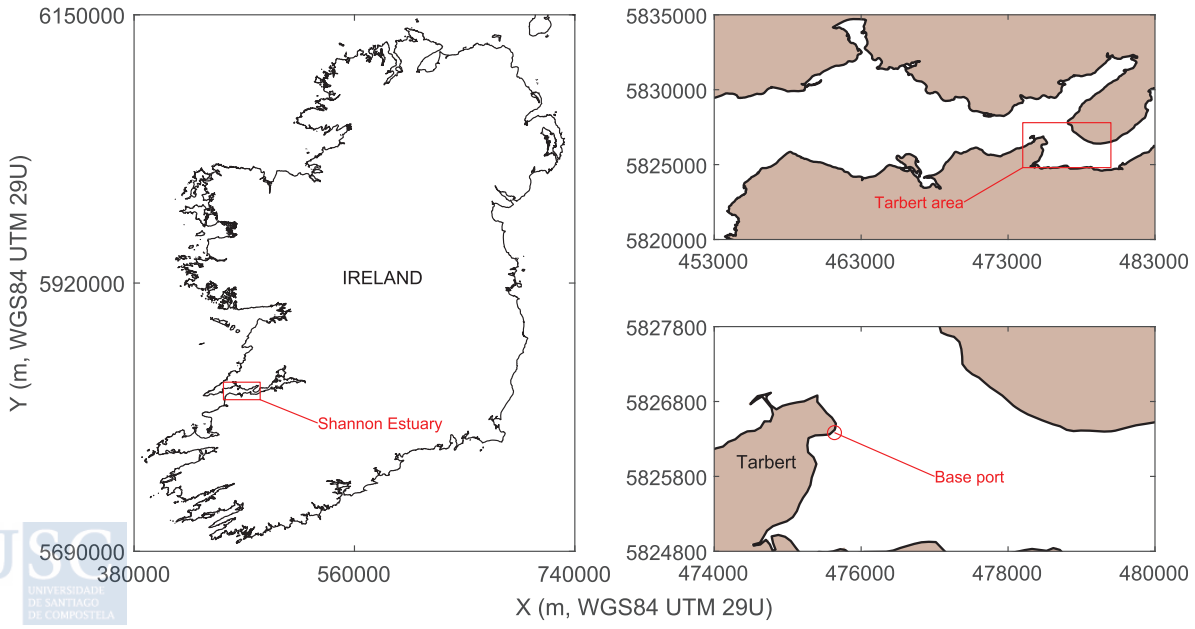


**Fig. 1.** Location of Shannon Estuary in W Ireland pinpointing Tarbert Area.

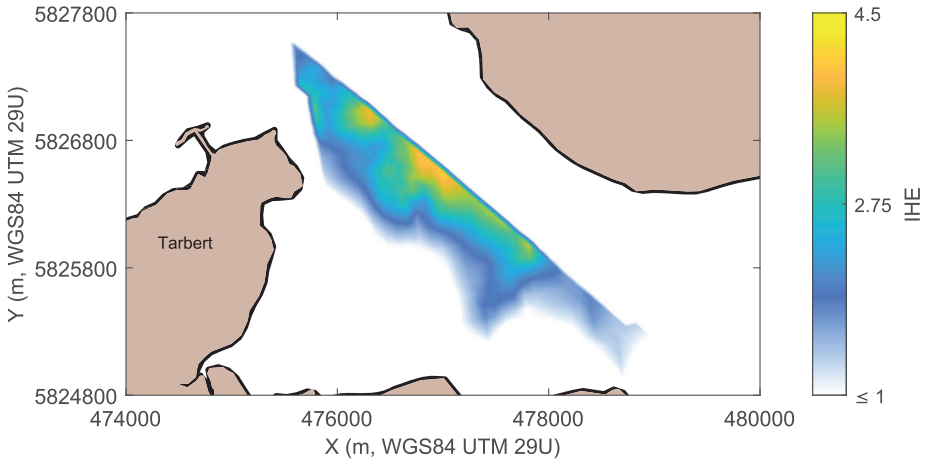


**Fig. 2.** IHE index over the exploitable threshold (IHE ≥1) in the Tarbert Area.

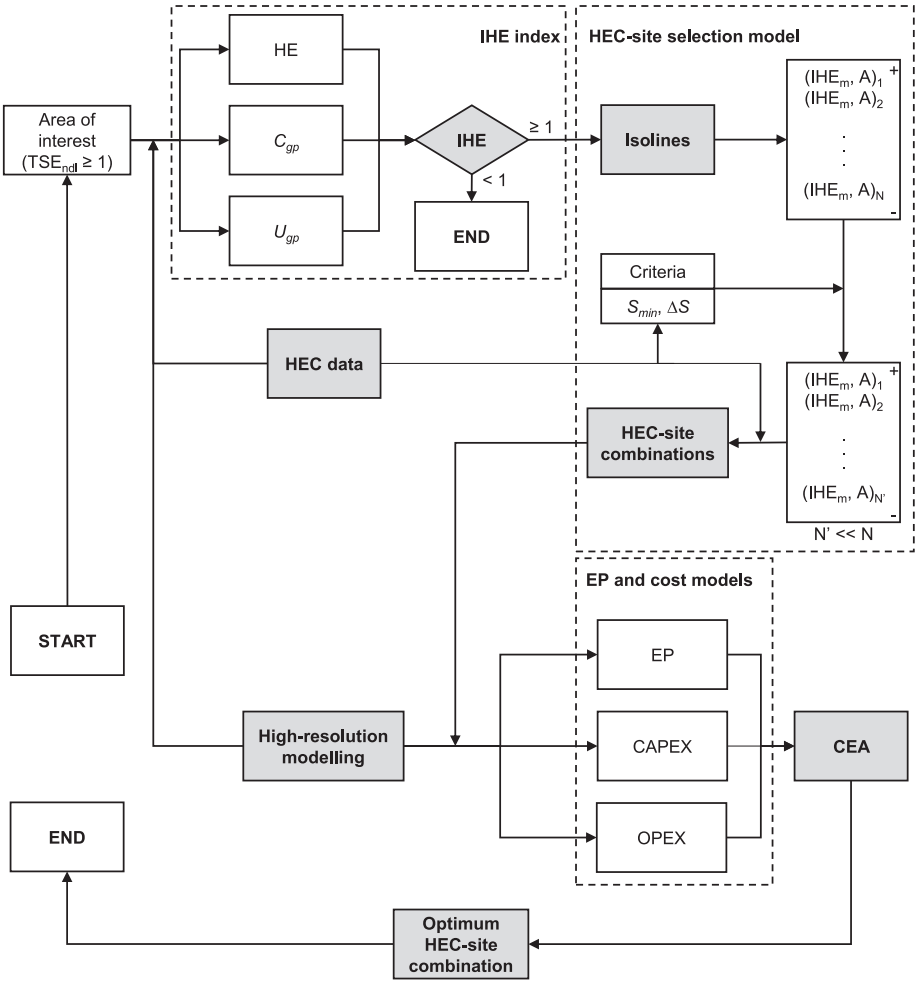


**Fig. 3.** Flowchart of the proposed procedure.

(i) The development of an HEC-site selection model (Section 3), which employs the IHE index and spatial analysis algorithms to define different HEC-site combinations, allowing for economies of scale by analysing various farm sizes based on specific criteria (Section 3).
(ii) The application of an energy production model leading to the computation of the Annual Energy Production (AEP) of the different HEC-site combinations previously defined, based on high-resolution numerical modelling.
(iii) The definition of a Capital Expenditures (CAPEX) model (Section 5), which is based on a detailed breakdown in unitary costs and an ad hoc algorithm for assessing the effects of the economies of scale resulting from the different farms analysed.
(iv) The definition of an Operational Expenditures (OPEX) model (Section 6), considering HEC-specific O&M procedures, including

the analysis of human and material resources and the definition of specific weather windows.

(v) The integration of previous results (ii to iv) to provide reliable CEA parameters for the different HEC-site combinations, leading to the selection of the best alternative.

For the sake of clarity, a flowchart of the procedure is provided in Fig. 3.

This procedure is illustrated through a case study in the Tarbert Area of the Shannon Estuary (Ireland) [30,31,41,42]. The CEA is carried out in terms of Levelized Cost of Energy (LCOE) – a metric widely used in marine renewable energy projects, including for the selection of sites for hydrokinetic energy farms [24–27,45,46].

## 3. HEC-site selection model

The first step of the proposed approach is the definition of all the feasible HEC-site combinations. This is a key stage upon which depend several parameters that influence the cost structure (inter alia, the final layout of the farm or maintenance strategies), including the possible effects of the economies of scale and the performance of the plant and, in consequence, the resulting CEA values.

With the aim of generalizing the results provided, generic taxonomies of energy converters are considered (Section 3.1), including information about their reliability, which will be retained for its use in further sections. As regards locations, the results of the IHE index in the surroundings of Tarbert are used as a starting point for the definition of different areas with homogeneous levels of energy resource, which are processed to identify the suitable areas under specific criteria by means of spatial analysis algorithms (Section 3.2).

### 3.1. Characteristics and reliability of the energy converters considered

The present work aims to provide results as accurate and realistic as possible in a nascent research field, hydrokinetic energy exploitation. As mentioned above, only horizontal-axis turbine-based devices are approaching commercial maturity, resulting in a lack of reliable economic information of HECs. In order to overcome these limitations, it is usual to resort to general taxonomies of HECs, grouping generic designs with a certain homogeneity, especially in the field of reliability, where surrogate data can be easily available from other renewables (e.g., wind energy). Likewise, despite the assumptions made, this approach is helpful to provide accurate figures of the cost structure of HECs and, in particular, of their costs of installation (Section 5), primarily due to the possibility of complementing their breakdown by means of different data sources, which are assumed to be common or scalable for the whole taxonomy considered [47].

Horizontal-axis turbines are usually classified depending on their seabed fixing as [48]: (i) bottom-fixed and (ii) floating devices. This division is connected with the available water depth and, in consequence, with the diameter of the turbine. Monopile bottom-fixed gravity foundations are usually prescribed up to 20–30 m depth, and floating, moored solutions for deeper areas [31]. This general picture is similar to offshore wind energy facilities, allowing us to use surrogate data to compute accurate reliability figures for HECs under an assembly or subassembly approach. The reader is referred to Ref. [47] for further information about this approach and its procedures.

Therefore, in order to select generic energy converter designs, representative of the aforementioned taxonomies and covering the most common horizontal-axis turbines and a wide range of diameters, two different HECs are considered: (i) a floating device of 4.5 m of diameter (F-HEC), which in turn could be applied to most of the areas of interest for hydrokinetic energy exploitation, and (ii) a bottom-fixed converter of 16 m of diameter (BF-HEC), which is of interest in a large number of non-depth limited coastal areas, such as deep estuaries. The main characteristics of the HECs selected, along with their reliability data in terms of average annual number of reparations required, which are retained for its use in further sections, are summarized in Table 1.

### 3.2. Selection of areas for CEA

Previous works have highlighted the energy potential of the Tarbert Area by considering not only its hydrokinetic energy resource, but also its morphological configuration, by applying the $TSE_{ndl}$ index [30], along with socioeconomic and environmental aspects, through the implementation of the IHE index [31]. On the basis of the application of the IHE index, a large area of approx. 3 $km^2$ with values above a minimum threshold of IHE = 1 (i.e., the threshold value of the IHE indicating suitability for hydrokinetic energy exploitation) has been delimited. The definition of suitable smaller areas for energy exploitation requires to take into account the spatial variability of the available resource within this large area; in fact, within it, the maximum value of the IHE index, IHE = 4.15, is roughly two times higher than its mean value, IHE = 2.10 [31]. The more reduced the area, the greater the IHE index; however, the larger the area considered, the higher the number of HECs, which would result in a cost reduction as a consequence of the economies of scale, not considered in the IHE index. With the aim of defining suitable areas for hydrokinetic energy exploitation considering this spatial variability of the energy resource and the resulting effects on the economies of scale, a complex spatial analysis algorithm (Fig. 3) is developed and applied to the Tarbert Area as follows.

First, the entire region delimited by the isoline IHE = 1 is subdivided into several sub-areas or polygons by considering isolines of a value ranging from 1 to the maximum value of the IHE index within the whole area by considering a given step. In the present application, a step of 0.2 is proposed; however, this value can be adapted based on the specific characteristics of the site. Second, the mean value of the IHE index at each polygon is computed along with their total surface. Third, the polygons subsequently obtained are rearranged according to their value of mean IHE index in decreasing order (i.e., increasing their total available surface). Finally, some of the polygons obtained are retained for further analysis from the rearranged list. To this end, the selection procedure considers the following criteria, being applied from the top to the bottom of the list.

The polygons to be retained must fulfil simultaneously two criteria: (i) to have, at least, a minimum total surface, $S_{min}$, and (ii) to provide a significant relative increase in the total available surface, $\Delta S$, with respect to the preceding selected polygon in the list. In the present work, these values are established as follows [27,49–54]: $S_{min} = 5\ hm^2$ and $\Delta S = 100\%$. This second criterion allows us to consider the effects of economies of scale on the cost structure of the hydrokinetic farm.

### 3.3. Application of HEC-site selection model

The results of the application of the proposed HEC-site selection model to the Tarbert Area in the Shannon Estuary are provided in Figs. 4 and 5.

In Fig. 4, the different polygons obtained by considering isolines of a value ranging from IHE = 1 to the maximum value of the IHE index by considering a step = 0.2 are plotted (in black). Likewise, in order to facilitate the understanding of the results and of the proposed HEC-site selection model, additional isolines with step = 0.6 are also plotted (colour code). A total of 30 polygons are apparent. Finally, as result of the application of the rest of the procedure and the surface criteria given by $S_{min} = 5\ hm^2$ and $\Delta S = 100\%$, in Fig. 5 the polygons retained are plotted. Only five polygons resulting from this procedure are considered for further analysis (A to E), allowing the consideration of the effects of economy scale. In addition, the polygon IHE = 1 is also retained. Their main characteristics are presented in Table 2.

Based on the characteristics (water depth) of the areas selected, and the characteristics of the selected devices (i.e., surface occupied per unit of HEC and minimum water depth required) (Table 1), a total of seven

**Table 1**
Main technical characteristics and reliability data of the HECs considered [rotor diameter (Ø), swept area ($A$), minimum water depth ($d_{min}$), total surface in plan view occupied per each device ($S_{unit}$), cut-in velocity ($V_{ci}$), rated velocity ($V_r$), cut-off velocity ($V_{co}$), rated power ($P_r$), power coefficient in normal operation ($C_{pNO}$), power coefficient in stall control ($C_{pSC}$), failure rate ($\lambda$)].

| HEC | Ø (m) | $A$ (m$^2$) | $d_{min}$ (m) | $S_{unit}$ (m$^2$) | $V_{ci}$ (m/s) | $V_r$ (m/s) | $V_{co}$ (m/s) | $P_r$ (kW) | $C_{pNO}$ | $C_{pSC}$ | $\lambda$ (no/yr) |
|---|---|---|---|---|---|---|---|---|---|---|---|
| BF-HEC | 16.00 | 200.00 | 25.00 | 1920.00 | 1.00 | 2.50 | 3.10 | 1200.00 | 0.48 | n.a. | 4.54 |
| F-HEC | 4.50 | 15.90 | 7.00 | 760.00 | 0.70 | 2.70 | 3.75 | 56.00 | 0.35 | 0.20 | 5.37 |

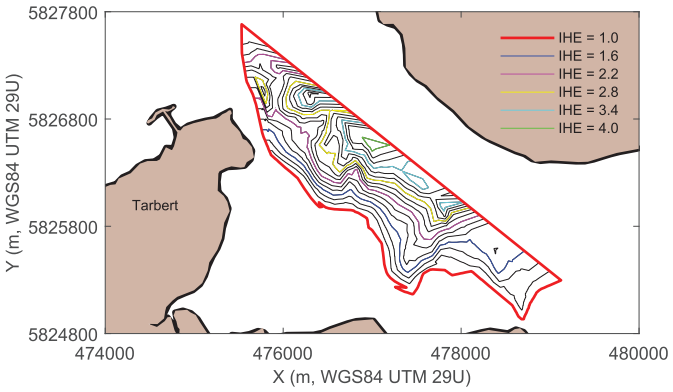


**Fig. 4.** Isolines of the IHE index (0.2 of step for isolines in black and 0.6 for isolines with colour code) within polygon IHE = 1. (For interpretation of the references to colour in this figure legend, the reader is referred to the Web version of this article.)

HEC-site combinations are retained for further CEA: F-HEC can be installed within polygons A to E and IHE = 1; in the case of BF-HEC, it can operate only within polygon E.

## 4. AEP model

### 4.1. Model description

Once defined the different HEC-site combinations resulting from the methodology described in Section 3, the next step in order to assess the techno-economic performance of these combinations is to accurately quantify their annual energy production (AEP). To this end, a high-resolution numerical model (Delft3D-FLOW) of the Shannon Estuary is implemented (in its 2DH form) and successfully validated, allowing the simulation of its hydrodynamics during a complete year [55–57]. For further details about the implementation and validation of the numerical model the reader is referred to Refs. [30,31]. Once the hydrodynamics of this coastal area are fully described in spatiotemporal terms, the electric energy production, $E_e$, of a HEC operating during a period of time $T$ can be computed as follows [58]:

$$E_e = \frac{AC_p\rho}{2}\int_{t=0}^{t=T}[V(t)]^3\,dt, \tag{1}$$

where $A$ represents the turbine swept area, $C_p$ is the power coefficient which models the efficiency of the HEC selected, $\rho$ stands for the water density and $V(t)$ is the instantaneous vertically averaged flow velocity.

However, an accurate computation of this energy production in a

**Table 2**
Main characteristics of the sites selected [mean value of the IHE index (IHE$_m$), standard deviation ($\sigma$), mean water depth ($h_m$), surface ($S$), distance between the centroid of the polygon and the base port ($d_{C\text{-}BP}$)].

| Polygon | IHE$_m$ $\pm$ $\sigma$ | $h_m \pm \sigma$ (m) | $S$ (hm$^2$) | $d_{C\text{-}BP}$ (km) |
|---|---|---|---|---|
| A | 3.93 $\pm$ 0.08 | 9.22 $\pm$ 1.09 | 8.26 | 1.36 |
| B | 3.74 $\pm$ 0.20 | 10.00 $\pm$ 1.68 | 18.37 | 1.38 |
| C | 3.43 $\pm$ 0.30 | 12.02 $\pm$ 2.96 | 46.32 | 1.54 |
| D | 3.11 $\pm$ 0.43 | 14.34 $\pm$ 3.69 | 99.17 | 1.30 |
| E | 2.53 $\pm$ 0.66 | 17.21 $\pm$ 5.00 | 208.96 | 1.26 |
| IHE = 1 | 2.15 $\pm$ 0.80 | 16.97 $\pm$ 5.07 | 297.97 | 1.48 |

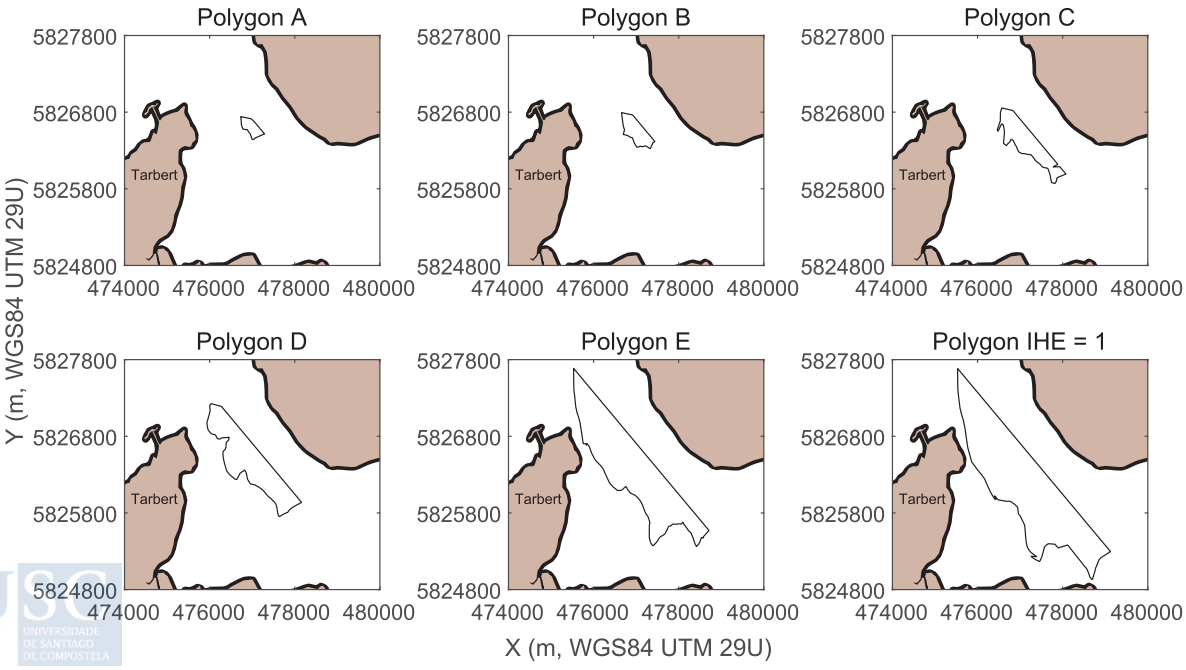


**Fig. 5.** Delimitation of the resulting polygons (A to E), along with polygon IHE = 1.

large coastal region, as is the case of the Tarbert Area, is not straightforward. Given the heterogeneity in terms of available surface of the different sub-areas or polygons of interest selected in Section 3, the spatial variability of the energy resource could result in inaccurate figures of energy production. To avoid this issue, a specific procedure is defined in order to compute the energy production of the different HEC-site combinations. Thus, the site-specific hydrodynamic regime of each polygon considered has been reconstructed based on high-resolution numerical results as follows: for each time step of the numerical simulation, the computed values of flow velocity of each grid cell contained in the polygon considered are averaged, constituting a site-specific and time-dependent hydrodynamic regime for each polygon analysed. So, the characteristic velocity at each polygon at each time step, $V_c$ ($t$), can be computed as:

$$V_c(t) = \frac{1}{n}\sum_{i=0}^{i=n} V_c(i), \tag{2}$$

where $i$ and $t$ represent the numerical cell number and time step, respectively. Thus, the characteristic mean velocity at each polygon, $V_c$, can be computed as:

$$V_c = \frac{1}{T}\sum_{t=0}^{t=T}\left[\frac{1}{n}\sum_{i=0}^{i=n} V_c(i,t)\right], \tag{3}$$

in this way, the energy production of the different HEC-site combinations can be accurately computed, including the effects of the spatial variability of the energy resource, by combining the time distribution of the characteristic velocity, $V_c$ ($t$), with the characteristics of each HEC considered (Table 1) by means of Eq. (1).

### 4.2. Application of AEP model

The results of the application of the proposed AEP model to the Tarbert Area are provided in Figs. 6 and 7.

In Fig. 6, the resulting time distribution of the characteristic velocity during a complete annual year at each polygon is shown. As a result of these time distributions, the following characteristic mean velocities, $V_c$, are attained: 1.20 m/s, 1.05 m/s, 1.16 m/s, 1.12 m/s, 1.03 m/s and 0.98 m/s for polygons A, B, C, D, E, and IHE = 1, respectively.

In Fig. 7, the figures of AEP and capacity factor ($C_f$) for the different HEC-site combinations retained are plotted. AEP is computed by combining the site-specific hydrodynamic regime and the power curve of the HECs considered as provided by the device developers. $C_f$ is obtained according to Ref. [59].

It can be observed that the polygon where F-HEC produces the largest amount of energy is that with the largest surface, IHE = 1 with 174.7 GWh, progressively reducing its energy production as the surface reduces: polygons E with 148.0 GWh, D with 89.9 GWh, C with 45.2 GWh, B with 14.3 GWh, and A with 8.9 GWh. In the case of BF-HEC, its annual energy production in polygon E is 45.1 GWh. This is the result of the significantly larger number of devices in the larger polygons (at least 100% of increase in the total surface with respect the preceding polygon according to the established criteria), which does not indicate a better performance. In fact, the smaller the polygons, the higher their IHE, and therefore the performance in terms of $C_f$ could tend to be the opposite. In the case of F-HEC: polygons A with 16.84%, B with 12.07%, C with 15.12%, D with 13.89%, E with 10.95% and IHE = 1 with 9.28%. In the case of BF-HEC, its $C_f$ in polygon E is 8.42%. This expected tendency does not apply to all cases, e.g. polygon B, given that IHE index also considers, in addition to the energy resource, the total costs although in

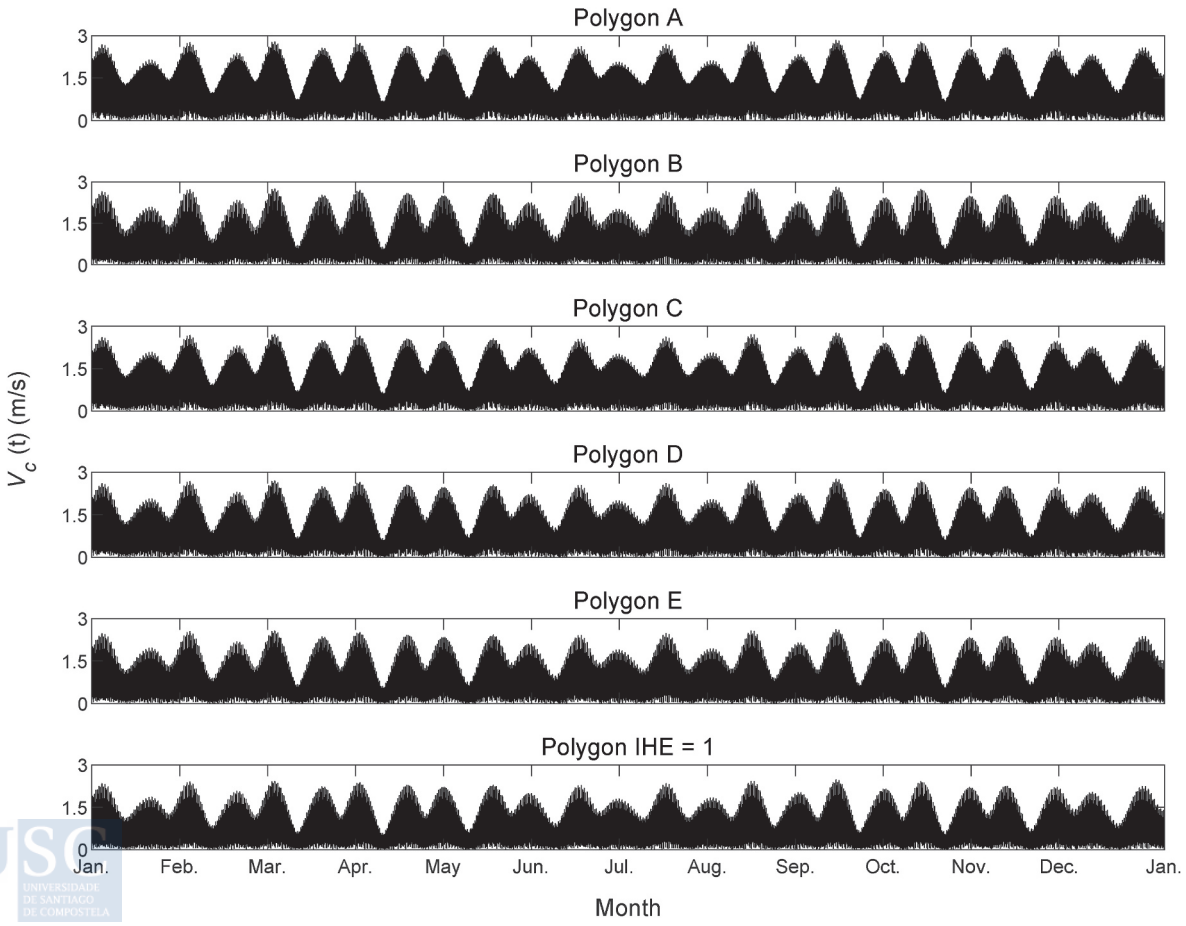


**Fig. 6.** Time distribution of the characteristic velocity, $V_c$ ($t$), in the selected polygons.

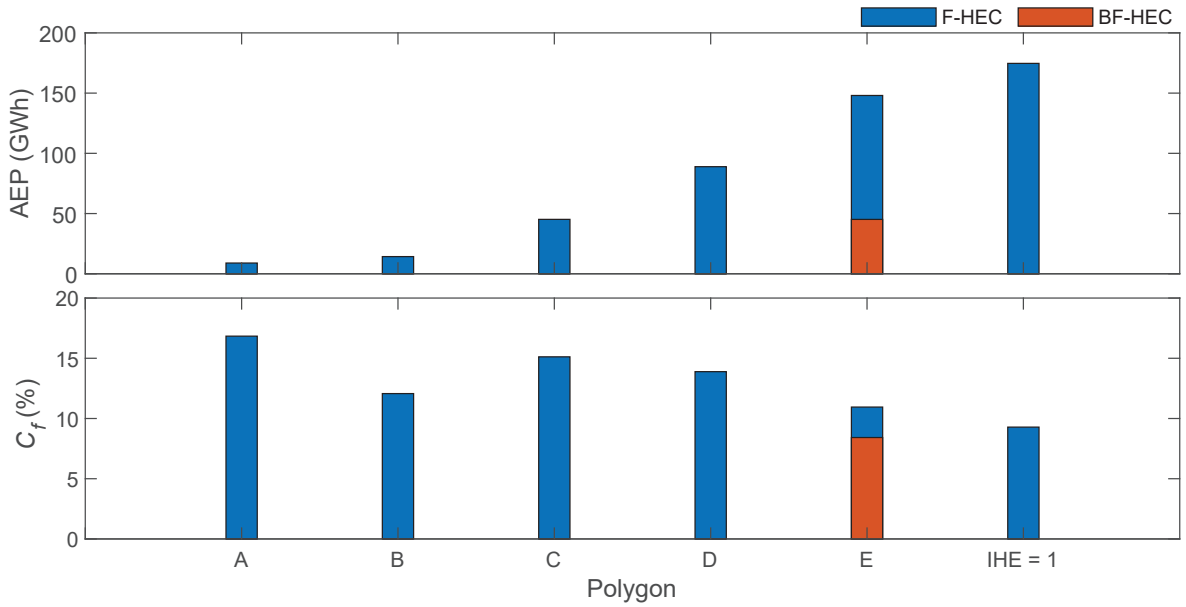


**Fig. 7.** AEP (above) and $C_f$ (below) for the selected HEC-site combinations.

a more simplified way than that proposed in the present work.

## 5. CAPEX model

### 5.1. Fundamentals of CAPEX estimation

CAPEX stand for the capital expenditures needed for the installation, in the present case, of a hydrokinetic farm. They are usually considered as a one-off expenditure, usually incurred in the first year of the project or in the first payment period (prior to the beginning of the operation of the farm). In consequence, CAPEX group all the construction costs of the plant, commonly representing more than 70% of its total expenses [45]. As a result of their economic magnitude, and in order to make available an accurate assessment of CAPEX, it is necessary to define in detail their cost items and structure, for which a widely used unitary costs model should be defined (Section 5.1) and subsequently implemented (Section 5.2) to compute the CAPEX of the different HEC-site combinations defined in Section 3 — instead of a global percentage, which might produce misleading results.

CAPEX is usually broken down into three cost categories [60]: (i) management and engineering costs ($CAPEX_1$), which encompasses the cost of different planning activities needed to ensure the viability of the project and the fulfilment of all its technical requirements (e.g., conceptualization, design, quality management, etc.); (ii) manufacturing costs ($CAPEX_2$), including the cost of the main structural elements of the farm and its equipment (e.g., devices, cabling, foundations or moorings, etc.); and (iii) installation costs ($CAPEX_3$), which include, among others, the expenses of the deployment and grid connection of the plant. The evaluation of these cost categories in the proposed model is explained in detail in Section 5.2.

### 5.2. Definition of CAPEX model

An accurate computation of $CAPEX_1$ to $CAPEX_3$ terms is a key point to develop the CEA of a hydrokinetic farm, especially in the case of $CAPEX_2$, which has been estimated at about 80% of the total CAPEX [45,61]. However, this value is highly dependent on the characteristics of the farm and should be accurately computed for each specific project. In this context, the only way to obtain realistic CAPEX figures is, as in the case of a conventional engineering project, to assess them by means of measurements and unitary costs. The definition of these data requires a detailed design of the HEC, e.g., through CAD tools [62], and a reliable breakdown of unitary costs, which is not typically available in the literature. To this end, the use of HEC types and representative generic designs are required.

In the present application, a detailed and validated unitary costs model [60,63–65] has been used by combining its breakdown (Table 3) with the specific measurements of the HECs considered, according to their significative taxonomic similarities. For further details about this model and its implementation, the reader is referred to Ref. [60].

Likewise, the present CAPEX model also considers the effects of the economies of scale resulting from the consideration of different farm sizes for installing the selected HECs, for which and ad hoc algorithmic procedure is applied. This procedure is based on a detailed analysis of the farm size (as a function of the installed power, $P$) and its influence on CAPEX figures for a wide range of proposed hydrokinetic plants, ranging from reduced plants, e.g., 0.5 MW [66], which were planned for the self-sufficiency of local facilities, to large offshore farms, e.g., 50 MW, with remarkable similarities with wind farms [25]. In this context, an increase in the number of HECs may lead to a considerable reduction in the costs in the case of initially proposed small to medium farm sizes; however, as the size of the farm grows, the increase in these effects progressively reduces up to a point at which are maximum [33]. In the present work, these limits have been widely analysed in terms of installed power in tidal energy and other renewables — for farms with installed power over approx. 30 MW the CAPEX presents maximum reductions of about 35% [67–69]. Moreover, as previously established, this reduction is more abrupt in the case of increasing the size of small farms than when approaching the aforementioned limit (i.e., 30 MW), which could be represented through a logarithmic function [70]. Based on these considerations, and by applying a parametric analysis to several hydrokinetic farms within a wide range of installed power (i.e., 0.5–50 MW), the effects of the economies of scale in terms of CAPEX reduction can be computed for hydrokinetic farms below 30 MW as follows:

$$CAPEX_{red}(\%) = 100 \times [8.4805 \ln(P) + 5.8782]. \quad (4)$$

Above this limit the CAPEX reduction would be set as a constant (35%).

### 5.3. Application of CAPEX model

The results of the application of the proposed CAPEX model to the

**Table 3**
CAPEX breakdown: unitary costs. Adapted from [60].

| Definition | Value | Units |
|---|---|---|
| Cost of occupation of the farm (taxes) | 2.00 | €/m$^2$ |
| Cost of carbon steel manufactured for the structure of the nacelle | 8.00 | €/kg |
| Cost of manufactured carbon steel for PTO frame | 4.00 | €/kg |
| Cost of manufactured fiberglass for the fairing | 10.00 | €/kg |
| Cost of thrust bearing | 40,000.00 | €/MW |
| Cost of brake system | 2000.000 | €/MW |
| Cost of electrical generator | 180,000.00 | €/MW |
| Cost of gearbox | 35,000.00 | €/MW |
| Cost of high-speed shaft | 3000.00 | €/MW |
| Cost of yaw system | 12.00 | €/kg |
| Cost of cooling system | 15,000.00 | €/MW |
| Cost of pressure oil system | 15,000.00 | €/MW |
| Cost of condition monitoring system | 110,000.00 | €/MW |
| Cost of protection and connection switches | 12.00 | €/kg |
| Cost of control system | 12.00 | €/kg |
| Cost of bilge system | 12.00 | €/kg |
| Cost of compressed air system | 12.00 | €/kg |
| Cost of circuit board | 12.00 | €/kg |
| Cost of added elements | 3.00 | €/kg |
| Cost of blades | 40.00 | €/m |
| Cost of pitch system | 500.00 | €/m |
| Cost of core of the rotor | 1000.00 | €/m |
| Cost of low-speed shaft | 500.00 | €/m |
| Cost of base support of the HEC structure | 3.00 | €/kg |
| Cost of transition structure of the HEC | 3.00 | €/kg |
| Cost of vertical column of the HEC | 3.00 | €/kg |
| Cost of elaborated concrete of the ballast | 0.20 | €/kg |
| Cost of special concrete bags | 0.30 | €/kg |
| Cost of mooring system (catenary anchor leg mooring) composed by three stud–link chain lines | 40.00 | €/m |
| Cost of concrete monopile foundation up to 30 m water depth | 15,000.00 | €/m |
| Cost of protection switch | 25,000.00 | €/MW |
| Cost of submarine connector | 25.00 | €/kg |
| Cost of submarine connector installed in the base of the HEC | 12.00 | €/kg |
| Cost of internal wiring | 12.00 | €/kg |
| Cost of connection box | 12.00 | €/kg |
| Cost of umbilical cables | 250.00 | €/m |
| Cost of rectifiers | 100,000.00 | €/MW |
| Cost of inverters | 100,000.00 | €/MW |
| Cost of electrical boxes | 20,000.00 | €/MW |
| Cost of transformers | 40,000.00 | €/MW |
| Cost of transformation platform | 3.00 | €/kg |
| Cost of submarine exportation cables | 500.00 | €/m |
| Cost of ground exportation cables | 150.00 | €/m |

Tarbert Area are presented in Table 4. As can be observed, $CAPEX_2$ represents the lion's share of the total capital investment, followed by $CAPEX_1$ (about ten times less) and $CAPEX_3$ (about forty times less). However, their relative importance for the different HEC-site combinations differs widely; in effect, as the surface considered (and therefore the number of HECs) increases, the value of $CAPEX_2$ significantly increases, whereas this increase in the case of $CAPEX_1$ is much more contained. This means that in the case of areas of reduced surface (e.g., about 5 hm$^2$), the contribution of $CAPEX_1$ to the total CAPEX could represent 50% of $CAPEX_2$.

## 6. OPEX model

### 6.1. Fundamentals of OPEX estimation

OPEX represent the expenditures incurred during the operation, in this case, of a hydrokinetic farm. They usually include all the expenses related with the fixed costs of exploitation and both scheduled and unscheduled O&M, such as insurances, taxes, salaries, facilities, etc [25]. In consequence, OPEX are highly influenced by the performance of the plant and the O&M strategy defined for each type of installation. As a general rule, they constitute an important driver of the cost structure of a hydrokinetic farm, reaching average figures greater than 30% of the total expenses [45]; however, they may widely vary amongst hydrokinetic farms depending on their specific characteristics [25]. Resulting from their importance on the cost structure of a hydrokinetic farm, it is necessary to estimate OPEX as realistically as possible, analysing in detail the actual limitations of the state of the art. To this end, an ad hoc OPEX model is developed (Section 6.2) by considering: (i) reliability HEC data (Section 3), (ii) high-resolution hydrodynamic numerical modelling (Section 4), and (iii) several O&M procedures. Finally, this model is applied to estimate the OPEX of the different HEC-site combinations defined for the Tarbert Area (Section 6.3).

In spite of their important weight on the cost structure of hydrokinetic farms, the assessment of OPEX is subject to a large number of uncertainties, which results from the lack of knowledge caused by the reduced number of real projects. In order to avoid these difficulties, OPEX estimations usually resort to considering either specific cost items or the total cost as a function of the installed power [46,71] or as percentage of CAPEX [25,72]. Recent works proposed more complex models for specific maintenance items, including O&M schemes based on metocean data [47,73,74]; however, high-resolution site-specific numerical modelling required for accurate OPEX estimations is not usually considered [25]. Moreover, previous studies are focused on specific designs of HECs and only take into account a specific O&M strategy [25,60,63–65]. These weaknesses are considered as a starting point for the development of an ad hoc OPEX model, which is detailed in the subsequent section (Section 6.2).

In this regard, prior to the development of an OPEX model, it is necessary to define an appropriate breakdown whose categories would allow a developer to consider all the aforementioned aspects. In the present work, as in the case of CAPEX, a breakdown of OPEX composed of three different categories is considered [25,60,63,75]: (i) insurances and fixed costs ($OPEX_1$), which represent one of the most expensive maintenance costs in renewables [76]; (ii) scheduled or preventive maintenance ($OPEX_2$), covering calendar- or condition-based supervising and reconditioning works; and (iii) unscheduled or corrective maintenance ($OPEX_3$), which stands for unplanned repairing operations. The evaluation of these cost categories in the proposed model is explained in detail in Section 6.2.

**Table 4**
CAPEX results (M€) for the different HEC-site combinations considered.

| Cost item | F-HEC—A | F-HEC—B | F-HEC—C | F-HEC—D | F-HEC—E | F-HEC—IHE | BF-HEC—E |
|---|---|---|---|---|---|---|---|
| $CAPEX_1$ | **5.72** | **5.92** | **6.48** | **7.53** | **9.73** | **11.38** | **5.75** |
| $CAPEX_2$ | **12.91** | **22.64** | **48.02** | **100.71** | **213.71** | **295.90** | **61.65** |
| HECs | 6.50 | 13.25 | 30.21 | 64.74 | 136.72 | 190.25 | 24.11 |
| Foundations | n.a. | n.a. | n.a. | n.a. | n.a. | n.a. | 13.54 |
| Moorings | 0.70 | 1.55 | 4.23 | 10.87 | 27.43 | 37.64 | n.a. |
| Cabling | 5.71 | 7.84 | 13.58 | 25.10 | 49.56 | 68.01 | 24.00 |
| $CAPEX_3$ | **0.15** | **0.33** | **0.99** | **1.77** | **3.53** | **5.64** | **1.40** |
| Power system | 0.02 | 0.04 | 0.13 | 0.23 | 0.47 | 0.75 | 0.19 |
| Cabling | 0.04 | 0.08 | 0.26 | 0.46 | 0.92 | 1.46 | 0.36 |
| HECs | 0.09 | 0.21 | 0.60 | 1.08 | 2.14 | 3.42 | 0.85 |
| CAPEX | **18.78** | **28.89** | **55.49** | **110.01** | **226.97** | **312.91** | **68.80** |

**Table 5**
Hydrodynamic thresholds for the operation and maintenance works using OSV and CTV vessels.

| Weather criteria | OSV O&M | CTV O&M |
|---|---|---|
| Significant wave height, $H_s$ (m). Safety and (max.) values | 1.50 (2.00) | 1.20 (1.50) |
| Tidal currents velocity, $V_{tc}$ (m/s) | 1.00 | 1.00 |
| Wind velocity at 10 m height, $U_{10}$ (m/s) | 10.00 | 10.00 |

### 6.2. Definition of OPEX model

The approach proposed in this work addresses the abovementioned limitations of current OPEX models by considering: (i) high-resolution site-specific numerical modelling; and (ii) different O&M procedures, as a result of analysing HECs representative of various taxonomies (Section 3). The first aspect is of paramount importance to provide the required accuracy for the definition of weather windows suitable for the O&M works; the second one has an important influence resulting from the differences in the maintenance protocol of floating and bottom-fixed technologies (e.g., number of technicians required, type of vessel, duration of works, etc.). Bearing this in mind, the evaluation of $OPEX_1$, $OPEX_2$ and $OPEX_3$ is developed as follows.

The accurate estimation of $OPEX_1$ represents a complex task given the low number of real projects developed; thus, reference values should be provided by developers and stakeholders, in particular from the offshore sector [76]. In this regard, as in the case of the abovementioned simplified estimations of OPEX, it is usual to estimate this term as a function of the installed power or as a percentage of the CAPEX. The approach followed in this work is the second, with $OPEX_1$ computed as a 1.5% of CAPEX, which has shown to provide accurate results [25,72].

Regarding $OPEX_2$, it encompasses very heterogeneous maintenance works, covering from cleaning and inspection activities to the replacement of minor components belonging to different systems of the hydrokinetic farm [75]. Thus, this term is the result of several cost items incurred during these works, whose amounts could be highly diverse (e.g., material, staff, transport, etc.). In this respect, the accurate definition of weather windows suitable for conducting maintenance works has a key role in driving the expenses included within the $OPEX_2$ term [60,63], and therefore lead to an optimization of resources and costs [75].

The computation of these weather windows requires the definition of specific hydrodynamic conditions, usually in form of threshold values, considering the different weather parameters that could influence the maintenance works and their implication for the security of the infrastructure and workers involved. In this regard there exist different types of vessels to conduct maintenance operations, which can be divided in two large categories [77]: (i) Crew Transport Vessel (CTV) for offshore reparations, and (ii) an Offshore Supply Vessel (OSV), usually equipped with a Remoted Operated Vehicle (ROV), in the case of onshore works. OSV operation requires specific wave, wind and current conditions, whereas CTV operation is only limited in terms of wave height [77]; however, given that specific specialized workers (e.g., divers or

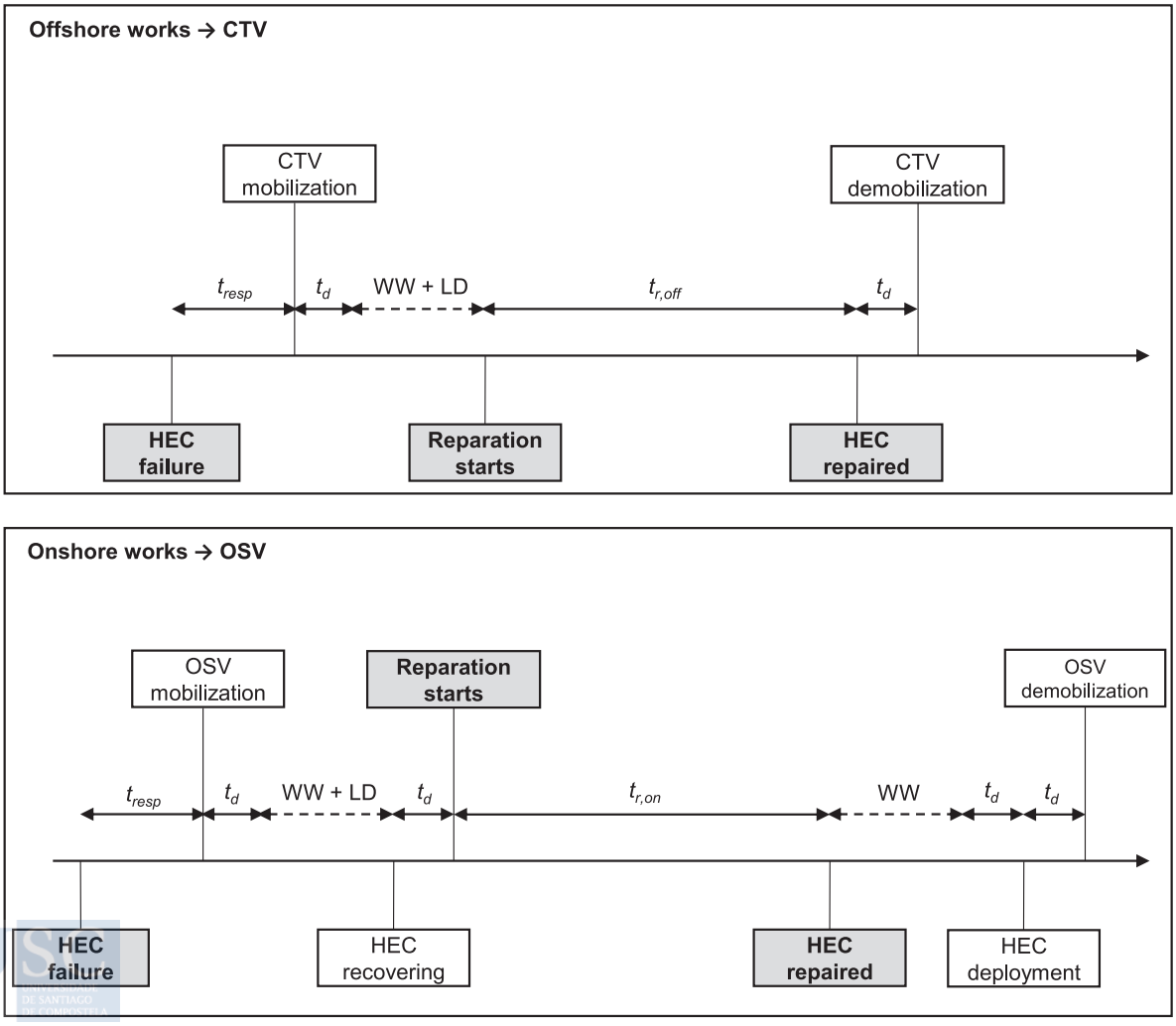


**Fig. 8.** Sketch of the operational protocol for offshore (above) and onshore (below) unplanned reparations ($OPEX_3$).

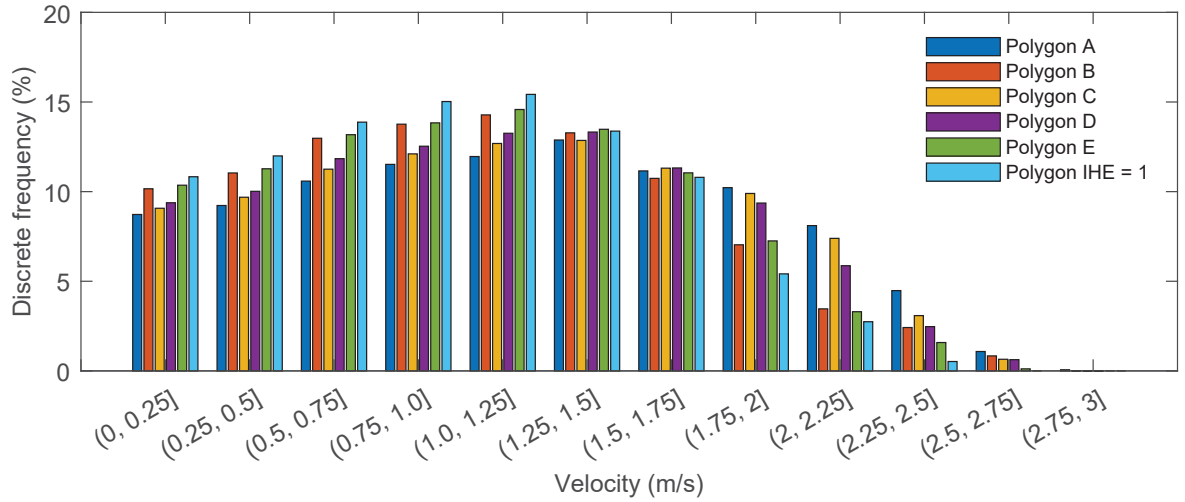


**Fig. 9.** Discrete frequency (non-exceedance) of velocity intervals (0.25 m/s wide) for the polygons considered.

submarine welders) also require specific conditions, CTV operation is also limited by wind and current conditions [25]. Table 5 summarizes the different hydrodynamic thresholds, which are defined by considering not only the limit conditions for the operation of the vessels but also, as abovementioned, the security of workers, which results in considerably restrictive conditions, especially in terms of current velocity [25].

In the case of areas of interest for HEC operation sheltered from wave action, it can be assumed that the only limiting condition is the magnitude of the currents, and therefore, weather windows should be computed based on high-resolution hydrodynamic numerical modelling (Shallow Water models) leading to the accurate computation of its discrete and cumulative annual velocity frequencies. This computation should be conducted by considering the time during which the aforementioned threshold is not exceeded and, therefore, the hydrodynamic conditions are suitable for maintenance operations. It is important to note that the need for considering waves and winds should be analysed for each case study.

In this work $OPEX_2$ is computed based on reference values for the different parameters involved in its computation [60] which are adapted to the site-specific conditions of the different HEC-site combinations (Section 3) in terms of weather windows appropriate for O&M works (Table 5).

In the case of $OPEX_3$, the definition of an appropriate operational protocol is a key aspect for conducting unplanned repairing operations, allowing the optimization of material and human resources [75]. In this context, the repairing strategy needs to be adapted according to the vertical configuration of the hydrokinetic farm, distinguishing between bottom-fixed and floating converters [77]. These vertical configuration influences not only the different resources involved in the repairing procedure and its location (i.e., onshore or offshore) but also the accessibility to the different components of HECs.

According to Ref. [77], these protocols are defined as follows: in the case of bottom-fixed HECs, their unplanned maintenance is, in any case, conducted at onshore facilities; on the contrary, the unplanned maintenance of floating HECs can be carried out either onshore or offshore, depending on the duration of the works, $t_r$. For trivial works ($t_r \leq 1$ h), the reparations can be conducted offshore. Minor reparations ($1\text{ h} < t_r \leq 24$ h) are usually prescribed offshore if the components of the HEC are easily accessible, and at onshore facilities in the opposite case. Finally, major reparations ($t_r > 24$ h), are always conducted onshore. This categorization has an effect on the type of vessel required for conducting the repairing works (CTV and OSV for offshore and onshore maintenance, respectively), as in the case of OPEX2 computation (see above). In Fig. 8 the operational protocol for both offshore and onshore unplanned reparations is presented in the terms of the following timing nomenclature [77]: $t_{resp}$ is the response time, which represents the time necessary to detect a failure and mobilize the human and technical resources required; $t_d$ stands for the displacement time, considering the distance between the base port and the hydrokinetic farm; WW represents the time increment incurred as a consequence of weather windows; LD stands for time increments resulting from logistic delays; and finally, $t_{r,off}$ and $t_{r,on}$ are representative timings of repairing operations for offshore and onshore works, respectively. Further information regarding the cost of the resources involved in both protocols can be found in Ref. [25]. As in the case of $OPEX_2$, an accurate computation of $OPEX_3$ should be based on the definition of the required weather windows as previously defined (Table 5).

Based on the aspects previously remarked, the computation of the $OPEX_3$ term can be summarized in the following steps: (i) definition of the operational protocol as a function of the vertical configuration of the hydrokinetic farm, (ii) computation of the costs incurred as a result of each repairing operation depending on the timing and resources involved, (iii) evaluation of the impact of weather windows and delays on the cost of each operation, (iv) computation of $OPEX_3$ term by considering the reliability of the devices (required annual number of interventions), and integrating the results of steps (i), (ii) and (iii).

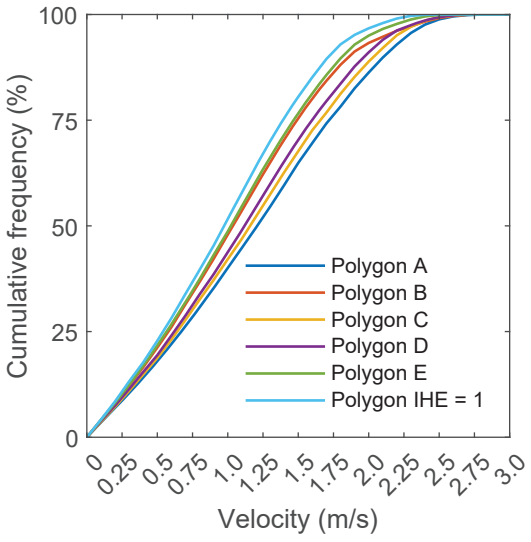


**Fig. 10.** Cumulative frequency (non-exceedance) of flow velocity for the polygons considered.

**Table 6**
Timing (average values) of the different activities conducted during repairing or unscheduled maintenance works ($OPEX_3$) for offshore and onshore operations.

| Variable | Duration |
|---|---|
| $t_c$ | 1.00 h |
| $t_d$ | 0.50 h |
| WW | Site-specific |
| LD | 30% (time increase) |
| $t_{r,off}$ | 4.00 h |
| $t_{r,on}$ | 32.00 h |

### 6.3. Application of OPEX model

For the application of the model, in the first place the annual discrete and cumulative velocity frequencies (non-exceedance) are obtained from the high-resolution shallow water model, and presented in Figs. 9 and 10, respectively.

The time available for O&M for the different areas is similar, despite their differences in total surface, with about 40.1%, 47.9%, 42.21%, 43.8%, 48.9% and 51.7% for polygons A, B, C, D, E, and IHE = 1, respectively (Fig. 10). It can be observed that the smaller the polygons, the higher IHE tend to have large resource, and therefore large current magnitude which reduce the available time for O&M. However, given that IHE index also considers the costs (in a somewhat simplistic way), this does not apply to all cases, as it can be observed in the case of polygon B which presents greater O&M windows than larger polygons such as C and D.

Based on these figures, the proposed OPEX model is applied to the Tarbert Area by considering the Tarbert facilities as base port (Fig. 1) in order to compute the timing of the works associated to the operational protocols for unplanned reparations shown in Fig. 8 (Table 6) [25]. The results of the application of the OPEX model are provided in Table 7.

As can be observed, $OPEX_1$ and $OPEX_2$ represent the lion's share of the operational expenditures, being about one order magnitude larger than $OPEX_3$. Overall $OPEX_2$ is larger than $OPEX_1$ (more than double considering all HEC-site combinations); however, their relative importance is highly dependent on the total surface and the resulting number of HECs considered, being $OPEX_1$ greater than $OPEX_2$ in the case of polygon A.

## 7. CEA parameters computation

The results obtained for AEP, OPEX and CAPEX can be straightforwardly used to compute the viability of the proposed HEC-site combination through CEA parameters. As previously mentioned, in this application CEA is developed in terms of Levelized Cost of Energy (LCOE), which is usually computed as follows [45]:

$$LCOE = \frac{CAPEX + \sum_{t=1}^{T} \frac{OPEX}{(1+k)^t}}{\sum_{t=1}^{T} \frac{AEP}{(1+k)^t}}, \quad (3)$$

where $k$ represents the discount rate and $T$ is the lifetime of the project. According to Ref. [24], values of 10% and 20 years are established for $k$ and $T$, respectively. In addition, it is important to note that the discount rate is not applied to CAPEX insofar as this term corresponds with initial investments which are not constant along the lifetime of the project. The interpretation of the LCOE is straightforward: the lower the value of the LCOE, the better the HEC-site combination for hydrokinetic energy exploitation.

In Fig. 11, LCOE results for the different HEC-site combinations are presented. It can be observed that LCOE values reduce as the polygons occupy progressively a larger area as a result of the effects of the economies of scale, and up to a point where they attain their largest influence (i.e., reach a constant peak value), thereby providing the largest cost reduction. In the case of F-HEC: polygons A with 0.314 €/kWh, B with 0.310 €/kWh, C with 0.196 €/kWh, D with 0.200 €/kWh, E with 0.247 €/kWh and IHE = 1 with 0.287 €/kWh. In the case of BF-HEC, its LCOE in polygon E is 0.260 €/kWh.

Thus, in spite of the smallest polygon (polygon A) being that with the largest $C_f$ and IHE index, the effects of the economies of scale lead to a polygon with larger available area and less available resource (power), polygon C, to be that providing the best cost-effective figures, which are attained by F-HEC.

The results of LCOE obtained are compared with those obtained by applying previous state-of-the-art procedures used in tidal energy projects. To this end, simplistic procedures for easily assessing the viability of projects at their initial steps (e.g. Refs. [24,78,79]), along with complex procedures providing more accurate results (e.g. Refs. [45,46,61]) are considered. The comparison is conducted for the selected combinations: F-HEC operating in polygon C and BF-HEC operating in

**Table 7**
Annual OPEX results (M€) for the HEC-site combinations considered.

| Cost item | F-HEC—A | F-HEC—B | F-HEC—C | F-HEC—D | F-HEC—E | F-HEC—IHE | BF-HEC—E |
|---|---|---|---|---|---|---|---|
| $OPEX_1$ | 0.28 | 0.43 | 0.83 | 1.65 | 3.40 | 4.69 | 1.03 |
| $OPEX_2$ | 0.26 | 0.56 | 1.47 | 3.12 | 6.38 | 8.70 | 2.53 |
| $OPEX_3$ | 0.04 | 0.04 | 0.04 | 0.04 | 0.04 | 0.04 | 0.1 |
| OPEX | **0.58** | **1.03** | **2.34** | **4.81** | **9.82** | **13.43** | **3.66** |

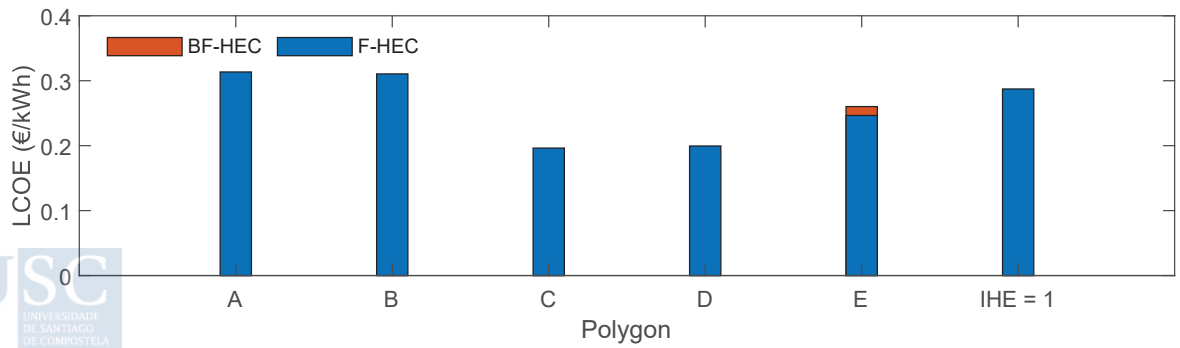


**Fig. 11.** LCOE of the HEC-site combinations considered.

**Table 8**
Comparison of the results of LCOE according to the proposed methodology ($LCOE_{IHE}$) and other state-of-the-art procedures ([24,78,79] and [45,45,61]).

| HEC-site combination | $LCOE_{IHE}$ (€/kWh) | LCOE [24,78,79] (€/kWh) | LCOE [45,45,61] (€/kWh) |
|---|---|---|---|
| F-HEC—C | 0.196 | 0.397 | 0.280 |
| BF-HEC—E | 0.260 | 0.688 | 0.560 |

polygon E. For the application of these methodologies CAPEX and OPEX terms are computed, whereas AEP is determined according to section 4. LCOE results are provided in Table 8.

As it can be observed, the implementation of more simplistic theories, in particular [24,78,79] leads to significant deviations in LCOE figures with respect to the proposed methodology in the present study, of about 103% and 165% for F-HEC in polygon C and BF-HEC in polygon E, respectively. The application of more detailed methodologies [45,46,61] provides more accurate results, with deviations of about 43% and 115%, for F-HEC in polygon C and BF-HEC in polygon E, respectively.

The deviations in the results obtained are primarily due to how OPEX is computed following the different procedures, which correspond to either predetermined values according to general farm characteristics, in the case of simple procedures, or are function of the installed power of the farm, in the case of more complex methodologies. In this way, the current available procedures do not consider cost reductions with increasing farm size, and therefore they usually overestimate OPEX values for large farm projects, as it is the case of the present study.

## 8. Conclusions

Cost-effective analyses (CEA) of proposed hydrokinetic farms are often based on highly simplified energy performance parameters and cost structure, which may lead to suboptimal planning decisions. In connection with the development of CEA is the delimitation of the areas of analysis, usually defined by merely considering the available energy resource and, in some occasions, certain geomorphological parameters, such as the total water depth. These simplified approaches could be adequate in the initial stages of the design of a hydrokinetic farm; however, further and more detailed information is required for the accurate definition of the most appropriate configuration. The current methodologies applied to tidal energy projects only approximate the correct values of the CEA parameters, as a result of their inability to consider specific aspects of the cost analysis, in particular O&M costs, and their disregard of the potential effects of economies of scale, which are related to the characteristics of the study areas (total surface, distance to existing ports, hydrodynamics, etc.).

In this work, a novel approach for accurately computing CEA parameters of hydrokinetic energy projects is developed, leading to the selection of the most appropriate HEC-site combination within a coastal area, and improving previous procedures. The proposed methodology is subsequently applied to the Shannon Estuary (W Ireland) and the results computed in terms of Levelized Cost of Energy (LCOE).

The proposed approach consists of five steps. First, a HEC-site selection model is developed by means of the IHE index and spatial analysis algorithms, leading to the definition of various HEC-site combinations which allow the consideration of economies of scale by retaining different areas for analysis based on specific criteria. Then, the application of an energy production model leads to the computation of the Annual Energy Production (AEP) for the different HEC-site combinations selected, for which high-resolution numerical modelling and specific algorithms are considered. With respect to the cost structure, a Capital Expenditures (CAPEX) model and an Operational Expenditures (OPEX) model are developed. The CAPEX model is based on the detailed breakdown in unitary costs and an ad hoc algorithm for assessing the effects of the economies of scale of the different HEC-site combinations retained. The OPEX model considers HEC-specific O&M procedures, including the analysis of the necessary human and material resources, along with the definition of specific O&M weather windows. Finally, the previous results are integrated to provide reliable CEA parameters for the different HEC-site combinations, leading to the selection of the best alternative.

This procedure is illustrated for the Shannon Estuary and, in particular, the Tarbert Area. The CEA parameters are obtained in terms of Levelized Cost of Energy (LCOE). It is found that the area with the largest $C_f$ and IHE index is not that with the best CEA parameters; instead, the economies of scale lead to a larger area with less available resource providing the best cost-effective figures. As a result, the HEC-site combination providing best cost-effective figures is F-HEC at polygon C with 0.196 €/kWh. The results of LCOE obtained are compared with those obtained by applying state-of-the art procedures used in tidal energy projects. Significant variations in LCOE results as obtained from the different methodologies considered are observed ranging from about 40% to 165%, which results from the overly simplistic OPEX computations leading to a significant overestimation of cost in the case of large farms. In sum, the proposed approach addresses the major difficulties and uncertainties when computing the main aspects affecting the CEA of hydrokinetic energy farms, avoiding simplistic assumptions, and overall improving on the current procedures. The procedure was illustrated through a case study in the Shannon Estuary, but it could be applied to any other coastal area with potential for hydrokinetic energy exploitation.

## CRediT authorship contribution statement

**D.M. Fouz:** Conceptualization, Methodology, Investigation, Formal analysis, Visualization, Writing – original draft. **R. Carballo:** Conceptualization, Methodology, Writing – review & editing, Supervision, Project administration, Funding acquisition. **I. López:** Methodology, Formal analysis, Writing – review & editing, Supervision. **X.P. González:** Methodology, Formal analysis, Visualization, Supervision. **G. Iglesias:** Conceptualization, Methodology, Writing – review & editing, Supervision.

## Declaration of competing interest

The authors declare that they have no known competing financial interests or personal relationships that could have appeared to influence the work reported in this paper.

## Data availability

The authors are unable or have chosen not to specify which data has been used.

## Acknowledgements

This work was supported by the PORTOS project, which is co-financed by the Interreg Atlantic Area Programme, through the European Regional Development Fund [grant number EAPA_784/2018] and 'Axudas para a consolidación e estruturación de unidades de investigación competitivas nas universidades do Sistema Universitario Galego (2020–22)' with reference number ED341B 2020/25.

During this work, D.M. Fouz was supported by a predoctoral grant of the 'Convocatoria de contratos predoutorais do Campus de Especialización Campus Terra' with reference number 8042-272B-64100.

## References

[1] Robbins JR, Buchet PJ, Miller DL, Evans PGH, Waggitt J, Ford AT, et al. Shipping in the north-east Atlantic: identifying spatial and temporal patterns of change. Mar Pollut Bull 2022;179:113681.

[2] Anticamara JA, Watson R, Gelchu A, Pauly D. Global fishing effort (1950–2010): trends, gaps, and implications. Fish Res 2011;107:131–6.
[3] Baxter T, Coombes M, Viles H. Identifying priorities for the joint conservation of maritime built heritage and marine biodiversity: an assessment of shoreline engineering on the Isles of Scilly, UK, using historical datasets. Ocean Coast Manag 2022;227:106288.
[4] Filho LM, Roebeling P, Villasante S, Bastos MI. Ecosystem services values and changes across the Atlantic coastal zone: considerations and implications. Mar Pol 2022;145:105265.
[5] Ramos V, Giannini G, Calheiros-Cabral T, Rosa-Santos P, Taveira-Pinto F. Legal framework of marine renewable energy: a review for the Atlantic region of Europe. Renew Sustain Energy Rev 2021;137:110608.
[6] Claus R, López M. Key issues in the design of floating photovoltaic structures for the marine environment. Renew Sustain Energy Rev 2022;164:112502.
[7] Pérez-Collazo C, Greaves D, Iglesias G. A review of combined wave and offshore wind energy. Renew Sustain Energy Rev 2015;42:141–53.
[8] Todeschini G, Coles D, Lewis M, Popov I, Angeloudis A, Fairley I, et al. Medium-term variability of the UK's combined tidal energy resource for a net-zero carbon grid. Energy 2022;238:121990.
[9] Almoghayer MA, Woolf DK, Kerr S, Davies G. Integration of tidal energy into an island energy system – a case study of Orkney islands. Energy 2022;242:122547.
[10] Li J, Pan S, Chen Y, Yao Y, Xu C. Assessment of combined wind and wave energy in the tropical cyclone affected region:An application in China seas. Energy 2022;260:125020.
[11] Neill SP, Angeloudis A, Robins PE, Walkington I, Ward SL, Masters I, et al. Tidal range energy resource and optimization – past perspectives and future challenges. Renew Energy 2018;127:763–78.
[12] Carballo R, Sánchez M, Ramos V, Taveira-Pinto F, Iglesias G. A high resolution geospatial database for a wave energy exploitation. Energy 2014;68:572–83.
[13] Pugh DT. Tides, surges, and mean sea-level/a handbook for engineers and scientists. John Wiley & Sons Inc; 1996.
[14] Dyer KE. Estuaries: a physical introduction. New York: John Wiley; 1997.
[15] Saini G, Saini RP. A review on technology, configurations, and performance of cross-flow hydrokinetic turbines. Int J Energy Res 2019;43:6639–79.
[16] Seo J, Yi J, Park J, Lee K. Review of tidal characteristics of Uldolmok Strait and optimal design of blade shape for horizontal axis tidal current turbines. Renew Sustain Energy Rev 2019;113:109273.
[17] Segura E, Morales R, Somolinos JA, López A. Techno-economic challenges of tidal energy conversion systems: current status and trends. Renew Sustain Energy Rev 2017;77:536–50.
[18] Kim ES, Bernitsas MM. Performance prediction of horizontal hydrokinetic energy converter using multiple-cylinder synergy in flow induced motion. Appl Energy 2016;170:92–100.
[19] Fouz DM, Carballo R, Ramos V, Iglesias G. Hydrokinetic energy exploitation under combined river and tidal flow. Renew Energy 2019;143:558–68.
[20] Iglesias I, Bio A, Bastos L, Avilez-Valente P. Estuarine hydrodynamic patterns and hydrokinetic energy production: the Douro estuary case study. Energy 2021;222:119972.
[21] Si Y, Liu X, Wang T, Feng B, Qian P, Ma Y, et al. State-of-the-art review and future trends of development of tidal current energy converters in China. Renew Sustain Energy Rev 2022;167:112720.
[22] Bahaj A, Blunden L, Anwar A. Tidal-current energy device development and evaluation protocol. University of Southampton; 2008. Southhampton, Tech.Rep.
[23] Robertson B, Bekker J, Buckham B. Renewable integration for remote communities: comparative allowable cost analyses for hydro, solar and wave energy. Appl Energy 2020;264:114677.
[24] Vazquez A, Iglesias G. LCOE (levelised cost of energy) mapping: a new geospatial tool for tidal stream energy. Energy 2015;91:192–201.
[25] López A, Morán JL, Núñez LR, Somolinos JA. Study of a cost model of tidal energy farms in early design phases with parametrization and numerical values. Application to a second-generation device. Renew Sustain Energy Rev 2020;117:109497.
[26] Rodrigues N, Pintassilgo P, Calhau F, González-Gorbeña E, Pacheco A. Cost-benefit analysis of tidal energy production in a coastal lagoon: the case of Ria Formosa – Portugal. Energy 2021;229:120812.
[27] Radfar S, Panahi R, Javaherchi T, Filom S, Mazyaki AR. A comprehensive insight into tidal stream energy farms in Iran. Renew Sustain Energy Rev 2017;79:323–38.
[28] de Andres A, Medina-Lopez E, Crooks D, Roberts O, Jeffrey H. On the reversed LCOE calculation: design constraints for wave energy commercialization. International Journal of Marine Energy 2017;18:88–108.
[29] Iglesias G, Sánchez M, Carballo R, Fernández H. The TSE index – a new tool for selecting tidal stream sites in depth-limited regions. Renew Energy 2012;48:350–7.
[30] Fouz DM, Carballo R, López I, Iglesias G. Tidal stream energy potential in the Shannon Estuary. Renew Energy 2022;185:61–74.
[31] Fouz DM, Carballo R, López I, Iglesias G. A holistic methodology for hydrokinetic energy site selection. Appl Energy 2022;317:119155.
[32] Castro-Santos L, Filgueira-Vizoso A, Lamas-Galdo I, Carral-Couce L. Methodology to calculate the installation costs of offshore wind farms located in deep waters. J Clean Prod 2018;170:1124–35.
[33] Dismukes DE, Upton GB. Economies of scale, learning effects and offshore wind development costs. Renew Energy 2015;83:61–6.
[34] Robins PE, Neill SP, Lewis MJ, Ward SL. Characterising the spatial and temporal variability of the tidal-stream energy resource over the northwest European shelf seas. Appl Energy 2015;147:510–22.
[35] Coles D, Angeloudis A, Greaves D, Hastie G, Lewis M, Mackie L, et al. A review of the UK and British Channel Islands practical tidal stream energy resource. Proc Roy Soc Lond 2021;477:20210469.
[36] Manchester S, Barzegar B, Swan L, Groulx D. Energy storage requirements for in-stream tidal generation on a limited capacity electricity grid. Energy 2013;61:283–90.
[37] Barbour E, I GB. Energy storage in association with tidal current generation systems. Proc Inst Mech Eng: J Power Energy 2011;225:443–55.
[38] Coles D, Angeloudis A, Goss Z, Miles J. Tidal stream vs. Wind energy: the value of cyclic power when combined with short-term storage in hybrid systems. Energies 2021;14.
[39] Clarke JA, Connor G, Grant AD, Johnstone CM. Regulating the output characteristics of tidal current power stations to facilitate better base load matching over the lunar cycle. Renew Energy 2006;31:173–80.
[40] Bryden IG, Macfarlane DM. The utilisation of short term energy storage with tidal current generation systems. Energy 2000;25:893–907.
[41] SIFP Steering Group. Strategic Integrated Framework Plan (SIFP) for the Shannon Estuary - an inter-jurisdictional land and marine based framework to guide the future developments and management of the Shannon Estuary. 2013.
[42] O'Rourke F, Boyle F, Reynolds A. Ireland's tidal energy resource; an assessment of a site in the Bulls Mouth and the Shannon Estuary using measured data. Energy Convers Manag 2014;87:726–34.
[43] Arean N, Carballo R, Iglesias G. An integrated approach for the installation of a wave farm. Energy 2017;138:910–9.
[44] Álvarez M, Carballo R, Ramos V, Iglesias G. An integrated approach for the planning of dredging operations in estuaries. Ocean Eng 2017;140:73–83.
[45] Vazquez A, Iglesias G. Capital costs in tidal stream energy projects – a spatial approach. Energy 2016;107:215–26.
[46] Vazquez A, Iglesias G. A holistic method for selecting tidal stream energy hotspots under technical, economic and functional constraints. Energy Convers Manag 2016;117:420–30.
[47] T MD, D Z, P JT. Tidal stream device reliability comparison models. Proc Inst Mech Eng O J Risk Reliab 2012;226:6–17.
[48] Sánchez M, Carballo R, Ramos V, Iglesias G. Energy production from tidal currents in an estuary: a comparative study of floating and bottom-fixed turbines. Energy 2014;77:802–11.
[49] Díaz H, Rodrigues JM, Guedes Soares C. Preliminary assessment of a tidal test site on the Minho estuary. Renew Energy 2020;158:642–55.
[50] Han J, Jung J, Hwang JH. Optimal configuration of a tidal current turbine farm in a shallow channel. Ocean Eng 2021;220:108395.
[51] Radfar S, Panahi R, Majidi Nezhad M, Neshat M. A numerical methodology to predict the maximum power output of tidal stream arrays. Sustainability 2022;14.
[52] Funke SW, Kramer SC, Piggott MD. Design optimisation and resource assessment for tidal-stream renewable energy farms using a new continuous turbine approach. Renew Energy 2016;99:1046–61.
[53] Ren Z, Wang Y, Li H, Liu X, Wen Y, Li W. A coordinated planning method for micrositing of tidal current turbines and collector system optimization in tidal current farms. IEEE Trans Power Syst 2019;34:292–302.
[54] Fakhri E, Thiébot J, Gualous H, Machmoum M, Bourguet S. Overall tidal farm optimal design–application to the alderney race and the fromveur strait (France). Appl Ocean Res 2021;106:102444.
[55] Iglesias G, Carballo R. Can the seasonality of a small river affect a large tide-dominated estuary? The case of the Ria de Viveiro, Spain. J Coast Res 2011;27:1170–82.
[56] Ramos V, Carballo R, Álvarez M, Sánchez M, Iglesias G. A port towards energy self-sufficiency using tidal stream power. Energy 2014;71:432–44.
[57] Pacheco A, Ferreira Ó, Carballo R, Iglesias G. Evaluation of the production of tidal stream energy in an inlet channel by coupling field data and numerical modelling. Energy 2014;71:104–17.
[58] Fouz DM, Carballo R, López I, Ramos V, Iglesias G. Hydrokinetic energy production in shallow estuaries: miño estuary, nw Spain. Proceedings of the European Wave and Tidal Energy Conference 2021. 1995-1.
[59] Ramos V, Iglesias G. Performance assessment of tidal stream turbines: a parametric approach. Energy Convers Manag 2013;69:49–57.
[60] Segura E, Morales R, Somolinos JA. Cost assessment methodology and economic viability of tidal energy projects. Energies 2017;10.
[61] Allan G, Gilmartin M, McGregor P, Swales K. Levelised costs of wave and tidal energy in the UK: cost competitiveness and the importance of "banded" renewables obligation certificates. Energy Pol 2011;39:23–39.
[62] Payne GS, Stallard T, Martinez R. Design and manufacture of a bed supported tidal turbine model for blade and shaft load measurement in turbulent flow and waves. Renew Energy 2017;107:312–26.
[63] Segura E, Morales R, Somolinos JA. Economic-financial modeling for marine current harnessing projects. Energy 2018;158:859–80.
[64] Segura E, Morales R, Somolinos JA. Increasing the competitiveness of tidal systems by means of the improvement of installation and maintenance maneuvers in first generation tidal energy converters—an economic argumentation. Energies 2019;12.
[65] Segura E, Morales R, Somolinos JA. Influence of automated maneuvers on the economic feasibility of tidal energy farms. Sustainability 2019;11.
[66] Carballo R, Iglesias G, Castro A. Numerical model evaluation of tidal stream energy resources in the Ría de Muros (NW Spain). Renew Energy 2009;34:1517–24.
[67] Goss ZL, Coles DS, Kramer SC, Piggott MD. Efficient economic optimisation of large-scale tidal stream arrays. Appl Energy 2021;295:116975.

[68] Santa Catarina A. Wind power generation in Brazil: an overview about investment and scale analysis in 758 projects using the Levelized Cost of Energy. Energy Pol 2022;164:112830.
[69] Shields M, Beiter P, Nunemaker J, Cooperman A, Duffy P. Impacts of turbine and plant upsizing on the levelized cost of energy for offshore wind. Appl Energy 2021; 298:117189.
[70] Low WZ, vanden Broucke SKLM, Wynn MT, ter Hofstede AHM, De Weerdt J, van der Aalst WMP. Revising history for cost-informed process improvement. Computing 2016;98:895–921.
[71] Vazquez A, Iglesias G. Grid parity in tidal stream energy projects: an assessment of financial, technological and economic LCOE input parameters. Technol Forecast Soc Change 2016;104:89–101.
[72] Núñez L, López A, Somolinos J, Robledo F, Espín M. Methodologies for Tidal Energies Converters evaluation on early project phases. 2014.
[73] Hudson B, Kay E, Lawless M, Bruce T. Advanced metocean planning tools for the wave and tidal energy sectors. 2017.
[74] Martini M, Guanche R, Losada-Campa I, Losada IJ. The impact of downtime over the long-term energy yield of a floating wind farm. Renew Energy 2018;117:1–11.
[75] Obdam T, Braam H, René Van DP, Rademakers L. O&M cost estimation & feedback of operational data. In: Suvire Gastón O, editor. Wind farm. Rijeka: IntechOpen; 2011. Ch. 2.
[76] O'Connor M, Lewis T, Dalton G. Operational expenditure costs for wave energy projects and impacts on financial returns. Renew Energy 2013;50:1119–31.
[77] RealTide Consortium. RealTide deliverable D1.2 - RAM assessment report. Bureau Veritas; 2020. D1.2.
[78] Ernst Y. Cost of a financial support for wave, tidal stream and tidal range generation in the UK. A report for the Department of Energy and Climate Change and the Scottish Government; 2010.
[79] Ernst Y. Impact of banding the renewables obligation: costs of electricity production. Prepared by ernst and young. Commisioned by Department of Trade and Industry (DTI); 2007.

# 7 GENERAL DISCUSSION

This thesis presents a comprehensive methodology for the decision-making regarding hydrokinetic energy exploitation within a coastal region, providing all the relevant information for installing a hydrokinetic energy farm. The methodology consists of three main procedures (Chapter 4 to Chapter 6), each resulting in a different index (i.e., $TSE_{ndl}$, IHE and $LCOE_{IHE}$), whose complexity and accuracy increase as project planning progresses, moving from preliminary identification of areas suitable for the installation of initial designs to the detailed assessment of specific locations for full-scale project installations.

The methodology developed in this thesis is applied to the Shannon Estuary, as detailed in Chapters 4, 5, and 6. Each chapter focuses on the development and implementation of a specific procedure so as to fully develop it for the characteristics of this coastal area, as well as to provide the required information for its application to any other coastal region of interest for hydrokinetic energy exploitation.

In **Chapter 4 – *Tidal stream energy potential in the Shannon Estuary***, the $TSE_{ndl}$ index is introduced and applied to the Shannon Estuary. This index represents an adapted version of the Tidal Stream Exploitability (TSE) index (Iglesias, G. et al., 2012), specifically designed for non-depth-limited coastal areas like the Shannon Estuary. The original TSE index was developed and successfully applied for selecting tidal stream energy conversion sites in regions characterised by limited water depth, such as shallow and intermediate-depth areas (e.g., Iglesias, G. et al., 2012; Ramos & Iglesias, 2013; Ramos et al., 2013; Ramos et al., 2014). However, its straightforward application to deep coastal regions may lead to an overestimation of the energy potential, particularly in areas with water depths larger than the operational requirements of most HECs. In such cases, the role of water depth differs from that in depth-limited areas, requiring adaptation for its accurate application to non-depth-limited areas. To address this, the analysis of areas with water depths exceeding a predetermined threshold is conducted by incorporating an additional resource-limiting expression in the TSE penalty function, $\xi$, leading to definition of the new penalty-limiting function, $\xi_{ndl}$. This new function resorts to a new water depth range given by the threshold $h_3$, above which $TSE_{ndl}$ values are limited to $h_3$, established by considering the characteristics of the currently available conversion technologies. The application of this procedure enables the delimitation of large areas of interest for MRE projects at preliminary stages by establishing various $TSE_{ndl}$ thresholds. Locations with $TSE_{ndl}$ values greater than or equal to 1 and $TSE_{ndl}$ values greater than or equal to 2 indicate areas of interest and high interest, respectively, for hydrokinetic energy conversion. However, implementing the TSEndl index is a complex process requiring extensive and precise geospatial data, particularly hydrodynamic and bathymetric data.

In the first instance, considering the substantial freshwater inflows into the Shannon Estuary, alongside tidal action, it becomes imperative to consider both baroclinic and barotropic flows (Iglesias, G. et al., 2008). Hence, achieving an accurate characterization of the hydrological regime is required. Freshwater inputs are sourced from gauging stations managed by the Irish Office of Public Works (OPW), facilitating the incorporation of intra-annual variations in the fluvial contributions of the main rivers discharging into the estuary, namely: Shannon, Fergus, Feale, Mulkear, Killimor, Deel, Maigue, Ollatrim, and Killimor. Seasonal variations in their discharge are observed (e.g., winter, spring, summer, and autumn scenarios),

with River Shannon contributing the lion's share of the total discharge, with seasonal contributions ranging from 68% to 86% of the aggregate river discharges.

The subsequent step consists in applying a high-resolution numerical model to comprehensively describe the hydrodynamics of the Shannon Estuary. In this application, a shallow water hydrodynamic model, Delft3D FLOW, is implemented and validated against current velocity field data gathered by Acoustic Doppler Current Profiler (ADCP). This open-source code resorts to a finite difference scheme to approximate the Navier-Stokes equations under the Shallow Water and Boussinesq assumptions, coupled with the transport equation, enabling the computation of the spatial distribution of temperature and salinity, and thereby density. To avoid spurious numerical disturbances on the area of interest, the model grid extends not only over the entire Shannon Estuary but also to the 100 m isobath, approximately 30 km offshore. The resultant grid comprises a total of 69,649 cells of varying size resolution: with a resolution of 100 × 100 m within the estuary, gradually increasing to 100 × 300 m from the estuary mouth towards the ocean boundary. Bathymetric data was obtained from the INFOMAR programme (Integrated Mapping for the Sustainable Development of Ireland's Marine Resource) (O'Toole et al., 2020), supplemented by topographic data to comprehensively characterize the extensive intertidal areas within the estuary. After validating the numerical model through the comparison of computed flow velocity results with field measurements, it is used to evaluate the hydrokinetic energy potential of the Shannon Estuary by conducting various case studies.

First, a preliminary analysis focused on the general distribution of the available energy resource is conducted by considering both the tide and river discharges, in addition to the thermohaline conditions at the open boundaries and the resulting baroclinic flows, over a complete mean spring-neap tidal cycle (≈ 14.75 days). Seasonal river discharges during this period are used to define four case studies: winter (CS1), spring (CS2), summer (CS3) and autumn (CS4). The vast datasets resulting from CS1 to CS4 are used to investigate for the first time the influence of the freshwater inputs on the general circulation patterns of the Shannon Estuary, showing that this influence is more limited than might have been expected according to the large fluvial discharges flowing into this estuary.

Once the general resource distribution has been analysed, the combined effects of the interaction of both energy resources are assessed over a long period (a complete year) (CS5) to accurately determine the total available energy. To this end, average monthly river discharges are input to the model. In this way, in terms of hydrokinetic energy availability, the intra-annual variability that might arise from variations in freshwater discharges is all but negligible, as it results from CS5, reinforcing the results from CS1 to CS4. The hydrodynamics of the Shannon Estuary can be established as clearly tide-dominated, resulting from its large tidal range and tidal prism. Moreover, a marked ebb dominance is apparent, probably as a result of the complex interaction of the tide with the bottom contours, especially in specific areas of the inner estuary, where this effect is reinforced by the action of river discharges.

Even though the above information would have been sufficient to identify the areas with the largest energy resource, the most suitable areas for its conversion also depend on other variables, such as the magnitude of peak velocities or water depth. With this in view, and in order to have a clearer understanding of the exploitability of the hydrokinetic energy resource in this coastal region, the spatial distribution of the $TSE_{ndl}$ index is computed in a tidal cycle during spring tides and mean river discharges and thermohaline conditions (CS6). As it emerges, extensive areas may be suitable for hydrokinetic energy exploitation. However, the installation of a hydrokinetic farm requires the accurate delimitation of the areas suited for its operation. More specifically, the areas above the two abovementioned thresholds of $TSE_{ndl}$ (i.e.,

$TSE_{ndl} \geq 1$ and $TSE_{ndl} \geq 2$) are delimited, resulting in a total of seven areas (Area I to VII) identified as suitable for hydrokinetic energy exploitation, five of them being of high interest (i.e., $TSE_{ndl} \geq 2$) (Areas I, II, IV, V and VI), and the remaining two of interest (i.e., $TSE_{ndl} \geq 1$) (Areas III and VI). The spatial distribution of the $TSE_{ndl}$ index, along with their specific characteristics, show the particular interest of Areas I, II and IV for hydrokinetic energy exploitation; however, Areas I and II are far from port facilities, and makes difficult the energy storage. Nearer to several facilities, but with a somewhat lower resource, are Areas III, VI and VII. On this basis, Areas III, IV, VI and VII are retained for further analysis.

To this end, two locations within these areas are selected for high-resolution analysis, one corresponding with the highest $TSE_{ndl}$, and the other representing the mean $TSE_{ndl}$ for each area. At these locations, the time distribution of the available resource is analysed for a complete mean spring-neap tidal cycle under mean river discharges and thermohaline conditions (CS7). As a result, the time distribution of the current velocity and power density at the abovementioned locations are computed. The available resource is found to differ greatly amongst areas, depending on their specific location within the estuary. Overall, there are reduced spatial variations in the available resource, except for Area IV, where the minimum and maximum value of the $TSE_{ndl}$ differ in roughly 400%, resulting from its large surface area.

For all the interest of the results obtained in Chapter 4, where the new $TSE_{ndl}$ index has been developed and applied in order to identify the most suitable areas for hydrokinetic energy conversion in deep-water areas and characterise their available energy resource, the final decision regarding the installation of a hydrokinetic energy farm should consider not only the available resource and specific geomorphological aspects (e.g., water depth), but also Marine Spatial Planning, and in particular the environmental and socioeconomic factors.

On these grounds, a new procedure, the Integrated Hydrokinetic Energy (IHE) index, is proposed in **Chapter 5 – *A holistic methodology for hydrokinetic energy site selection***, where it is developed and applied again to the Shannon Estuary. The IHE index takes into account all relevant aspects influencing the decision-making process for selecting optimal areas for hydrokinetic energy exploitation in coastal regions. These aspects include energy resource availability, costs, as well as socioeconomic and environmental factors. By doing so, it transcends the limitations of specific conversion technologies or farm layouts, thereby significantly enhancing existing methodologies. Finally, the IHE index aims to reduce uncertainties in the decision-making of hydrokinetic energy projects by using a new comprehensive and integrated approach with application to MRE projects at early stages.

This procedure is carried out through four steps: (i) a thorough characterisation of the energy resource by high-resolution spatiotemporal numerical modelling; (ii) the development of a geospatial penalty function that considers the relationship between primary drivers of capital expenditures (CAPEX) and coastal configuration (depth and distance to coast), thereby penalizing areas with higher installation costs; (iii) an accurate geospatial analysis of socioeconomic and environmental uses to assess their compatibility with hydrokinetic energy exploitation, resulting in an additional penalty function; and finally, (iv) the integration of the results from steps (i) to (iii) to provide a reliable indicator of the viability of hydrokinetic energy exploitation across a coastal region.

Firstly, the exploitable energy resource —defined as that can be harnessed within the operational range of HECs— is characterized and compared with a reference energy level, representing the minimum annual energy required for hydrokinetic energy exploitation. This leads to the computation of the HE index, the first term of the IHE index. The exploitable energy is calculated by using high-resolution numerical results (Chapter 4), but now limiting the energy output between specific lower and upper thresholds of current velocity required for HEC

operation (in this case, 0.7 and 3.1 $ms^{-1}$, respectively). The reference energy level, set at 0.2 $kWm^{-2}$, is based on a comprehensive review of previous research on hydrokinetic energy potential across numerous coastal regions (Carballo et al., 2009; Fouz et al., 2019; Iglesias, I. et al., 2021; Liu et al., 2021; Marsh et al., 2021; Neill et al., 2014; O'Rourke et al., 2014; Ramos et al., 2014; Ramos & Ringwood, 2016; Robins et al., 2015; Sánchez et al., 2014; Thiébot et al., 2020; Yang et al., 2021), where current velocity data obtained either by numerical modelling or in situ measurements are analysed. Accordingly, five categories defining the hydrokinetic energy potential of coastal regions are established based on the HE index: Categories I to V, from lower to higher potential. Applying this categorization to the Shannon Estuary and using the nomenclature from Chapter 4 (i.e., Areas I to VII), most previous identified areas fall into Categories II (Areas V, VI and VII) and III (Areas I, II, and IV), but also into Category I (Area III). More specifically, Area IV boasts the largest exploitable resource, followed by Areas II and I with slightly lower resources, Areas V and VI with significantly lower energy, and finally, Areas VII and III, which are near the threshold of viability from an exploitable energy resource perspective.

Next, in order to develop and implement a geospatial cost penalty function, it is necessary to accurately identify the main drivers of costs, particularly CAPEX, and relate them to the coastal configuration so as to penalise areas where energy exploitation will incur higher expenses. CAPEX are usually broken down as follows (Dalton et al., 2015; Vázquez & Iglesias, 2016a): (i) device costs, (ii) cable costs, (iii) foundation or mooring system costs, (iv) installation costs (e.g., transportation and deployment costs), and (v) grid connection costs. Device and grid connection costs are generally independent of the coastal geomorphology of the study area, and instead they depend on the specific type of technology. However, cable and foundation or mooring system costs are clearly dependent on key geomorphological aspects, namely shoreline distance and water depth, respectively. By considering the main formulations available in the scientific literature, the relationship between these cost elements and the abovementioned geomorphological aspects can be established, requiring the definition of a minimum pre-sizing scheme for a "standard" hydrokinetic farm, including the total plant power and the number of devices required to fulfil it. Both aspects are analysed with a particular emphasis on the current trends and prospects of hydrokinetic technology, focused on second- or third-generation HECs (Segura, E. et al., 2017), and considering representative designs of a wide range of different technologies applied to real hydrokinetic energy projects, whose main geomorphological aspects are also assessed, leading to the definition of threshold reference values. This analysis leads to the definition of a penalty function, $C_{gp}$, relating the costs and the characteristics of a given location (depth and distance to coast).

The application of the $C_{gp}$ penalty function to the Shannon Estuary shows an excellent correlation with the estuary's coastal configuration. Specifically, values of approximately 0.4-0.6 are found within the central channel of the inner and middle estuary, around 0.9 in the nearest shoreline areas (which are virtually not penalized due to their reduced depth and proximity to the coast) and dropping to about 0.2 near the mouth (due to greater water depths and distance from the coast). The highest costs are observed in Area V, closely followed by Areas I and III, then by Areas II, VI, and IV, with Area VII having the lowest costs. However, similar to the exploitable resource analysis, the large surface occupied by these areas means that the costs of installing a hydrokinetic farm can vary significantly within each area, with a mean variation (the difference between mean and maximum $C_{gp}$ values) of 24%. In particular, Areas V and I exhibit variations of 39% and 33%, respectively. These variations can substantially affect the identification of the best sites for hydrokinetic farm installation and must be taken into account in the decision-making process.

The next step in applying the IHE index is to assess the compatibility between hydrokinetic energy exploitation and existing marine uses. To achieve this, a water use penalty function, $U_{gp}$, is defined and applied to the Shannon Estuary. The development of this function involves several stages. First, the marine uses in the coastal region are identified, categorised into (i) socioeconomic activities and (ii) environmental uses. The socioeconomic activities considered are aquaculture, shellfish harvesting, and navigation. For environmental uses, Special Areas of Conservation (SACs) and Special Protection Areas (SPAs) are analysed. A quantitative approach is then proposed to assess the coexistence of these marine uses with hydrokinetic energy exploitation. This method involves defining the penalty function $U_{gp}$, with values ranging from 0 (totally restricted, indicating no coexistence) to 1 (no restrictions, indicating full coexistence), and intermediate values adapted to the specific characteristics of each marine use (Galparsoro et al., 2021). Regarding its physical interpretation, lower $U_{gp}$ values indicate higher restrictions. Lastly, in areas where multiple marine uses overlap, the most restrictive $U_{gp}$ value is used.

Regarding the spatial distribution of the different aforementioned marine uses within the Shannon Estuary, the following observations can be made: (i) extensive areas are occupied by or are suitable for aquaculture farming; (ii) virtually the entire estuary is used for navigation, with a legally delimited navigation area encompassing the main channel and various approaches to the nearby coast; and (iii) environmental uses occupy much larger areas than those dedicated to socioeconomic activities, but overall not imposing significant restrictions on hydrokinetic energy operations.

The most compatible area for hydrokinetic energy operation, with fewer socioeconomic and environmental restrictions, is Area I, followed by Area VII, and subsequently, with similar values, Areas IV, V, and II. However, Areas III and VI are deemed unsuitable for energy conversion due to the presence of higher restrictions. In contrast to the resource and cost results, the variations in $U_{gp}$ within each area are less pronounced, except in Area IV.

Finally, the computation of the IHE index for the Shannon Estuary involves combining the results obtained from previous steps (i to iii), with each result corresponding to a term constituting the proposed index (i.e., HE, $C_{gp}$, and $U_{gp}$). For further details, the reader is referred to Eq. (1) in Chapter 5. The computation of the IHE index results in the identification of a total of six areas with potential interest for hydrokinetic energy exploitation (Areas $I_{IHE}$ to $VI_{IHE}$), corresponding to those with an IHE greater than 1, which significantly differs from previous analyses. Area $IV_{IHE}$, near Tarbet, is identified as the most suitable area, as in previous studies, but now occupying a smaller surface within the previously identified Area IV (delimited in Chapter 4 by means of the $TSE_{ndl}$ index). This new Area $IV_{IHE}$ presents a lower available resource, but also lower costs and fewer restrictions for hydrokinetic energy operation than in the case of former Area IV. The other newly identified areas do not correspond to previously identified areas; instead, they are close to the previous areas, occupying a more limited surface with somewhat lower resource, but lower costs and fewer restrictions for energy conversion.

The results of the IHE index indicate that Area $IV_{IHE}$ is of high interest for energy operation, with a mean value of IHE belonging to category III and specific locations falling within category IV. Additionally, Area $I_{IHE}$ and Area $III_{IHE}$, with somewhat less potential, are also of significant interest, with mean values of IHE belonging to category II and specific locations falling within category III. Finally, the remaining areas, Area $II_{IHE}$, Area $V_{IHE}$, and Area $VI_{IHE}$, could be of interest, albeit with more limited potential, as indicated by their mean values of the IHE index close to 1.

The results demonstrate the capacity of the IHE index for identifying the most suitable locations for hydrokinetic energy conversion in a coastal region, thereby reducing uncertainties at the early stages of MRE projects. Furthermore, the final design of the farm configuration in subsequent project stages necessitates a detailed cost analysis of specific HEC-site combinations, encompassing all relevant expenses incurred during installation and operation. While installation costs are partially considered in the IHE index, operation costs are beyond its scope, necessitating the development of complex cost models considering a wide range of operational parameters (e.g., transport distance by sea and land, vessel requirements, climate conditions, etc.).

In order to address the limitations outlined in Chapter 5 and to extend the analysis to specific HEC-site combinations, in **Chapter 6 – *A methodology for cost-effective analysis of hydrokinetic energy projects***, the IHE index is used as a basis for developing a specific procedure for conducting cost-effective analysis (CEA) of hydrokinetic energy farms. This CEA is conducted in terms of Levelized Costs of Energy (LCOE), which are computed based on the results provided by the IHE index ($LCOE_{IHE}$) through a newly developed *ad hoc* procedure which is also illustrated by its application to the Shannon Estuary.

The novelty of this procedure lies in the integrated analysis of the following aspects: (i) the energy production, assessed by combining high-resolution numerical modelling results (Chapter 5) with spatial analysis algorithms; (ii) the installation costs, analysed in terms of unitary costs, including the effects of economies of scale often disregarded; and (iii) the operation costs, computed through an *ad hoc* Operation and Maintenance (O&M) model, incorporating various operational parameters and strategies typically evaluated through simplified methods.

The proposed approach encompasses five steps: (i) developing an HEC-site selection model by using IHE index results and spatial analysis algorithms to define different HEC-site combinations, enabling the analysis of economies of scale by analysing various farm sizes defined based on specific criteria; (ii) applying an energy production model to compute the Annual Energy Production (AEP) of the different HEC-site combinations based on high-resolution numerical modelling; (iii) defining a Capital Expenditures (CAPEX) model, which incorporates a detailed breakdown of unitary costs and an algorithm to assess economies of scale resulting from the different farm sizes analysed; (iv) establishing an Operational Expenditures (OPEX) model, considering HEC-specific O&M procedures, including analysis of human and material resources and defining specific weather windows; and finally, (v) integrating previous results (ii to iv) to provide reliable CEA parameters for the different HEC-site combinations, leading to the selection of the best alternative, and therefore its detailed analysis in MRE projects at final stages.

The first step of the proposed approach is the definition of the feasible HEC-site combinations. To generalize the results, representative designs of horizontal axis turbine-based devices, considering those with the largest commercial maturity, are retained: (i) BF-HEC (bottom-fixed, Ø 16 m) and (ii) F-HEC (floating, Ø 4.5 m). Their reliability, estimated through surrogate data, is retained for use in step (iv). For the Shannon Estuary application, the area with greater IHE index, Area $IV_{IHE}$, corresponding to Tarbert surroundings, is retained. IHE index results are used to define polygons with homogeneous energy resource levels, processed to identify suitable areas via spatial analysis algorithms. First, the region within the isoline IHE = 1 is subdivided into sub-areas by isolines ranging from 1 to the maximum IHE value, using a step of 0.2, which could be adapted to site-specific characteristics. Second, the mean IHE value and total surface of each polygon are computed. Third, polygons are rearranged in decreasing order of mean IHE value. Finally, polygons are selected based on two criteria: having at least a

minimum total surface ($S_{min}$ = 5 $hm^2$) and providing a significant relative increase in total available surface ($\Delta S$ = 100%) compared to the preceding polygon, considering economies of scale in the cost structure of the hydrokinetic farm.

By applying the spatial analysis algorithm, a total of 30 polygons are obtained. However, after applying the aforementioned criteria, only five polygons (A to E) are retained for further analysis. Additionally, the polygon IHE = 1 is also retained. Based on the characteristics of the selected areas (water depth) and the selected devices (surface occupied per HEC unit and minimum water depth required), a total of seven HEC-site combinations are considered for further CEA: F-HEC can be installed within polygons A to E and IHE = 1, while BF-HEC can operate only within polygon E.

Once the different HEC-site combinations are defined, the next step in conducting the CEA is to accurately quantify their AEP. This involves the analysis of high-resolution hydrodynamic numerical results of the Shannon Estuary for a complete year, which are made available in Chapter 5. With the hydrodynamics of the estuary fully described in spatiotemporal terms, calculating the electric energy production of an HEC over time at a particular site becomes feasible. However, accurately computing the energy production in a large and heterogeneous coastal region like the Tarbert Area is complex due to the spatial variability of the energy resource. To address this, a specific procedure is established as follows. For each time step of the numerical simulation, the flow velocity values at each grid cell within the considered polygon are averaged, creating a site-specific, time-dependent hydrodynamic regime for each polygon. This method leads to an accurate computation of the energy production for different HEC-site combinations by integrating the site-specific hydrodynamic patterns with the characteristics of each HEC, thereby accounting for the spatial variability of the energy resource.

The energy production analysis reveals that the polygon with the largest surface area, IHE = 1, where F-HEC operates, provides the greatest amount of energy with 174.7 GWh annually. Energy production decreases progressively as the polygon surface area reduces: polygon E generates148.0 GWh, polygon D 89.9 GWh, polygon C 45.2 GWh, polygon B 14.3 GWh, and polygon A 8.9 GWh. For BF-HEC, polygon E yields an annual energy production of 45.1 GWh. This trend correlates with the significantly larger number of devices in the larger polygons, attributed to the criteria requiring at least a 100% increase in total surface compared to the preceding polygon, rather than improved performance per device. Indeed, smaller polygons tend to present higher values of the IHE index, and therefore better performance in terms of capacity factor ($C_f$) (Ramos & Iglesias, 2013), which could tend to be the opposite than in the case of the energy production. $C_f$ attained by F-HEC at the different polygons are: A with 16.84%, B with 12.07%, C with 15.12%, D with 13.89%, E with 10.95%, and IHE = 1 with 9.28%. For BF-HEC, the $C_f$ in polygon E is 8.42%. However, this expected trend of higher IHE indices corresponding to higher $C_f$ does not apply to polygon B, where the IHE index also reflects total costs, albeit in a more simplified manner than the detailed analysis conducted in this study.

The third step involves defining and applying a Capital Expenditures (CAPEX) model, categorized into: (i) management and engineering costs ($CAPEX_1$), which include planning activities essential for project viability and technical requirements, such as conceptualization, design, and quality management; (ii) manufacturing costs ($CAPEX_2$), covering the main structural elements and equipment of the farm, including devices, cabling, foundations, or moorings; and (iii) installation costs ($CAPEX_3$), which encompass expenses related to the deployment and grid connection of the plant. Accurately calculating $CAPEX_1$ to $CAPEX_3$ is crucial for the cost-effective analysis (CEA) of a hydrokinetic farm, particularly for $CAPEX_2$,

estimated to account for about 80% of the total CAPEX (Allan et al., 2011; Vázquez & Iglesias, 2016a). However, this percentage varies significantly depending on farm characteristics and requires an accurate computation for each specific project. Realistic CAPEX figures can only be obtained by assessing measurements and unitary costs, akin to conventional engineering projects. To this end, detailed HEC designs and reliable unitary cost breakdowns are necessary, often lacking in literature. To address this, representative generic designs are used, enabling the adaptation and implementation of a detailed and validated unitary costs model (Segura, E. et al., 2018; Segura, Eva et al., 2017; Segura, Eva et al., 2019a; Segura, Eva et al., 2019b).

Moreover, the CAPEX model accounts for the effects of economies of scale by considering different farm sizes. An algorithmic procedure is employed for this purpose, conducting a parametric cost analysis for a wide range of proposed hydrokinetic plants, spanning from small nearshore installations to large offshore farms. The analysis reveals a varying influence of economies of scale based on farm size (Dismukes & Upton, 2015): while smaller to medium-sized farms benefit significantly from increased device numbers leading to considerable cost reductions, this effect diminishes as farm size grows, eventually reaching a maximum. Specifically, maximum CAPEX reductions of approximately 35% are observed for hydrokinetic energy farms with installed power exceeding roughly 30 MW (Goss et al., 2021; Santa Catarina, 2022; Shields et al., 2021), with reductions becoming less pronounced as installed power approaches this threshold, following a logarithmic profile (Low et al., 2016). Beyond the 30 MW limit, the CAPEX reduction can be considered a constant value (i.e., 35%).

The analysis of the CAPEX model applied to the Tarbert Area reveals that $CAPEX_2$ constitutes the lion's share of the total capital investment, with $CAPEX_1$ and $CAPEX_3$ representing about 10% and 2.5% of $CAPEX_2$, respectively. However, their relative contribution varies significantly for the different HEC-site combinations. In particular, as the surface area increases (and so the number of HECs), the value of $CAPEX_2$ also experiences a notable increase, whereas the increase in $CAPEX_1$ is comparatively more restrained. This indicates that in areas with smaller surface areas (e.g., around 5 $hm^2$), the contribution of $CAPEX_1$ to the total CAPEX could amount to approximately 50% of $CAPEX_2$.

The fourth step involves the development and implementation of an Operational Expenditures (OPEX) model, which considers three main cost categories: (i) insurances and fixed costs ($OPEX_1$), (ii) scheduled or preventive maintenance ($OPEX_2$), and (iii) unscheduled or corrective maintenance ($OPEX_3$). OPEX are significantly influenced by plant performance and the defined O&M strategy, often constituting a substantial portion of the total expenses in hydrokinetic farms, averaging over 30% (Vázquez & Iglesias, 2016a). However, these costs can vary widely based on the specific characteristics of each hydrokinetic farm (López et al., 2020). Therefore, an accurate estimation of OPEX is crucial, requiring a detailed analysis of the current state of the art, as described in Chapter 6, along with specific aspects involved in the economic assessment of various OPEX terms. The novelty of this OPEX model lies in the consideration of HEC-specific O&M procedures, including the analysis of the necessary human and material resources, as well as the definition of specific O&M weather windows.

Upon application of the OPEX model, it is observed that $OPEX_1$ and $OPEX_2$ constitute the majority of operational expenditures, with $OPEX_2$ being approximately double than the magnitude of $OPEX_1$ for all HEC-site combinations. However, the relative importance of these categories varies depending on the total surface area and the resulting number of HECs considered, with $OPEX_1$ surpassing $OPEX_2$ in the case of polygon A.

In the final step, the results from steps (ii) to (iv) —AEP, CAPEX, and OPEX, respectively— are used to determine the viability of the proposed HEC-site combinations resulting from step (i) through Levelized Cost of Energy (LCOE) computations. For further

details, the reader is referred to Eq. (3) in Chapter 6. A lower LCOE value indicates a better HEC-site combination for hydrokinetic energy exploitation. It is obtained that LCOE values decrease as the polygons occupy larger areas, reflecting the effects of economies of scale, until reaching a point where these effects peak, at which the greatest cost reduction is attained. For instance, in the case of F-HEC, LCOE values decrease from 0.314 €/kWh in polygon A to 0.196 €/kWh in polygon C. Similarly, for BF-HEC, its LCOE in polygon E is 0.260 €/kWh. Despite polygon A having the highest $C_f$ and IHE index, the effects of economies of scale lead to polygon C, with a larger available surface but less available resource, providing the best cost-effective figures, particularly for F-HEC.

The comparison of LCOE results obtained by using the proposed approach with those resulting from previous works reveal significant overestimations, ranging from about 40% to 165% (Allan et al., 2011; Ernst, 2007; Ernst, 2010; Vázquez & Iglesias, 2015; Vázquez & Iglesias, 2016a; Vázquez & Iglesias, 2016b). These variations stem from previous methodologies' overly simplistic OPEX computations, leading to a substantial overestimation of costs, especially in the case of large farms. Overall, the proposed approach addresses major difficulties and uncertainties in computing the main aspects affecting the CEA of hydrokinetic energy farms. By avoiding simplistic assumptions and improving upon current procedures, it provides more accurate and reliable results for decision-making in MRE projects at final stages.

# 8 CONCLUSIONS

In this thesis a comprehensive methodology for the exploitation of the hydrokinetic energy resource in a coastal region of interest is developed whose application will provide all the relevant elements required for a proper decision-making process. This methodology, which involves the obtention of a large dataset of high-resolution hydrodynamic numerical modelling results, along with socioeconomic and environmental data, and their analysis through cutting-edge geospatial techniques, is applied on the Shannon Estuary, a waterbody located on the Western Irish coast, well known for its vast hydrokinetic energy potential. The herein developed methodology is based on the development and application of three different procedures, whose final objective is the computation of a specific metric or index, made available for providing a reliable support in the decision-making process of a specific stage of hydrokinetic energy farm planning, from initial designs to full-scale projects, increasing in complexity and accuracy as planning progresses, namely: (i) Tidal Stream Exploitability index adapted to non-depth-limited areas, $TSE_{ndl}$ index (Chapter 4); (ii) Integrated Hydrokinetic Energy index, IHE index (Chapter 5); and (iii) Cost-Effective Analysis (CEA) in terms of Levelized Costs of Energy based on the IHE index, $LCOE_{IHE}$ (Chapter 6).

The $TSE_{ndl}$ index constitutes an adaptation of the so-called TSE index, formerly applied for preliminary tidal stream farm sitting in depth-limited coastal areas (e.g., inner or middle part of shallow estuaries), but now revised for its proper implementation to non-depth-limited areas (e.g., deep estuaries), such as the Shannon Estuary, allowing the selection of large areas of interest for MRE projects at preliminary stages, suitable of requiring further analysis at subsequent project stages. The application of the TSE index to non-depth-limited coastal areas would lead to an inappropriate site selection, resulting from considering overestimated energy resource figures, as a consequence of the role of water depth, which differs from that in depth-limited areas, requiring adaptation for its accurate application. To this end, a new penalty-limiting function, $\xi_{ndl}$, is developed by defining a new range in the former penalty function, $\xi$, given by a threshold above which $TSE_{ndl}$ values are limited to those corresponding to threshold water depths, established by considering the characteristics of the currently available energy conversion technologies. Resulting from the implementation of the $TSE_{ndl}$ index, a total of seven areas (Areas I to VII) suitable for hydrokinetic energy conversion have been preliminarily delimited by considering specific thresholds of the index and applying spatial analysis techniques. However, subsequent steps of hydrokinetic energy farm planning should consider not only the available energy resource but also other relevant aspects, such as the exploitability of this energy resource, along with socioeconomic and environmental restraints.

With this in mind, the IHE index is developed, consisting in a comprehensive tool for selecting optimal areas for hydrokinetic energy exploitation in coastal regions, considering energy resource availability, installation costs, and socioeconomic and environmental factors, thus overcoming the limitations of considering specific conversion technologies or farm layouts, and therefore allowing its application to MRE projects at early stages. This index is composed of four terms, each of them obtained at a specific step: (i) characterising the spatial distribution of the exploitable energy resource by means of the Hydrokinetic Energy (HE) index; (ii) determining installation costs resulting from coastal configuration (i.e., water depth

and shoreline distance) through the geospatial cost penalty function ($C_{gp}$); (iii) assessing the coexistence of hydrokinetic energy exploitation with the remaining existing or potential coastal uses by implementing the geospatial water use penalty function ($U_{gp}$); and finally, (iv) integrating previous steps (i to iii) to obtain the IHE index. The physical interpretation of the index and the terms that constitute it is as follows. HE values equal or higher than 1 indicate suitability for hydrokinetic energy operation, without considering other restrictions; regarding the penalty functions, $C_{gp}$ and $U_{gp}$, they range from 1 (no restriction) to 0 (total restriction). Consequently, the higher the IHE index, the more favourable the site for hydrokinetic energy exploitation, with values equal or above 1 indicating suitability threshold. Resulting from its application to the Shannon Estuary, six areas (Area $I_{IHE}$ to Area $VI_{IHE}$) are identified as suitable for hydrokinetic energy conversion, which differ from those selected in previous studies. The most suitable area, Area $IV_{IHE}$, near Tarbert, occupies a smaller surface with somewhat lower resource and fewer restrictions compared to those identified by the $TSE_{ndl}$ index. Nevertheless, once identified the best area for installing a hydrokinetic farm, the final definition of this farm will require a detailed cost-effective analysis of the different feasible HEC-site combinations, for which a detailed methodology is subsequently developed and implemented in terms of LCOE based on the results of the IHE index, $LCOE_{IHE}$.

CEA expressed in terms of $LCOE_{IHE}$ constitutes a brand-new procedure for conducting an accurate cost-effective analysis of hydrokinetic energy projects, avoiding simplified approaches, and therefore suboptimal farm planning. In sum, it provides a novel approach leading to the selection of the most appropriate HEC-site combination within a coastal area of interest, allowing its detailed analysis in MRE projects at final stages, and improving previous procedures. Its implementation consists of five steps: (i) the definition of the different feasible HEC-site combinations through a cutting-edge HEC-site selection model based on the IHE index and spatial analysis algorithms; (ii) the assessment of the energy production of the different alternatives defined in (i); (iii) the computation of CAPEX through a detailed breakdown; (iv) the assessment of OPEX considering HEC-specific O&M procedures, including the analysis of the different resources and the timing involved; and finally, (v) the integration of results from previous steps (i to iv) to provide reliable CEA parameters for the different HEC-site combinations, leading to the selection of the best combination. This procedure is illustrated for the Shannon Estuary, specifically the Tarbert Area, obtaining CEA parameters in terms of LCOE. This analysis reveals that the area with the highest energy production, performance or IHE index figures is not necessarily the most cost-effective; instead, economies of scale may lead to a larger area with fewer available resource presenting better cost-effective figures. $LCOE_{IHE}$ results show that the most cost-effective HEC-site combination is F-HEC operating in polygon C, with 0.196 €/kWh. When comparing the $LCOE_{IHE}$ results to those obtained in previous works, significant overestimations are observed, ranging from about 40% to 165%. From a detailed analysis of the procedure and results obtained, it can be established that previous results are inaccurate primarily resulting from their overly simplistic OPEX computations which significantly overestimate costs for large farms.

The present methodology and procedures involved could be used to provide similar information in any other coastal region of interest for hydrokinetic energy exploitation where the required geospatial data are available (i.e., socioeconomic, geomorphological and environmental restraints). Finally, an intensive effort has been made over the last months in order to extend the procedures herein developed for considering in detail the intra-annual variability on the hydrokinetic energy resource (e.g., time periods shorter than seasons), leading to their application in estuarine areas whose hydrodynamics are indeed dominated by river

discharges. In this regard, new parameters accounting for the variability in the hydrokinetic energy resource are now under development.

# REFERENCES


Agrawal, G., Mohan, D., & Rahman, H. (2021). Ambient air pollution in selected small cities in India: Observed trends and future challenges. *IATSS Research, 45*(1), 19-30. 10.1016/j.iatssr.2021.03.004.

Akbari, N., Jones, D., & Arabikhan, F. (2021). Goal programming models with interval coefficients for the sustainable selection of marine renewable energy projects in the UK. *European Journal of Operational Research, 293*(2), 748-760. 10.1016/j.ejor.2020.12.038.

Allan, G., Gilmartin, M., McGregor, P., & Swales, K. (2011). Levelised costs of Wave and Tidal energy in the UK: Cost competitiveness and the importance of "banded" Renewables Obligation Certificates. *Energy Policy, 39*(1), 23-39. 10.1016/j.enpol.2010.08.029.

Almoghayer, M. A., Woolf, D. K., Kerr, S., & Davies, G. (2022). Integration of tidal energy into an island energy system – A case study of Orkney islands. *Energy, 242*, 122547. 10.1016/j.energy.2021.122547.

Alsaleh, M., & Abdul-Rahim, A. S. (2022). The pathway toward pollution mitigation in EU28 region: Does hydropower growth make a difference? *Renewable Energy, 185*, 291-301. 10.1016/j.renene.2021.12.045.

Álvarez, E. A., Rico-Secades, M., Suárez, D. F., Gutiérrez-Trashorras, A. J., & Fernández-Francos, J. (2016). Obtaining energy from tidal microturbines: A practical example in the Nalón River. *Applied Energy, 183*, 100-112. 10.1016/j.apenergy.2016.08.173.

Álvarez, M., Carballo, R., Ramos, V., & Iglesias, G. (2017). An integrated approach for the planning of dredging operations in estuaries. *Ocean Engineering, 140*, 73-83. 10.1016/j.oceaneng.2017.05.014.

Álvarez, M., Ramos, V., Carballo, R., Areán, N., Torres, M., & Iglesias, G. (2020). The influence of dredging for locating a tidal stream energy farm. *Renewable Energy, 146*, 242-253. 10.1016/j.renene.2019.06.125.

Anticamara, J. A., Watson, R., Gelchu, A., & Pauly, D. (2011). Global fishing effort (1950–2010): Trends, gaps, and implications. *Fisheries Research, 107*(1), 131-136. 10.1016/j.fishres.2010.10.016.

Areán, N., Carballo, R., & Iglesias, G. (2017). An integrated approach for the installation of a wave farm. *Energy, 138*, 910-919. 10.1016/j.energy.2017.07.114.

Astariz, S., & Iglesias, G. (2016). Co-located wind and wave energy farms: Uniformly distributed arrays. *Energy, 113*, 497-508. 10.1016/j.energy.2016.07.069.

Bachvarova, E., Spasova, T., & Marinski, J. (2018). Air Pollution and Specific Meteorological Conditions at the Adjacent Areas of Sea Ports. *IFAC-PapersOnLine, 51*(30), 378-383. 10.1016/j.ifacol.2018.11.336.

Bahaj, A. S., Blunden, L., & Anwar, A. A. (2008). Tidal-current Energy Device Development and Evaluation Protocol. *University of Southampton, Southhampton, Tech.Rep*.

Bailey, D., & Solomon, G. (2004). Pollution prevention at ports: clearing the air. *Environmental Impact Assessment Review, 24*(7), 749-774. 10.1016/j.eiar.2004.06.005.

Barbour, E., & I, G. B. (2011). Energy storage in association with tidal current generation systems. *Proceedings of the Institution of Mechanical Engineers, Part A: Journal of Power and Energy, 225*(4), 443-455. 10.1177/0957650911399014.

Baxter, T., Coombes, M., & Viles, H. (2022). Identifying priorities for the joint conservation of maritime built heritage and marine biodiversity: An assessment of shoreline engineering on the Isles of Scilly, UK, using historical datasets. *Ocean & Coastal Management, 227*, 106288. 10.1016/j.ocecoaman.2022.106288.

Bhattacharya, S., Pennock, S., Robertson, B., Hanif, S., Alam, M. J. E., Bhatnagar, D., Preziuso, D., & O'Neil, R. (2021). Timing value of marine renewable energy resources for potential grid applications. *Applied Energy, 299*, 117281. 10.1016/j.apenergy.2021.117281.

Blunden, L. S., & Bahaj, A. S. (2006). Initial evaluation of tidal stream energy resources at Portland Bill, UK. *Renewable Energy, 31*, 121-132. 10.1016/j.renene.2005.08.016.

Brooks, D. A. (2011). The hydrokinetic power resource in a tidal estuary: The Kennebec River of the central Maine coast. *Renewable Energy, 36*(5), 1492-1501. 10.1016/j.renene.2010.10.029.

Bryden, I. G., & Macfarlane, D. M. (2000). The utilisation of short term energy storage with tidal current generation systems. *Energy, 25*(9), 893-907. 10.1016/S0360-5442(00)00020-7.

Cabral, T., Clemente, D., Rosa-Santos, P., Taveira-Pinto, F., Morais, T., Belga, F., & Cestaro, H. (2020). Performance Assessment of a Hybrid Wave Energy Converter Integrated into a Harbor Breakwater. *Energies, 13*(1), 236. 10.3390/en13010236.

Carballo, R., Iglesias, G., & Castro, A. (2009a). Numerical model evaluation of tidal stream energy resources in the Ría de Muros (NW Spain). *Renewable Energy, 34*(6), 1517-1524. 10.1016/j.renene.2008.10.028.

Carballo, R., Iglesias, G., & Castro, A. (2009b). Residual circulation in the Ría de Muros (NW Spain): A 3D numerical model study. *Journal of Marine Systems, 75*(1-2), 130. 10.1016/j.jmarsys.2008.08.004.

Carballo, R., López, I., Areán, N., & Fouz, D. M. (2020). PORTOS Deliverable D5.6 - Technology-site selection based on high-resolution performance analysis. Universidade de Santiago de Compostela.

Carballo, R., Sánchez, M., Ramos, V., Taveira-Pinto, F., & Iglesias, G. (2014). A high resolution geospatial database for a wave energy exploitation. *Energy, 68*, 572-583. 10.1016/j.energy.2014.02.093.

Castro-Santos, L., Filgueira-Vizoso, A., Lamas-Galdo, I., & Carral-Couce, L. (2018). Methodology to calculate the installation costs of offshore wind farms located in deep waters. *Journal of Cleaner Production, 170*, 1124-1135. 10.1016/j.jclepro.2017.09.219.

Castro-Santos, L., Garcia, G. P., Simões, T., & Estanqueiro, A. (2018). Planning of the installation of offshore renewable energies: a GIS approach of the Portuguese roadmap. *Renewable Energy, 132*, 1251-1262. 10.1016/j.renene.2018.09.031.

Castro-Santos, L., Lamas-Galdo, M. I., & Filgueira-Vizoso, A. (2020). Managing the oceans: Site selection of a floating offshore wind farm based on GIS spatial analysis. *Marine Policy, 113*, 103803. 10.1016/j.marpol.2019.103803.

Chowdhury, M. S., Rahman, K. S., Selvanathan, V., Nuthammachot, N., Suklueng, M., Mostafaeipour, A., Habib, A., Akhtaruzzaman, M., Amin, N., & Techato, K. (2021). Current trends and prospects of tidal energy technology. *Environment, Development and Sustainability, 23*(6), 8179-8194. 10.1007/s10668-020-01013-4.

Clarke, J. A., Connor, G., Grant, A. D., & Johnstone, C. M. (2006). Regulating the output characteristics of tidal current power stations to facilitate better base load matching over the lunar cycle. *Renewable Energy, 31*(2), 173-180. 10.1016/j.renene.2005.08.024.

Claus, R., & López, M. (2022). Key issues in the design of floating photovoltaic structures for the marine environment. *Renewable and Sustainable Energy Reviews, 164*, 112502. 10.1016/j.rser.2022.112502.

Coles, D., Angeloudis, A., Goss, Z., & Miles, J. (2021). Tidal Stream vs. Wind Energy: The Value of Cyclic Power When Combined with Short-Term Storage in Hybrid Systems. *Energies, 14*(4)10.3390/en14041106.

Coles, D., Angeloudis, A., Greaves, D., Hastie, G., Lewis, M., Mackie, L., McNaughton, J., Miles, J., Neill, S., Piggott, M., Risch, D., Scott, B., Sparling, C., Stallard, T., Thies, P., Walker, S., White, D., Willden, R., & Williamson, B. (2021). A review of the UK and British Channel Islands practical tidal stream energy resource. *Proceedings of the Royal Society of London, 477*, 20210469. 10.1098/rspa.2021.0469.

Dallavalle, E., Cipolletta, M., Moreno, V. C., Cozzani, V., & Zanuttigh, B. (2021). Towards green transition of touristic islands through hybrid renewable energy systems. A case study in Tenerife, Canary Islands. *Renewable Energy, 174*, 426-443. 10.1016/j.renene.2021.04.044.

Dalton, G., Allan, G., Beaumont, N., Georgakaki, A., Hacking, N., Hooper, T., Kerr, S., O'Hagan, A. M., Reilly, K., Ricci, P., Sheng, W., & Stallard, T. (2015). Economic and socio-economic assessment methods for ocean renewable energy: Public and private perspectives. *Renewable and Sustainable Energy Reviews, 45*, 850-878. 10.1016/j.rser.2015.01.068.

de Andrés, A., Medina-López, E., Crooks, D., Roberts, O., & Jeffrey, H. (2017). On the reversed LCOE calculation: Design constraints for wave energy commercialization. *International Journal of Marine Energy, 18*, 88-108. 10.1016/j.ijome.2017.03.008.

Deltares. (2010). *User Manual Delft3D-FLOW* (Deltares ed.).

Des, M., deCastro, M., Sousa, M. C., Dias, J. M., & Gómez-Gesteira, M. (2019). Hydrodynamics of river plume intrusion into an adjacent estuary: The Minho River and Ria de Vigo. *Journal of Marine Systems, 189*, 87-97. 10.1016/j.jmarsys.2018.10.003.

Díaz, H., Rodrigues, J. M., & Guedes Soares, C. (2020). Preliminary assessment of a tidal test site on the Minho estuary. *Renewable Energy, 158*, 642-655. 10.1016/j.renene.2020.05.072.

Dismukes, D. E., & Upton, G. B. (2015). Economies of scale, learning effects and offshore wind development costs. *Renewable Energy, 83*, 61-66. 10.1016/j.renene.2015.04.002.

Dyer, K. E. (1997). *Estuaries: A Physical Introduction*. John Wiley.

ed-Dîn Fertahi, S., Bouhal, T., Rajad, O., Kousksou, T., Arid, A., El Rhafiki, T., Jamil, A., & Benbassou, A. (2018). CFD performance enhancement of a low cut-in speed current Vertical Tidal Turbine through the nested hybridization of Savonius and Darrieus. *Energy Conversion and Management, 169*, 266-278. 10.1016/j.enconman.2018.05.027.

Egbert, G. D., Bennett, A. F., & Foreman, M. G. G. (1994). Topex/Poseidon tides estimated using a global inverse model. *Journal of Geophysical Research, 99*, 24821-52. 10.1029/94JC01894.

Ernst, Y. (2007). Impact of Banding the Renewables Obligation: Costs of Electricity Production. *A report for the Department of Trade and Industry (DTI). United Kingdom.*

Ernst, Y. (2010). Cost of a financial support for wave, tidal stream and tidal range generation in the UK. *A Report for the Department of Energy and Climate Change and the Scottish Government.*

European Comission. (1996). *The exploitation of tidal marine currents. Report EUR16683EN*.

Fakhri, E., Thiébot, J., Gualous, H., Machmoum, M., & Bourguet, S. (2021). Overall tidal farm optimal design–Application to the Alderney Race and the Fromveur Strait (France). *Applied Ocean Research, 106*, 102444. 10.1016/j.apor.2020.102444.

Falco, L., Pittito, A., Adnams, W., Earwaker, N., & Greidanus, H. (2019). Eu Vessel density map. Detailed method. https://www.emodnet-humanactivities.eu/documents/Vessel%20density%20maps_method_v1.5.pdf.

Fallon, D., Hartnett, M., Olbert, A., & Nash, S. (2014). The effects of array configuration on the hydro-environmental impacts of tidal turbines. *Renewable Energy, 64*(0), 10-25. 10.1016/j.renene.2013.10.035.

Filho, L. M., Roebeling, P., Villasante, S., & Bastos, M. I. (2022). Ecosystem services values and changes across the Atlantic coastal zone: Considerations and implications. *Marine Policy, 145*, 105265. 10.1016/j.marpol.2022.105265.

Fiorini, M., Capata, A., & Bloisi, D. D. (2016). AIS Data Visualization for Maritime Spatial Planning (MSP). *International Journal of E-Navigation and Maritime Economy, 5*, 45-60. 10.1016/j.enavi.2016.12.004.

Fouz, D. M., Carballo, R., López, I., & Iglesias, G. (2022a). A holistic methodology for hydrokinetic energy site selection. *Applied Energy, 317*, 119155. 10.1016/j.apenergy.2022.119155.

Fouz, D. M., Carballo, R., López, I., & Iglesias, G. (2022b). Tidal stream energy potential in the Shannon Estuary. *Renewable Energy, 185*, 61-74. 10.1016/j.renene.2021.12.055.

Fouz, D. M., Carballo, R., López, I., Ramos, V., & Iglesias, G. (2021). Hydrokinetic energy production in shallow estuaries: Miño Estuary, NW Spain. Proceedings of the 14th European Wave and Tidal Energy Conference (EWTEC).

Fouz, D. M., Carballo, R., Ramos, V., & Iglesias, G. (2019). Hydrokinetic energy exploitation under combined river and tidal flow. *Renewable Energy, 143*, 558-568. 10.1016/j.renene.2019.05.035.

Fraenkel, P. (2010). Practical tidal turbine design considerations: a review of technical alternatives and key design decisions leading to the development of the SeaGen 1.2 MW tidal turbine. Paper presented at the *Ocean Power Fluid Machinery Seminar, 19* 1-19.

Funke, S. W., Kramer, S. C., & Piggott, M. D. (2016). Design optimisation and resource assessment for tidal-stream renewable energy farms using a new continuous turbine approach. *Renewable Energy, 99*, 1046-1061. 10.1016/j.renene.2016.07.039.

Galparsoro, I., Korta, M., Subirana, I., Borja, Á, Menchaca, I., Solaun, O., Muxika, I., Iglesias, G., & Bald, J. (2021). A new framework and tool for ecological risk assessment of wave energy converters projects. *Renewable and Sustainable Energy Reviews, 151*, 111539. 10.1016/j.rser.2021.111539.

González, C. J., Reyes, E., Álvarez, Ó, Izquierdo, A., Bruno, M., & Mañanes, R. (2019). Surface currents and transport processes in the Strait of Gibraltar: Implications for modeling and management of pollutant spills. *Ocean & Coastal Management, 179*, 104869. 10.1016/j.ocecoaman.2019.104869.

Goss, Z. L., Coles, D. S., Kramer, S. C., & Piggott, M. D. (2021). Efficient economic optimisation of large-scale tidal stream arrays. *Applied Energy, 295*, 116975. 10.1016/j.apenergy.2021.116975.

Han, J., Jung, J., & Hwang, J. H. (2021). Optimal configuration of a tidal current turbine farm in a shallow channel. *Ocean Engineering, 220*, 108395. 10.1016/j.oceaneng.2020.108395.

Hudson, B., Kay, E., Lawless, M., & Bruce, T. (2017). Advanced metocean planning tools for the wave and tidal energy sectors. Proceedings of the 12th European Wave and Tidal Energy Conference (EWTEC).

Hunt, J. D., Nascimento, A., Caten, C. S. t., Tomé, F. M. C., Schneider, P. S., Thomazoni, A. L. R., Castro, N. J. d., Brandão, R., Freitas, M. A. V. d., Martini, J. S. C., Ramos, D. S., & Senne, R. (2022). Energy crisis in Brazil: Impact of hydropower reservoir level on the river flow. *Energy, 239*, 121927. 10.1016/j.energy.2021.121927.

Iglesias, G., & Carballo, R. (2009). Seasonality of the circulation in the Ría de Muros (NW Spain). *Journal of Marine Systems, 78*(1), 94-108. 10.1016/j.jmarsys.2009.04.002.

Iglesias, G., & Carballo, R. (2010). Effects of high winds on the circulation of the using a mixed open boundary condition: the Ría de Muros, Spain. *Environmental Modelling & Software, 25*(4), 455-466. 10.1016/j.envsoft.2009.10.013.

Iglesias, G., & Carballo, R. (2011). Can the seasonality of a small river affect a large tide-dominated estuary? The case of the Ria de Viveiro, Spain. *Journal of Coastal Research, 27*(6), 1170-1182. 10.2112/JCOASTRES-D-11-00021.1.

Iglesias, G., Carballo, R., & Castro, A. (2008). Baroclinic modelling and analysis of tide- and wind-induced circulation in the Ría de Muros (NW Spain). *Journal of Marine Systems, 74*(1-2), 475-484. 10.1016/j.jmarsys.2008.03.009.

Iglesias, G., Sánchez, M., Carballo, R., & Fernández, H. (2012). The TSE index – A new tool for selecting tidal stream sites in depth-limited regions. *Renewable Energy, 48*(0), 350-357. 10.1016/j.renene.2012.05.012.

Iglesias, I., Bio, A., Bastos, L., & Avilez-Valente, P. (2021). Estuarine hydrodynamic patterns and hydrokinetic energy production: The Douro estuary case study. *Energy, 222*, 119972. 10.1016/j.energy.2021.119972.

J. Serrano González, M. Burgos Payán, & J. M. Riquelme Santos. (2011). An improved evolutive algorithm for large offshore wind farm optimum turbines layout. Proceedings of the IEEE Trondheim PowerTech Conference, 1-6. 10.1109/PTC.2011.6019366.

Joy, R., Wood, J. D., Sparling, C. E., Tollit, D. J., Copping, A. E., & McConnell, B. J. (2018). Empirical measures of harbor seal behavior and avoidance of an operational tidal turbine. *Marine Pollution Bulletin, 136*, 92-106. 10.1016/j.marpolbul.2018.08.052.

Kamal, M. M., & Saini, R. P. (2022). A review on modifications and performance assessment techniques in cross-flow hydrokinetic system. *Sustainable Energy Technologies and Assessments, 51*, 101933. 10.1016/j.seta.2021.101933.

Kazancoglu, Y., Ozbiltekin-Pala, M., & Ozkan-Ozen, Y. D. (2021). Prediction and evaluation of greenhouse gas emissions for sustainable road transport within Europe. *Sustainable Cities and Society, 70*, 102924. 10.1016/j.scs.2021.102924.

Khan, M. J., Bhuyan, G., Iqbal, M. T., & Quaicoe, J. E. (2009). Hydrokinetic energy conversion systems and assessment of horizontal and vertical axis turbines for river and tidal applications: A technology status review. *Applied Energy, 86*(10), 1823-1835. 10.1016/j.apenergy.2009.02.017

Khojasteh, D., Lewis, M., Tavakoli, S., Farzadkhoo, M., Felder, S., Iglesias, G., & Glamore, W. (2022). Sea level rise will change estuarine tidal energy: A review. *Renewable and Sustainable Energy Reviews, 156*, 111855. 10.1016/j.rser.2021.111855.

Kim, E. S., & Bernitsas, M. M. (2016). Performance prediction of horizontal hydrokinetic energy converter using multiple-cylinder synergy in flow induced motion. *Applied Energy, 170*, 92-100. 10.1016/j.apenergy.2016.02.116.

Kotrikla, A. M., Lilas, T., & Nikitakos, N. (2017). Abatement of air pollution at an aegean island port utilizing shore side electricity and renewable energy. *Marine Policy, 75*, 238-248. 10.1016/j.marpol.2016.01.026.

Lange, M., & Cummins, V. (2021). Managing stakeholder perception and engagement for marine energy transitions in a decarbonising world. *Renewable and Sustainable Energy Reviews, 152*, 111740. 10.1016/j.rser.2021.111740.

Le Provost, C., Bennett, A. F., & Cartwright, D. E. (1995). Ocean tides for and from Topex/Poseidon. *Science, 267*(5198), 639-647. 10.1126/science.267.5198.639.

Lewis, M., McNaughton, J., Márquez-Dominguez, C., Todeschini, G., Togneri, M., Masters, I., Allmark, M., Stallard, T., Neill, S., Goward-Brown, A., & Robins, P. (2019). Power variability of tidal-stream energy and implications for electricity supply. *Energy, 183*, 1061-1074. 10.1016/j.energy.2019.06.181.

Lewis, M., O'Hara Murray, R., Fredriksson, S., Maskell, J., de Fockert, A., Neill, S. P., & Robins, P. E. (2021). A standardised tidal-stream power curve, optimised for the global resource. *Renewable Energy, 170*, 1308-1323. 10.1016/j.renene.2021.02.032.

Li, J., Pan, S., Chen, Y., Yao, Y., & Xu, C. (2022). Assessment of combined wind and wave energy in the tropical cyclone affected region:An application in China seas. *Energy, 260*, 125020. 10.1016/j.energy.2022.125020.

Liu, X., Chen, Z., Si, Y., Qian, P., Wu, H., Cui, L., & Zhang, D. (2021). A review of tidal current energy resource assessment in China. *Renewable and Sustainable Energy Reviews, 145*, 111012. 10.1016/j.rser.2021.111012.

Lonati, G., Cernuschi, S., & Sidi, S. (2010). Air quality impact assessment of at-berth ship emissions: Case-study for the project of a new freight port. *Science of the Total Environment, 409*(1), 192-200. 10.1016/j.scitotenv.2010.08.029.

López, A., Morán, J. L., Núñez, L. R., & Somolinos, J. A. (2020). *Study of a cost model of tidal energy farms in early design phases with parametrization and numerical values. Application to a second-generation device*10.1016/j.rser.2019.109497.

López, I., Carballo, R., Fouz, D. M., & Iglesias, G. (2021). Design Selection and Geometry in OWC Wave Energy Converters for Performance. *Energies, 14*(6), 1707 10.3390/en14061707.

López, M., Rodríguez, N., & Iglesias, G. (2020). Combined Floating Offshore Wind and Solar PV. *Journal of Marine Science and Engineering, 8*(8), 576. 10.3390/jmse8080576.

Low, W. Z., vanden Broucke, S. K. L. M., Wynn, M. T., ter Hofstede, A. H. M., De Weerdt, J., & van der Aalst, W. M. P. (2016). Revising history for cost-informed process improvement. *Computing, 98*(9), 895-921. 10.1007/s00607-015-0478-1.

Manchester, S., Barzegar, B., Swan, L., & Groulx, D. (2013). Energy storage requirements for in-stream tidal generation on a limited capacity electricity grid. *Energy, 61*, 283-290. 10.1016/j.energy.2013.08.036.

Marsh, P., Penesis, I., Nader, J. R., Cossu, R., Auguste, C., Osman, P., & Couzi, C. (2021). Tidal current resource assessment and study of turbine extraction effects in Banks Strait, Australia. *Renewable Energy*, 10.1016/j.renene.2021.08.051.

Martini, M., Guanche, R., Losada-Campa, I., & Losada, I. J. (2018). The impact of downtime over the long-term energy yield of a floating wind farm. *Renewable Energy, 117*, 1-11. 10.1016/j.renene.2017.10.032.

Mejía-Olivares, C. J., Haigh, I. D., Wells, N. C., Coles, D. S., Lewis, M. J., & Neill, S. P. (2018). Tidal-stream energy resource characterization for the Gulf of California, México. *Energy, 156*, 481-491. 10.1016/j.energy.2018.04.074.

Mestres, M., Griñó, M., Sierra, J. P., & Mösso, C. (2016). *Analysis of the optimal deployment location for tidal energy converters in the mesotidal Ria de Vigo (NW Spain)*10.1016/j.energy.2016.06.055.

Neill, S. P., Angeloudis, A., Robins, P. E., Walkington, I., Ward, S. L., Masters, I., Lewis, M. J., Piano, M., Avdis, A., Piggott, M. D., Aggidis, G., Evans, P., Adcock, T. A. A., Židonis, A., Ahmadian, R., & Falconer, R. (2018). Tidal range energy resource and optimization – Past perspectives and future challenges. *Renewable Energy, 127*, 763-778. 10.1016/j.renene.2018.05.007.

Neill, S. P., Hashemi, M. R., & Lewis, M. J. (2014). The role of tidal asymmetry in characterizing the tidal energy resource of Orkney. *Renewable Energy, 68*, 337-350. 10.1016/j.renene.2014.01.052.

Njoh, A. J. (2021). Renewable energy as a determinant of inter-country differentials in $CO_2$ emissions in Africa. *Renewable Energy, 172*, 1225-1232. 10.1016/j.renene.2021.03.096.

Núñez, L. R., López, A., Somolinos, J. A., Robledo, F., & Espín, M. (2014). Methodologies for Tidal Energies Converters evaluation on early project phases. Proceedings of the 1st International Conference on Renewable Energies Offshore (RENEW).

O'Rourke, F., Boyle, F., & Reynolds, A. (2014). Ireland's tidal energy resource; An assessment of a site in the Bulls Mouth and the Shannon Estuary using measured data. *Energy Conversion and Management, 87*, 726-734. 10.1016/j.enconman.2014.06.089.

Obdam, T., Braam, H., René Van, D. P., & Rademakers, L. (2011). O&M Cost Estimation & Feedback of Operational Data. In Gastón O. Suvire (Ed.), *Wind Farm* (pp. Ch. 2). IntechOpen. 10.5772/17011.

O'Carroll, J. P. J., Kennedy, R. M., Creech, A., & Savidge, G. (2017). Tidal Energy: The benthic effects of an operational tidal stream turbine. *Marine Environmental Research, 129*, 277-290. 10.1016/j.marenvres.2017.06.007.

O'Connor, M., Lewis, T., & Dalton, G. (2013). Operational expenditure costs for wave energy projects and impacts on financial returns. *Renewable Energy, 50*, 1119-1131. 10.1016/j.renene.2012.08.059.

O'Toole, R., Judge, M., Sacchetti, F., Furey, T., Mac Craith, E., Sheehan, K., Kelly, S., Cullen, S., McGrath, F., & Monteys, X. (2020). Mapping Ireland's coastal, shelf and deep-water environments using illustrative case studies to highlight the impact of seabed mapping on the generation of blue knowledge. *Geological Society, London, Special Publications, 505*, SP505-207. 10.1144/SP505-2019-207.

Pacheco, A., Ferreira, Ó, Carballo, R., & Iglesias, G. (2014). *Evaluation of the production of tidal stream energy in an inlet channel by coupling field data and numerical modelling*10.1016/j.energy.2014.04.075.

Pallotta, G., Vespe, M., & Bryan, K. (2013). Vessel Pattern Knowledge Discovery from AIS Data: A Framework for Anomaly Detection and Route Prediction. *Entropy, 15*(6), 2218-2245. 10.3390/e15062218

Payne, G. S., Stallard, T., & Martinez, R. (2017). Design and manufacture of a bed supported tidal turbine model for blade and shaft load measurement in turbulent flow and waves. *Renewable Energy, 107*, 312-326. 10.1016/j.renene.2017.01.068.

Peñalba, M., Aizpurua, J. I., & Martinez-Perurena, A. (2021). On the definition of a risk index based on long-term metocean data to assist in the design of Marine Renewable Energy systems. *Ocean Engineering, 242*, 110080. 10.1016/j.oceaneng.2021.110080.

Pérez-Collazo, C., Greaves, D., & Iglesias, G. (2015). A review of combined wave and offshore wind energy. *Renewable and Sustainable Energy Reviews, 42*, 141-153. 10.1016/j.rser.2014.09.032.

Pérez-Collazo, C., Pemberton, R., Greaves, D., & Iglesias, G. (2019). Monopile-mounted wave energy converter for a hybrid wind-wave system. *Energy Conversion and Management, 199*, 111971. 10.1016/j.enconman.2019.111971.

Pinon, G., Mycek, P., Germain, G., & Rivoalen, E. (2012). Numerical simulation of the wake of marine current turbines with a particle method. *Renewable Energy, 46*(0), 111-126. 10.1016/j.renene.2012.03.037.

Pudur, R., & Gao, S. (2016). Performance Analysis of Savonius Rotor Based Hydropower Generation Scheme with Electronic Load Controller. *Journal of Renewable Energy, 2016*, 4127619. 10.1155/2016/4127619.

Pugh, D. T. (1996). *Tides, Surges, and Mean Sea-Level/a Handbook for Engineers and Scientists*. John Wiley & Sons Inc.

Qian, P., Feng, B., Liu, H., Tian, X., Si, Y., & Zhang, D. (2019). Review on configuration and control methods of tidal current turbines. *Renewable and Sustainable Energy Reviews, 108*, 125-139. 10.1016/j.rser.2019.03.051.

Radfar, S., Panahi, R., Javaherchi, T., Filom, S., & Mazyaki, A. R. (2017). A comprehensive insight into tidal stream energy farms in Iran. *Renewable and Sustainable Energy Reviews, 79*, 323-338. 10.1016/j.rser.2017.05.037.

Radfar, S., Panahi, R., Majidi Nezhad, M., & Neshat, M. (2022). A Numerical Methodology to Predict the Maximum Power Output of Tidal Stream Arrays. *Sustainability, 14*(3), 1664. 10.3390/su14031664.

Ramos, V., & Iglesias, G. (2013). Performance assessment of Tidal Stream Turbines: A parametric approach. *Energy Conversion and Management, 69*(0), 49-57. 10.1016/j.enconman.2013.01.008.

Ramos, V., & Ringwood, J. V. (2016). Implementation and evaluation of the International Electrotechnical Commission specification for tidal stream energy resource assessment: A case study. *Energy Conversion and Management, 127*, 66-79. 10.1016/j.enconman.2016.08.078.

Ramos, V., Carballo, R., Álvarez, M., Sánchez, M., & Iglesias, G. (2013). Assessment of the impacts of tidal stream energy through high-resolution numerical modeling. *Energy, 61*(0), 541-554. 10.1016/j.energy.2013.08.051.

Ramos, V., Carballo, R., Álvarez, M., Sánchez, M., & Iglesias, G. (2014). A port towards energy self-sufficiency using tidal stream power. *Energy, 71*, 432-444. 10.1016/j.energy.2014.04.098.

Ramos, V., Giannini, G., Calheiros-Cabral, T., Rosa-Santos, P., & Taveira-Pinto, F. (2021). Legal framework of marine renewable energy: A review for the Atlantic region of Europe. *Renewable and Sustainable Energy Reviews, 137*, 110608. 10.1016/j.rser.2020.110608.

RealTide Consortium. (2020). *RealTide Deliverable D1.2 - RAM Assessment Report. Bureau Veritas.* (No. D1.2).

Robbins, J. R., Bouchet, P. J., Miller, D. L., Evans, P. G. H., Waggitt, J., Ford, A. T., & Marley, S. A. (2022). Shipping in the north-east Atlantic: Identifying spatial and temporal patterns of change. *Marine Pollution Bulletin, 179*, 113681. 10.1016/j.marpolbul.2022.113681.

Robertson, B., Bekker, J., & Buckham, B. (2020). Renewable integration for remote communities: Comparative allowable cost analyses for hydro, solar and wave energy. *Applied Energy, 264*, 114677. 10.1016/j.apenergy.2020.114677.

Robins, P. E., Neill, S. P., Lewis, M. J., & Ward, S. L. (2015). Characterising the spatial and temporal variability of the tidal-stream energy resource over the northwest European shelf seas. *Applied Energy, 147*, 510-522. 10.1016/j.apenergy.2015.03.045.

Rodrigues, N., Pintassilgo, P., Calhau, F., González-Gorbeña, E., & Pacheco, A. (2021). Cost-benefit analysis of tidal energy production in a coastal lagoon: The case of Ria Formosa – Portugal. *Energy, 229*, 120812. 10.1016/j.energy.2021.120812.

Rosa-Santos, P., Taveira-Pinto, F., Rodríguez, C. A., Ramos, V., & López, M. (2019). The CECO wave energy converter: Recent developments. *Renewable Energy, 139*, 368-384. 10.1016/j.renene.2019.02.081.

Saini, G., & Saini, R. P. (2019). A review on technology, configurations, and performance of cross-flow hydrokinetic turbines. *International Journal of Energy Research, 43*(13), 6639-6679. 10.1002/er.4625.

Sánchez, M., Carballo, R., Ramos, V., & Iglesias, G. (2014). Energy production from tidal currents in an estuary: A comparative study of floating and bottom-fixed turbines. *Energy, 77*, 802-811. 10.1016/j.energy.2014.09.053.

Sánchez-Úbeda, J. P., Calvache, M. L., Duque, C., & López-Chicano, M. (2016). Filtering methods in tidal-affected groundwater head measurements: Application of harmonic analysis and continuous wavelet transform. *Advances in Water Resources, 97*, 52-72. 10.1016/j.advwatres.2016.08.016.

Santa Catarina, A. (2022). Wind power generation in Brazil: An overview about investment and scale analysis in 758 projects using the Levelized Cost of Energy. *Energy Policy, 164*, 112830. 10.1016/j.enpol.2022.112830.

Segura, E., Morales, R., & Somolinos, J. A. (2017). Cost Assessment Methodology and Economic Viability of Tidal Energy Projects. *Energies, 10*(11), 1806. 10.3390/en10111806.

Segura, E., Morales, R., & Somolinos, J. A. (2018). Economic-financial modeling for marine current harnessing projects. *Energy, 158*, 859-880. 10.1016/j.energy.2018.06.035.

Segura, E., Morales, R., & Somolinos, J. A. (2019a). Increasing the Competitiveness of Tidal Systems by Means of the Improvement of Installation and Maintenance Maneuvers in First Generation Tidal Energy Converters—An Economic Argumentation. *Energies, 12*(13), 2464. 10.3390/en12132464.

Segura, E., Morales, R., & Somolinos, J. A. (2019b). Influence of Automated Maneuvers on the Economic Feasibility of Tidal Energy Farms. *Sustainability, 11*(21), 5965. 10.3390/su11215965.

Segura, E., Morales, R., Somolinos, J. A., & López, A. (2017). Techno-economic challenges of tidal energy conversion systems: Current status and trends. *Renewable and Sustainable Energy Reviews, 77*, 536-550. 10.1016/j.rser.2017.04.054.

Seo, J., Yi, J., Park, J., & Lee, K. (2019). Review of tidal characteristics of Uldolmok Strait and optimal design of blade shape for horizontal axis tidal current turbines. *Renewable and Sustainable Energy Reviews, 113*, 109273. 10.1016/j.rser.2019.109273.

Sheehan, T. L., & Healy, M. G. (2006). Sub-Recent Changes in Annual Average Water Level in the Shannon Estuary, Western Ireland. *Journal of Coastal Research, 39*, 193-197.

Shields, M., Beiter, P., Nunemaker, J., Cooperman, A., & Duffy, P. (2021). Impacts of turbine and plant upsizing on the levelized cost of energy for offshore wind. *Applied Energy, 298*, 117189. 10.1016/j.apenergy.2021.117189.

Si, Y., Liu, X., Wang, T., Feng, B., Qian, P., Ma, Y., & Zhang, D. (2022). State-of-the-art review and future trends of development of tidal current energy converters in China. *Renewable and Sustainable Energy Reviews, 167*, 112720. 10.1016/j.rser.2022.112720.

Sibtain, M., Li, X., Bashir, H., & Azam, M. I. (2021). Hydropower exploitation for Pakistan's sustainable development: A SWOT analysis considering current situation, challenges, and prospects. *Energy Strategy Reviews, 38*, 100728. 10.1016/j.esr.2021.100728.

SIFP Steering Group. (2013). Strategic Integrated Framework Plan (SIFP) for the Shannon Estuary - An inter-jurisdictional land and marine based framework to guide the future developments and management of the Shannon Estuary.

Souto, C., Gilcoto, M., Fariña-Busto, L., & Pérez, F. F. (2003). Modeling the residual circulation of a coastal embayment affected by wind-driven upwelling: Circulation of the Ría de Vigo (NW Spain). *Journal of Geophysical Research, 108*(C11), 4-18. 10.1029/2002JC001512.

Delorm, T., Zappala, D. & Tavner, P.J. (2012). Tidal stream device reliability comparison models. *Proceedings of the Institution of Mechanical Engineers, Part O: Journal of Risk and Reliability, 226*(1), 6-17. 10.1177/1748006X11422620.

Taveira-Pinto, F., Rosa-Santos, P., & Fazeres-Ferradosa, T. (2020). Marine renewable energy. *Renewable Energy, 150*, 1160-1164. 10.1016/j.renene.2019.10.014.

Technomare SpA, I. P. L. (1996). *Non Nuclear Energy – JOULE II. Wave energy project results. The Exploitation of Tidal Marine Currents*. EU JOULE contract JOU2-CT94-0355.

Thiébaut, M., & Sentchev, A. (2016). Tidal stream resource assessment in the Dover Strait (eastern English Channel). *International Journal of Marine Energy, 16*, 262-278. 10.1016/j.ijome.2016.08.004.

Thiébot, J., Guillou, S., & Droniou, E. (2020). Influence of the 18.6-year lunar nodal cycle on the tidal resource of the Alderney Race, France. *Applied Ocean Research, 97*, 102107. 10.1016/j.apor.2020.102107.

Todeschini, G., Coles, D., Lewis, M., Popov, I., Angeloudis, A., Fairley, I., Johnson, F., Williams, A. J., Robins, P., & Masters, I. (2022). Medium-term variability of the UK's combined tidal energy resource for a net-zero carbon grid. *Energy, 238*, 121990. 10.1016/j.energy.2021.121990.

Torres López, S., Varela, R. A., & Delhez, E. (2001). Residual circulation and thermohaline distribution of the Ría de Vigo: a 3-D hydrodynamic model. *Scientia Marina, 65*(1), 277-289. 10.3989/scimar.2001.65s1277.

Tunio, I. A., Shah, M. A., Hussain, T., Harijan, K., Mirjat, N. H., & Memon, A. H. (2020). Investigation of duct augmented system effect on the overall performance of straight blade Darrieus hydrokinetic turbine. *Renewable Energy, 153*, 143-154. 10.1016/j.renene.2020.02.012.

Vázquez, A., & Iglesias, G. (2015). LCOE (levelised cost of energy) mapping: A new geospatial tool for tidal stream energy. *Energy, 91*, 192-201. 10.1016/j.energy.2015.08.012.

Vázquez, A., & Iglesias, G. (2016a). Capital costs in tidal stream energy projects – A spatial approach. *Energy, 107*, 215-226. 10.1016/j.energy.2016.03.123.

Vázquez, A., & Iglesias, G. (2016b). A holistic method for selecting tidal stream energy hotspots under technical, economic and functional constraints. *Energy Conversion and Management, 117*, 420-430. 10.1016/j.enconman.2016.03.012.

Vázquez, A., & Iglesias, G. (2016c). Grid parity in tidal stream energy projects: An assessment of financial, technological and economic LCOE input parameters. *Technological Forecasting and Social Change, 104*, 89-101. 10.1016/j.techfore.2015.12.007.

Vespe, M., Gibin, M., Alessandrini, A., Natale, F., Mazzarella, F., & Osio, G. C. (2016). Mapping EU fishing activities using ship tracking data. *Journal of Maps 12*, 520-525. 10.1080/17445647.2016.1195299.

Yang, Z., Wang, T., Branch, R., Xiao, Z., & Deb, M. (2021). Tidal stream energy resource characterization in the Salish Sea. *Renewable Energy, 172*, 188-208. 10.1016/j.renene.2021.03.028.

Z. Ren, Y. Wang, H. Li, X. Liu, Y. Wen, & W. Li. (2019). A Coordinated Planning Method for Micrositing of Tidal Current Turbines and Collector System Optimization in Tidal Current Farms. *IEEE Transactions on Power Systems, 34*(1), 292-302. 10.1109/TPWRS.2018.2865310.

Zhai, M., Huang, G., Liu, L., Zheng, B., & Li, Y. (2021). Economic modeling of national energy, water and air pollution nexus in China under changing climate conditions. *Renewable Energy, 170*, 375-386. 10.1016/j.renene.2021.01.011.

Zhang, J., Cheng, C., Yu, S., Wu, H., & Gao, M. (2021). Sharing hydropower flexibility in interconnected power systems: A case study for the China Southern power grid. *Applied Energy, 288*, 116645. 10.1016/j.apenergy.2021.116645.

Zhao, Y., Xu, K., Dong, N., & Wang, H. (2022). Projection of climate change impacts on hydropower in the source region of the Yangtze River based on CMIP6. *Journal of Hydrology, 606*, 127453. 10.1016/j.jhydrol.2022.127453.

# INDEX OF FIGURES

## Chapter 4

**Chapter 5**



**Chapter 6**

# INDEX OF TABLES

## Chapter 4



## Chapter 5



## Chapter 6

# APPENDIX 1
# EXTENDED ABSTRACT
# (IN GALICIAN)

O cambio climático e o quecemento global centraron o interese das sociedades do século XXI en dous aspectos medioambientais clave: (i) as emisións de gases de efecto invernadoiro e (ii) a contaminación do aire. Estes problemas teñen unha importancia particular nas zonas costeiras, caracterizadas por unha intensa actividade socioeconómica e, en consecuencia, por un elevado consumo de enerxía (Bailey & Solomon, 2004; Lonati et al., 2010). Neste contexto, o interese polas fontes de enerxía libres de carbono experimentou un crecemento exponencial, coas enerxías renovables mariñas (ERMs) gañando recoñecemento coma un contribuínte significativo ao sector da enerxía verde e tendo o potencial de reducir de xeito significativo as emisións de gases de efecto invernadoiro e, polo tanto, mitigar o cambio climático (Ramos et al., 2021).

Entre as diferentes formas de ERM, a enerxía hidrocinética sitúase como unha opción a destacar. Representa un tipo específico de enerxía hidroeléctrica resultante da acción combinada das correntes de marea e dos fluxos barotrópicos resultantes das descargas fluviais (Fouz et al., 2019), destacando pola súa facilidade de predición (Carballo et al., 2009), a produción de electricidade de alta calidade (Lewis et al., 2019) e o seu reducido impacto ambiental (Brooks, 2011). Os estuarios, caracterizados por fortes correntes de marea e, en ocasións, cuantiosas descargas fluviais, representan lugares prometedores para a explotación da enerxía hidrocinética (Fouz et al., 2019; Iglesias, I. et al., 2021). Nos últimos anos, realizáronse esforzos significativos no desenvolvemento de convertedores de enerxía hidrocinética (HECs, polas súas siglas en inglés), particularmente turbinas hidrocinéticas (Kamal & Saini, 2022; Khan et al., 2009), e na identificación de áreas óptimas para a súa operación. Habitualmente, os procedementos de selección de emprazamento realízanse en base ao recurso enerxético dispoñible (p.ex., Carballo et al., 2009; Fouz et al., 2019; Mejía-Olivares et al., 2018; Ramos et al., 2014; Robins et al., 2015; Sánchez et al., 2014; Yang et al., 2021), con só un puñado de estudos que incorporan parámetros xeomorfolóxicos como a profundidade da auga (p.ex., Iglesias, G. et al., 2012). Con todo, á medida que avanzan os proxectos, consideracións adicionais como factores socioeconómicos e ambientais vólvense cruciais. Neste contexto, asegurar a coexistencia da explotación enerxética con outras actividades mariñas e considerar os custos de instalación e operación específicos do emprazamento (Castro-Santos et al., 2018) resulta de suma importancia, especialmente en zonas estuarinas, onde varias localizacións poden ter potencial para a implantación de granxas hidrocinéticas (Vázquez & Iglesias, 2016a). Dadas estas complexidades, requírense estudos de detalle para levar a cabo unha tomar de decisións informada. Así, deben desenvolverse métricas fiables para apoiar este proceso, garantindo a viabilidade técnica e económica, incluso nas primeiras etapas do proxecto, permitindo así que os investidores vexan reducidas as incertezas inherentes aos proxectos e á planificación de granxas de enerxía hidrocinética.

Con todo, o desenvolvemento de tales métricas non é sinxelo e require unha descrición detallada de tódolos aspectos relevantes asociados á instalación e operación dunha granxa hidrocinética nunha área costeira específica. Esta descrición debe abarcar non só consideracións técnico-económicas (p.ex., requisitos e restricións técnicas, estrutura de custos, fiabilidade,

mantemento, etc.), senón tamén factores hidrodinámicos. Unha caracterización detallada da hidrodinámica costeira é particularmente crucial, especialmente en estuarios suxeitos a importantes descargas fluviais, onde a súa influencia na variabilidade do recurso enerxético dispoñible (p.ex., variabilidade intraanual ou estacionalidade) e a súa interacción cos fluxos de marea non foron investigadas adecuadamente.

Polo contrario, numerosas investigacións intentaron abordar o desafío da localización de granxas de corrente de marea en zonas costeiras onde a hidrodinámica está principalmente dominada pola acción da marea e a variabilidade do recurso enerxético é practicamente nula. Aínda que as descargas fluviais están habitualmente presentes nesas zonas costeiras, estas xogan, en xeral, un papel secundario, como resultado da súa reducida importancia en comparación co prisma de marea; non obstante, poden ter unha importancia significativa en localizacións específicas. Ademais, estes estudos xeralmente céntranse en zonas costeiras de profundidade limitada (p.ex., partes internas e medias de estuarios pouco profundos) onde a xeomorfoloxía, e especialmente a profundidade da auga, é fundamental para definir os mellores emprazamentos para a explotación da enerxía hidrocinética. Non obstante, no caso de estuarios profundos, a profundidade da auga non xoga o mesmo papel, e a súa influencia nos procedementos de selección de localizacións non foi analizada exhaustivamente, resultando xeralmente na sobreestimación da dispoñibilidade enerxética.

**Esta tese presenta unha metodoloxía cuxa aplicación nunha zona costeira conducirá a un proceso de toma de decisións informado para a explotación do recurso enerxético hidrocinético, superando as limitacións antes mencionadas dos estudos actualmente dispoñibles**. A metodoloxía comprende tres procedementos diferentes, de xeito que cada un dos cales da como resultado unha métrica ou índice diferente, deseñados para etapas específicas da planificación de granxas de enerxía hidrocinética, desde deseños iniciais ata proxectos a gran escala, aumentando en complexidade e precisión á medida que avanza a planificación do proxecto. Estes procedementos, baseados en modelaxe numérica hidrodinámica de alta resolución e técnicas avanzadas de análise xeoespacial e algoritmos, exemplifícanse a través da súa aplicación a un caso de estudo no estuario do Shannon (Oeste de Irlanda), un corpo de auga non limitado pola profundidade, suxeito a importantes descargas fluviais, e amplamente coñecido polo seu potencial para a explotación da enerxía hidrocinética.

A presente tese está estruturada en oito capítulos, dos cales os Capítulos 4, 5 e 6 correspóndense con sendas publicacións en revistas científicas, constituíndo o núcleo principal da tese. Primeiro, o Capítulo 1 ofrece unha perspectiva xeral deste traballo. A continuación, no Capítulo 2, preséntase brevemente a hipótese principal xunto cos obxectivos finais e intermedios, definíndose estes últimos de acordo cos diferentes pasos necesarios para cumprir o obxectivo final proposto. Seguidamente, no Capítulo 3, introdúcense brevemente os principais aspectos metodolóxicos desta tese poñéndoos en conexión co obxectivo intermedio e artigo de investigación no cal son desenvolvidos e implementados. A continuación, nos **Capítulos 4** – ***Tidal stream energy potential in the Shannon Estuary***, publicado en *Renewable Energy*, **5** – ***A holistic methdolody for hydrokinetic energy site selection***, publicado en *Applied Energy*, e **6** – ***A methodology for cost-effective analysis of hydrokinetic energy projects***, publicado en *Energy*, exponse de xeito detallado o desenvolvemento metodoloxía proposta, así coma a súa aplicación no estuario do Shannon, abordándose en cada un deles diferentes aspectos específicos e fundamentais para a consecución do obxectivo final desta tese. Posteriormente, no Capítulo 7, realízase unha análise integral dos resultados obtidos nos capítulos precedentes (Capítulos 4 a 6) para describir adecuadamente a súa importancia dentro do contexto xeral deste traballo, e garantindo así a comprensión do lector sobre a presente investigación coma un conxunto. Finalmente, no Capítulo 8, preséntanse os principais

resultados de forma sintética xunto cos futuros traballos de investigación xa planificados, parte dos cales está actualmente en desenvolvemento.

A continuación, preséntase de forma sintética a metodoloxía proposta, resumindo os seus aspectos máis destacados, así coma os resultados e as principais conclusións obtidas.

Esta tese presenta unha metodoloxía completa para a toma de decisións respecto da explotación da enerxía hidrocinética dentro dunha rexión costeira, proporcionando toda a información relevante para instalar unha granxa de enerxía hidrocinética. A metodoloxía consta de tres procedementos principais, cada un deles dando lugar a un índice diferente, cuxa complexidade e precisión aumentan á medida que avanza a planificación do proxecto, pasando da identificación preliminar de áreas axeitadas para a instalación de deseños iniciais á avaliación detallada de localizacións específicas para a instalación de proxectos a gran escala. Estes procedementos son os correspondentes aos índices: (i) $TSE_{ndl}$, *Tidal Stream Exploitability index adapted to non-depth-limited areas* (Capítulo 4); (ii) IHE, *Integrated Hydrokinetic Energy index* (Capítulo 5); e (iii) $LCOE_{IHE,}$ *Cost-Effective Analysis* (CEA) *in terms of Levelized Costs of Energy based on the* IHE *index* (Capítulo 6).

O desenvolvemento e implementación do índice $TSE_{ndl}$ —unha versión revisada do *Tidal Stream Exploitability* (TSE) *index* (Iglesias, G. et al., 2012), adaptada para a súa aplicación zonas costeiras de profundidade non limitada— implica varios pasos clave. Primeiramente, é necesario avaliar o potencial da enerxía hidrocinética (isto é, resultante da acción conxunta das correntes de marea e os fluxos fluviais) dentro dunha rexión costeira. Isto require dunha caracterización precisa dos fluxos mareais e fluviais, así como da súa interacción, a cal se leva a cabo a través da implementación de alta resolución dun modelo numérico de augas pouco profundas no estuario do Shannon. A aplicación desta técnica de modelaxe numérica permite unha análise precisa da distribución espazo-temporal do recurso enerxético mediante a consideración de varios casos de estudo.

Dada a variabilidade dos réximes hidrolóxicos, á hora de definir estes casos de estudo, é importante poder capturar non só a variabilidade dos ciclos mareais, senón tamén das descargas fluviais, de xeito que permita analizar a variación intraanual das correntes inducidas por ditas descargas. Polo tanto, analízanse catro escenarios estacionais característicos, cubrindo un ciclo completo de mareas vivas-mortas medias (é dicir, 14.75 días, aproximadamente) baixo descargas fluviais estacionais. Esta análise proporciona información sobre a magnitude e distribución dos recursos de enerxía hidrocinética e a súa dependencia dos caudais fluviais. Posteriormente, unha vez determinadas as características xerais do recurso hidrocinético, o modelo é executado durante todo un ano considerando as descargas medias mensuais dos ríos para calcular con precisión o recurso total dispoñible xunto con outros parámetros de interese (Álvarez et al., 2020). Non obstante, estes escenarios estacionais e anuais non son suficientes para unha selección axeitada do emprazamento, xa que non consideran factores cruciais como a profundidade da auga. Por iso, o índice $TSE_{ndl}$ calcúlase nun ciclo de marea durante mareas vivas e baixo a acción de descargas fluviais medias e das condicións termohalinas.

Este índice permite delimitar zonas aptas para o aproveitamento enerxético hidrocinético, caracterizando as zonas seleccionadas en función do seu nivel de interese en base a límites específicos. Na presente aplicación, adóptanse os valores de $TSE_{ndl}$ maior ou igual que 1 e 2 para denotar zonas de interese e de moito interese respectivamente. A selección preliminar do emprazamento baseada no índice $TSE_{ndl}$ é examinada máis a fondo a través dunha análise numérica de alta resolución temporal, seleccionando para isto dous puntos significativos dentro de cada zona previamente delimitada: aqueles correspondentes ao valor máximo e medio do índice dentro de cada zona.

Aínda que a información proporcionada polo índice $TSE_{ndl}$ pode resultar valiosa nas etapas preliminares do proxecto, a decisión final respecto á instalación dunha granxa de enerxía hidrocinética require un enfoque integrado, tendo en conta aspectos relativos á Planificación Espacial Mariña, e en particular os factores ambientais e socioeconómicos, incluíndo o cálculo dos custos de instalación da mesma. Estes aspectos abórdanse detalladamente no segundo procedemento considerado, o índice IHE.

O segundo procedemento desenvolvido na presente tese consiste na conceptualización e aplicación do índice IHE, que integra tres factores clave para a selección de emprazamentos para o aproveitamento da enerxía hidrocinética (Vázquez & Iglesias, 2016b): (i) o recurso explotable (é dicir, aquel que é efectivamente aproveitable por un convertedor, xa que se atopa dentro do seu rango de operación), que se determina a través do modelo numérico de alta resolución implementado no Capítulo 4; (ii) a configuración xeomorfolóxica, cuxa influencia se determina de xeito paramétrico mediante a relación entre os principais custos de instalación (CAPEX, polas súas siglas en inglés) e as variables máis características da configuración costeira, distancia a costa e profundidade da auga, permitindo así penalizar aquelas zonas onde a instalación dun aproveitamento enerxético resultaría máis antieconómica; e, finalmente, (iii) os aspectos socioeconómicos (acuicultura, marisqueo e navegación) e ambientais (Zonas de Especial Conservación e Zonas de Especial Protección, SACs e SPAs polas súas siglas en inglés respectivamente, ambas contempladas na Rede Natura 2000), que son considerados no índice mediante o tratamento dunha inxente cantidade de datos xeoespaciais, permitindo así analizar a coexistencia do aproveitamento enerxético con outros usos costeiros actuais ou potenciais.

Deste xeito, a interpretación física do índice IHE é sinxela. Canto máis alto sexa o índice IHE, mellor será o emprazamento para a explotación da enerxía hidrocinética, con valores superiores a 1 indicando a idoneidade para a explotación da enerxía hidrocinética. Isto correspondería cun emprazamento cun IHE = 1 (valor mínimo para a idoneidade), e sen ningunha penalización en termos de CAPEX (e por tanto xeomorfolóxicos) e aspectos socioeconómicos ou ambientais. Así, ao ter en consideración tódolos aspectos involucrados na definición do emprazamento, o índice proporciona unha interpretación clara da idoneidade deste. Os resultados da implementación do índice IHE servirán de base para seleccionar as localizacións máis apropiadas para a conversión de enerxía hidrocinética nunha rexión costeira, reducindo as incertezas na planificación de proxectos comerciais nas súas primeiras etapas. O deseño final da configuración do aproveitamento enerxético en etapas posteriores do proxecto requiriría dunha análise detallada da rendibilidade das diferentes alternativas posibles de convertedor e emprazamento, para o cal se deseña o derradeiro procedemento contemplado na presente tese, o $LCOE_{IHE}$.

Finalmente, o terceiro e último procedemento desenvolvido nesta tese consiste en facer dispoñible un novo enfoque para calcular con precisión os parámetros de análise custo-beneficio (CEA, polas súas siglas en inglés) dos proxectos de enerxía hidrocinética. Para isto, na presente aplicación recórrese ao calculo dos custos nivelados da enerxía (LCOE, polas súas siglas en inglés), baseados nos resultados da aplicación do índice IHE, o que dá lugar a un novo parámetro denominado $LCOE_{IHE}$, cuxa determinación levaría á selección da combinación óptima de convertedor e emprazamento para instalar unha granxa hidrocinética nunha zona costeira (Bahaj et al., 2008; Si et al., 2022).

Este novo enfoque abrangue catro aspectos: (i) a definición de combinacións factibles de convertedor e emprazamento, baseada na análise espacial do índice IHE e na delimitación de zonas de interese realizada a partir deste (Capítulo 5); (ii) a avaliación da produción de enerxía das diferentes alternativas definidas en (i), calculada mediante resultados numéricos de alta resolución (Capítulo 5), que son tratados novamente para considerar adecuadamente a

variabilidade espacial do recurso enerxético e garantir a precisión dos resultados; (iii) a análise detallada do CAPEX do aproveitamento, incluíndo custos de enxeñaría e xestión, fabricación e instalación, xunto cos efectos das economías de escala, realizada mediante a combinación dun estudo de detalle dos custos unitarios, deseños xenéricos representativos de HECs e análises paramétricas das granxas hidrocinéticas propostas respectivamente; e finalmente, (iv) o cálculo do OPEX da granxa, incluíndo seguros e custos fixos, mantemento programado ou preventivo e mantemento non programado ou correctivo, considerando datos de fiabilidade dos HECs, a definición de fiestras meteorolóxicas baseadas en modelaxe numérica hidrodinámica de alta resolución (Capítulo 5) e varios procedementos de operación e mantemento (O&M) dependendo da configuración da granxa.

Deste xeito, a interpretación física do índice $LCOE_{IHE}$ é sinxela. Canto máis baixo sexa o índice, e en consecuencia o parámetro coste-beneficio da alternativa analizada (neste caso, €/kWh, xa que se leva a cabo en termos de LCOE), mellor será o emprazamento para a explotación da enerxía hidrocinética. Ademais, o enfoque proposto aborda as principais dificultades e incertezas á hora de calcular os aspectos que, dun xeito máis destacado, afectan ao CEA das granxas de enerxía hidrocinética, evitando suposicións simplistas e non fiables que poidan resultar nunha sobreestimación significativa do OPEX, especialmente no caso de grandes granxas, e mellorando en xeral os procedementos actuais.

A metodoloxía presentada é aplicada ao estuario do Shannon nos Capítulos 4, 5 e 6, cada un deles focalizado nun aspecto específico da súa aplicación, e por tanto nun procedemento ou índice, de modo que esta pode ser totalmente desenvolvida para as características desta zona costeira, así como proporcionar a información necesaria para poder aplicala noutra rexión costeira de interese para o aproveitamento enerxético hidrocinético. Cabe destacar que o seu desenvolvemento implica facer dispoñible un gran conxunto de datos de modelaxe numérica hidrodinámica de alta resolución e a súa análise a través de procedementos de análise xeoespacial de vangarda, conducindo á aplicación dos diferentes procedementos, cuxo obxectivo final é o cálculo dunha métrica ou índice específico, que sirva para proporcionar un apoio fiable no proceso de toma de decisións dunha etapa concreta da planificación do aproveitamento hidrocinético, desde deseños iniciais ata proxectos a gran escala, aumentando en complexidade e precisión á medida que avanzan as fases do proxecto.

No **Capítulo 4 – *Tidal stream energy potential in the Shannon Estuary***, lévase a cabo o desenvolvemento e aplicación do índice $TSE_{ndl}$. Este constitúe unha adaptación do chamado índice TSE, anteriormente aplicado para a selección preliminar de emprazamentos de granxas de correntes de marea en zonas costeiras con limitación de profundidade (p.ex., parte interior ou media de estuarios pouco profundos), pero agora revisado para a súa aplicación axeitada a zonas sen limitación de profundidade (p.ex., estuarios profundos), como o estuario do Shannon. A aplicación do índice TSE a zonas costeiras sen profundidade limitada levaría a unha selección inadecuada do emprazamento, como resultado de considerar cifras de recurso enerxético sobreestimadas, en consecuencia co papel que xoga a profundidade da auga, que difire daquel en zonas de profundidade limitada, requirindo dunha adaptación para a súa aplicación precisa. Con este fin, desenvolveuse unha nova función de penalización-limitación, $\xi_{ndl}$, definindo un novo rango na anterior función de penalización, $\xi$, dado por un valor límite de profundidade por riba do cal os valores de $TSE_{ndl}$ están limitados aos correspondentes a esta profundidade da auga limitada, que se estableceu tendo en conta as características das tecnoloxías de conversión de enerxía actualmente dispoñibles. A aplicación deste procedemento posibilita a delimitación de grandes áreas con potencialidade para o aproveitamento da enerxía hidrocinética, permitindo así a súa aplicación en proxectos de ERM en fases preliminares. Como resultado da aplicación do índice $TSE_{ndl}$ ao estuario do Shannon, un total de sete áreas (Áreas I a VII) adecuadas para

a conversión de enerxía hidrocinética foron delimitadas de xeito preliminar, considerando límites específicos do valor do índice e aplicando técnicas de análise espacial. Con todo, os pasos seguintes na planificación de granxas de enerxía hidrocinética deberían considerar non só o recurso enerxético dispoñible, senón tamén outros aspectos relevantes, como a explotabilidade deste recurso enerxético, xunto con restricións socioeconómicas e ambientais, cuxa consideración conduciu ao paso inicial para o desenvolvemento e implementación do índice IHE.

Neste senso, no **Capítulo 5 – *A holistic methodology for hydrokinetic energy site selection***, preséntase o desenvolvemento e aplicación do índice IHE. Dito índice constitúe unha ferramenta integral para seleccionar as mellores zonas para a explotación de enerxía hidrocinética en rexións costeiras, considerando a dispoñibilidade de recursos enerxéticos, os custos de instalación e os factores socioeconómicos e ambientais, superando así as limitacións de considerar tecnoloxías de conversión específicas ou deseños concretos de granxa e permitindo a súa aplicación en proxectos de ERM en fases pouco avanzadas. A súa implementación implica catro pasos: (i) caracterizar a distribución espacial do recurso enerxético explotable mediante o índice de Enerxía Hidrocinética (HE, polas súas siglas en inglés); (ii) determinar os custos de instalación resultantes da configuración costeira (isto é, profundidade da auga e distancia á liña de costa) a través da función de penalización xeoespacial de custos ($C_{gp}$, polas súas siglas en inglés); (iii) avaliar a coexistencia da explotación de enerxía hidrocinética co resto dos usos costeiros existentes ou potenciais mediante a implementación da función de penalización xeoespacial de uso da auga ($U_{gp}$, polas súas siglas en inglés); e, finalmente, (iv) integrar os pasos anteriores (i a iii) para obter o índice IHE. A interpretación física do índice e os termos que o constitúen son os seguintes. Os valores de HE iguais ou superiores a 1 indican aptitude para a operación de enerxía hidrocinética, sen considerar outras restricións; en relación cos termos de penalización, $C_{gp}$ e $U_{gp}$, varían de 1 (sen restrición) a 0 (restrición total). Por conseguinte, canto maior sexa o índice IHE, máis favorable será o emprazamento para a explotación de enerxía hidrocinética, con valores iguais ou superiores a 1 indicando aptitude para tales operacións. Como resultado da súa aplicación ao estuario do Shannon, o índice IHE identificou seis áreas (Área $I_{IHE}$ a Área $VI_{IHE}$) con valores de IHE superiores a 1 e, polo tanto, indicativos de aptitude para a conversión de enerxía hidrocinética, que difiren das seleccionadas en estudos anteriores. A área máis adecuada, Área $IV_{IHE}$, preto de Tarbert, ocupa unha superficie menor con recursos algo inferiores e menos restricións en comparación coa identificada mediante o índice $TSE_{ndl}$. Con todo, unha vez identificada a mellor área para instalar unha granxa hidrocinética, a definición final desta granxa require unha análise detallada dos custos das diferentes combinacións de convertedor e emprazamento, para o que se desenvolve e aplica unha metodoloxía en termos de LCOE baseada nos resultados do índice IHE, $LCOE_{IHE}$.

Así, finalmente, no **Capítulo 6 – *A methodology for cost-effective analysis of hydrokinetic energy projects***, preséntase o desenvolvemento e aplicación do procedemento conducente ao calculo do parámetro $LCOE_{IHE}$. Este constitúe un procedemento totalmente novo para realizar unha análise precisa e efectiva de custos de proxectos de enerxía hidrocinética, evitando enfoques simplificados e, por tanto, unha planificación subóptima do aproveitamento enerxético. En resumo, proporciona unha nova aproximación que leva á selección da combinación de convertedor e emprazamento máis adecuada dentro dunha área costeira de interese, posibilitando a súa análise detallada en proxectos de ERM na súa fase final e mellorando así os procedementos anteriormente dispoñibles. A súa implementación consta de cinco pasos: (i) a definición das diferentes combinacións de convertedor e emprazamento factibles a través dun modelo de vangarda para a selección destas combinacións baseado no

índice IHE e algoritmos de análise espacial; (ii) a avaliación da produción de enerxía das diferentes alternativas definidas en (i); (iii) o cálculo do CAPEX a través dun estudo de detalle do seus custos unitarios; (iv) a avaliación do OPEX considerando procedementos de O&M específicos para diferentes tipos de convertedores, incluíndo a análise dos diferentes recursos e o tempo implicado; e, finalmente, (v) a integración dos resultados dos pasos anteriores (i a iv) para proporcionar parámetros de análise de custo-beneficio fiables para as diferentes combinacións de convertedor e emprazamento, levando á selección da mellor alternativa. Este procedemento ilústrase para o estuario do Shannon, especificamente a Área de Tarbert, obtendo os parámetros de análise de custo-beneficio en termos de LCOE. Esta análise revela que a área con mellor rendemento e cifras do índice IHE non é necesariamente a máis rendible; polo contrario, as economías de escala favorecen unha área maior con menos recursos dispoñibles pero mellores cifras en termos de custo-beneficio. Consecuentemente, a combinación de convertedor e emprazamento con mellores resultados en termos de custo-beneficio é instalar a tecnoloxía F-HEC (flotante) no polígono C, cun $LCOE_{IHE}$ de 0.196 €/kWh. Ao comparar os resultados de $LCOE_{IHE}$ cos obtidos mediante a aplicación de procedementos desenvolvidos en traballos previos (Allan et al., 2011; Ernst, 2007; Ernst, 2010; Vázquez & Iglesias, 2015; Vázquez & Iglesias, 2016a; Vázquez & Iglesias, 2016b), obsérvanse sobreestimacións significativas, que van desde aproximadamente o 40% ao 165%. Estas discrepancias derivan dos cálculos do OPEX, excesivamente simplificados nas metodoloxías anteriores, as cales sobreestiman de xeito significativo os custos para grandes instalacións de aproveitamento enerxético.

A metodoloxía presentada e os procedementos que a constitúen poderían ser utilizado para proporcionar información semellante en calquera outra rexión costeira de interese para a explotación de enerxía hidrocinética onde estean dispoñibles os datos xeoespaciais necesarios (condicionantes socioeconómicos, xeomorfolóxicos e medioambientais). Finalmente, cabe mencionar que se fixo un esforzo intenso nos últimos meses para ampliar os procedementos aquí desenvolvidos para considerar detalladamente a variabilidade intraanual no recurso enerxético hidrocinético (p.ex., períodos de tempo máis curtos que as estacións), o que conduce á súa aplicación en áreas estuarinas cuxa hidrodinámica está totalmente dominada polas descargas fluviais. Neste senso, están en desenvolvemento novos parámetros que teñen en conta a variabilidade no recurso hidrocinético.

# APPENDIX 2
# EXTENDED ABSTRACT
# (IN SPANISH)

El cambio climático y el calentamiento global centraron el interés de las sociedades del siglo XXI en dos aspectos medioambientales clave: (i) las emisiones de gases de efecto invernadero y (ii) la contaminación del aire. Estos problemas tienen una importancia particular en las zonas costeras, caracterizadas por una intensa actividad socioeconómica y, en consecuencia, por un elevado consumo de energía (Bailey & Solomon, 2004; Lonati et al., 2010). En este contexto, el interés por las fuentes de energía libres de carbono ha experimentado un crecimiento exponencial, con las energías renovables marinas (ERMs) ganando reconocimiento como un contribuyente significativo al sector de la energía verde y con el potencial de reducir de manera significativa las emisiones de gases de efecto invernadero y, por lo tanto, mitigar el cambio climático (Ramos et al., 2021).

Entre las diferentes formas de ERM, la energía hidrocinética se sitúa como una opción a destacar. Representa un tipo específico de energía hidroeléctrica resultante de la acción combinada de las corrientes de marea y de los flujos barotrópicos resultantes de las descargas fluviales (Fouz et al., 2019), destacando por su facilidad de predicción (Carballo et al., 2009), la producción de electricidad de alta calidad (Lewis et al., 2019) y su reducido impacto ambiental (Brooks, 2011). Los estuarios, caracterizados por fuertes corrientes de marea y, en ocasiones, cuantiosas descargas fluviales, representan lugares prometedores para la explotación de la energía hidrocinética (Fouz et al., 2019; Iglesias, I. et al., 2021). En los últimos años se realizaron esfuerzos significativos en el desarrollo de convertidores de energía hidrocinética (HECs, por sus siglas en inglés), particularmente turbinas hidrocinéticas (Kamal & Saini, 2022; Khan et al., 2009), y en la identificación de zonas óptimas para su operación. Habitualmente, los procedimientos de selección de emplazamiento se realizan en base al recurso energético disponible (p.ej., Carballo et al., 2009; Fouz et al., 2019; Mejía-Olivares et al., 2018; Ramos et al., 2014; Robins et al., 2015; Sánchez et al., 2014; Yang et al., 2021), con sólo un puñado de estudios que incorporan parámetros geomorfológicos como la profundidad del agua (p.ej., Iglesias, G. et al., 2012). Con todo, a medida que avanzan los proyectos, consideraciones adicionales como factores socioeconómicos y ambientales se vuelven cruciales. En este contexto, asegurar la coexistencia de la explotación energética con otras actividades marinas y considerar los costes de instalación y operación específicos del emplazamiento (Castro-Santos et al., 2018) resulta de suma importancia, especialmente en zonas estuarinas, donde varias localizaciones pueden tener potencial para la implantación de granjas hidrocinéticas (Vázquez & Iglesias, 2016a). Dadas estas complejidades, se requieren estudios de detalle para llevar a cabo una tomar de decisiones informada. Así, deben desarrollarse métricas fiables para apoyar este proceso, garantizando la viabilidad técnica y económica, incluso en las primeras etapas del proyecto, permitiendo así que los inversores vean reducidas las incertidumbres inherentes a los proyectos y a la planificación de granjas de energía hidrocinética.

Con todo, el desarrollo de tales métricas no es sencillo y requiere una descripción detallada de todos los aspectos relevantes asociados a la instalación y operación de una granja hidrocinética en una zona costera específica. Esta descripción debe abarcar no sólo consideraciones técnico-económicas (p.ej., requisitos y restricciones técnicas, estructura de

costes, fiabilidad, mantenimiento, etc.), sino también factores hidrodinámicos. Una caracterización detallada de la hidrodinámica costera es particularmente crucial, especialmente en estuarios sujetos a importantes descargas fluviales, donde su influencia en la variabilidad del recurso energético disponible (p.ej., variabilidad intraanual o estacionalidad) y su interacción con los flujos de marea no fueron investigados adecuadamente.

Por el contrario, numerosas investigaciones intentaron abordar el desafío de la localización de granjas de corriente de marea en zonas costeras donde la hidrodinámica está principalmente dominada por la acción de la marea y la variabilidad del recurso energético es prácticamente nula. Aunque las descargas fluviales están habitualmente presentes en esas zonas costeras, estas juegan, en general, un papel secundario, como resultado de su reducida importancia en comparación con el prisma de marea; no obstante, pueden tener una importancia significativa en localizaciones específicas. Además, estos estudios generalmente se centran en zonas costeras de profundidad limitada (p.ej., partes internas y medias de estuarios poco profundos) donde la geomorfología, y especialmente la profundidad del agua, es fundamental para definir los mejores emplazamientos para la explotación de la energía hidrocinética. No obstante, en el caso de estuarios profundos, la profundidad del agua no juega el mismo papel, y su influencia en los procedimientos de selección de localizaciones no fue analizada exhaustivamente, resultando generalmente en la sobreestimación de la disponibilidad energética.

**Esta tesis presenta una metodología cuya aplicación en una zona costera conducirá a un proceso de toma de decisiones informado para la explotación del recurso energético hidrocinético, superando las limitaciones antes mencionadas de los estudios actualmente disponibles**. La metodología comprende tres procedimientos diferentes, de forma que cada uno de los cuales da como resultado una métrica o índice diferente, diseñados para etapas específicas de la planificación de granjas de energía hidrocinética, desde diseños iniciales hasta proyectos a gran escala, aumentando en complejidad y precisión a la medida que avanza la planificación del proyecto. Estos procedimientos, basados en modelización numérica hidrodinámica de alta resolución y técnicas avanzadas de análisis geoespacial y algoritmos, se ejemplifican a través de su aplicación a un caso de estudio en el estuario del Shannon (Oeste de Irlanda), un cuerpo de agua no limitado por la profundidad, sujeto a importantes descargas fluviales, y ampliamente conocido por su potencial para la explotación de la energía hidrocinética.

La presente tesis está estructurada en ocho capítulos, de los cuales los Capítulos 4, 5 y 6 se corresponden con sendas publicaciones en revistas científicas, constituyendo el núcleo principal de la tesis. Primero, el Capítulo 1 ofrece una perspectiva general de este trabajo. A continuación, en el Capítulo 2, se presenta brevemente la hipótesis principal junto con los objetivos finales e intermedios, definiéndose estos últimos de acuerdo con los diferentes pasos necesarios para cumplir el objetivo final propuesto. Seguidamente, en el Capítulo 3, se introducen brevemente los principales aspectos metodológicos de esta tesis poniéndolos en conexión con el objetivo intermedio y artículo de investigación en el cual son desarrollados e implementados. A continuación, en los Capítulos **4 – *Tidal stream energy potential in the Shannon Estuary***, publicado en *Renewable Energy*, **5 – *A holistic methodology for hydrokinetic energy site selection***, publicado en *Applied Energy*, y **6 – *A methodology for cost-effective analysis of hydrokinetic energy projects***, publicado en *Energy*, se expone de manera detallada el desarrollo metodología propuesta, así como su aplicación al estuario del Shannon, abordándose en cada uno de ellos diferentes aspectos específicos y fundamentales para la consecución del objetivo final de esta tesis. Posteriormente, en el Capítulo 7, se realiza un análisis integral de los resultados obtenidos en los capítulos precedentes (Capítulos 4 a 6) para describir adecuadamente su importancia dentro del contexto general de este trabajo, y garantizando así

la comprensión del lector sobre la presente investigación como un conjunto. Finalmente, en el Capítulo 8, se presentan los principales resultados de forma sintética junto con los futuros trabajos de investigación ya planificados, parte de los cuales está actualmente en desarrollo.

A continuación, se presenta de forma sintética la metodología propuesta, resumiendo sus aspectos más destacados, así como los resultados y las principales conclusiones obtenidas.

Esta tesis presenta una metodología completa para la toma de decisiones respecto de la explotación de la energía hidrocinética dentro de una región costera, proporcionando toda la información relevante para instalar una granja de energía hidrocinética. La metodología consta de tres procedimientos principales, cada uno de ellos dando lugar a un índice diferente, cuya complejidad y precisión aumentan a la medida que avanza la planificación del proyecto, pasando de la identificación preliminar de áreas adecuadas para la instalación de diseños iniciales a la evaluación detallada de localizaciones específicas para la instalación de proyectos a gran escala. Estos procedimientos son los correspondientes a los índices: (i) $TSE_{ndl}$, *Tidal Stream Exploitability index adapted to non-depth-limited areas* (Capítulo 4); (ii) IHE, *Integrated Hydrokinetic Energy index* (Capítulo 5); e (iii) $LCOE_{IHE,}$ *Cost-Effective Analysis* (CEA) *in terms of Levelized Costs of Energy based on the* IHE *index* (Capítulo 6).

El desarrollo e implementación del índice $TSE_{ndl}$ —una versión revisada del *Tidal Stream Exploitability* (TSE) *index* (Iglesias, G. et al., 2012), adaptada para su aplicación zonas costeras de profundidad no limitada— implica varios pasos clave. Primeramente, es necesario evaluar el potencial de la energía hidrocinética (esto es, resultante de la acción conjunta de las corrientes de marea y los flujos fluviales) dentro de una región costera. Esto requiere de una caracterización precisa de los flujos mareales y fluviales, así como de su interacción, la cual se lleva a cabo a través de la implementación de alta resolución de un modelo numérico de aguas poco profundas en el estuario del Shannon. La aplicación de esta técnica de modelización numérica permite un análisis preciso de la distribución espacio-temporal del recurso energético mediante la consideración de varios casos de estudio.

Dada la variabilidad de los regímenes hidrológicos, a la hora de definir estos casos de estudio, es importante poder capturar no sólo la variabilidad de los ciclos mareales, sino también de las descargas fluviales, de forma que permita analizar la variación intraanual de las corrientes inducidas por dichas descargas. Por lo tanto, se analizan cuatro escenarios estacionales característicos, cubriendo un ciclo completo de mareas vivas-muertas medias (es decir, 14.75 días, aproximadamente) bajo descargas fluviales estacionales. Este análisis proporciona información sobre la magnitud y distribución de los recursos de energía hidrocinética y su dependencia de los caudales fluviales. Posteriormente, una vez determinadas las características generales del recurso hidrocinético, el modelo es ejecutado durante todo un año considerando las descargas medias mensuales de los ríos para calcular con precisión el recurso total disponible junto con otros parámetros de interés (Álvarez et al., 2020). No obstante, estos escenarios estacionales y anuales no son suficientes para una selección idónea del emplazamiento, ya que no consideran factores cruciales como la profundidad del agua. Por eso, el índice $TSE_{ndl}$ se calcula en un ciclo de marea durante mareas vivas y bajo la acción de descargas fluviales medias y de las condiciones termohalinas.

Este índice permite delimitar zonas aptas para el aprovechamiento energético hidrocinético, caracterizando las zonas seleccionadas en función de su nivel de interés en base a límites específicos. En la presente aplicación, se adoptan los valores de $TSE_{ndl}$ mayor o igual que 1 y 2 para denotar zonas de interés y de mucho interés respectivamente. La selección preliminar del emplazamiento basada en el índice $TSE_{ndl}$ es examinada más a fondo a través de un análisis numérico de alta resolución temporal, seleccionando para esto dos puntos

significativos dentro de cada zona previamente delimitada: aquellos correspondientes al valor máximo y medio del índice dentro de cada zona.

Aunque la información proporcionada por el índice $TSE_{ndl}$ puede resultar valiosa en las etapas preliminares del proyecto, la decisión final respecto a la instalación de una granja de energía hidrocinética requiere un enfoque integrado, teniendo en cuenta aspectos relativos a la Planificación Espacial Marina, y en particular los factores ambientales y socioeconómicos, incluyendo el cálculo de los costes de instalación de la misma. Estos aspectos se abordan detalladamente en el segundo procedimiento considerado, el índice IHE.

El segundo procedimiento desarrollado en la presente tesis consiste en la conceptualización y aplicación del índice IHE, que integra tres factores clave para la selección de emplazamientos para el aprovechamiento de la energía hidrocinética (Vázquez & Iglesias, 2016b): (i) el recurso explotable (es decir, aquel que es efectivamente aprovechable por un convertidor, ya que se encuentra dentro de su rango de operación), que se determina a través del modelo numérico de alta resolución implementado en el Capítulo 4; (ii) la configuración geomorfológica, cuya influencia se determina de forma paramétrica mediante la relación entre los principales costes de instalación (CAPEX, por sus siglas en inglés) y las variables más características de la configuración costera, distancia la costa y profundidad del agua, permitiendo así penalizar aquellas zonas donde la instalación de un aprovechamiento energético resultaría más antieconómica; y, finalmente, (iii) los aspectos socioeconómicos (acuicultura, marisqueo y navegación) y ambientales (Zonas de Especial Conservación y Zonas de Especial Protección, SACs y SPAs por sus siglas en inglés respectivamente, ambas contempladas en la Red Natura 2000), que son considerados en el índice mediante el tratamiento de una ingente cantidad de datos geoespaciales, permitiendo así analizar la coexistencia del aprovechamiento energético con otros usos costeros actuales o potenciales.

De este modo, la interpretación física del índice IHE es sencilla. Cuanto más alto sea el índice IHE, mejor será el emplazamiento para la explotación de la energía hidrocinética, con valores superiores a 1 indicando la idoneidad para la explotación de la energía hidrocinética. Esto se correspondería con un emplazamiento con un IHE = 1 (valor mínimo para la idoneidad), y sin ninguna penalización en términos de CAPEX (y por tanto geomorfológicos) y aspectos socioeconómicos o ambientales. Así, al tener en consideración todos los aspectos involucrados en la definición del emplazamiento, el índice proporciona una interpretación clara de la idoneidad del mismo. Los resultados de la implementación del índice IHE servirán de base para seleccionar las localizaciones más apropiadas para la conversión de energía hidrocinética en una región costera, reduciendo las incertidumbres en la planificación de proyectos comerciales en sus primeras etapas. El diseño final de la configuración del aprovechamiento energético en etapas posteriores del proyecto requeriría de un análisis detallado de la rentabilidad de las diferentes alternativas posibles de convertidor y emplazamiento, para lo cual se diseña el último procedimiento contemplado en la presente tesis, el $LCOE_{IHE}$.

Finalmente, el tercero y último procedimiento desarrollado en esta tesis consiste en hacer disponible un nuevo enfoque para calcular con precisión los parámetros de análisis coste-beneficio (CEA, por sus siglas en inglés) de los proyectos de energía hidrocinética. Para esto, en la presente aplicación se recurre al cálculo de los costes nivelados de la energía (LCOE, por sus siglas en inglés), basados en los resultados de la aplicación del índice IHE, lo que da lugar a un nuevo parámetro denominado $LCOE_{IHE}$, cuya determinación llevaría a la selección de la combinación óptima de convertidor y emplazamiento para instalar una granja hidrocinética en una zona costera (Bahaj et al., 2008; Si et al., 2022).

Este nuevo enfoque abarca cuatro aspectos: (i) la definición de combinaciones factibles de convertidor y emplazamiento, basada en el análisis espacial del índice IHE y en la delimitación

de zonas de interés realizada a partir de este (Capítulo 5); (ii) la evaluación de la producción de energía de las diferentes alternativas definidas en (i), calculada mediante resultados numéricos de alta resolución (Capítulo 5), que son tratados nuevamente para considerar adecuadamente la variabilidad espacial del recurso energético y garantizar la precisión de los resultados; (iii) el análisis detallado del CAPEX del aprovechamiento, incluyendo costes de ingeniería y gestión, fabricación e instalación, junto con los efectos de las economías de escala, realizado mediante la combinación de un estudio de detalle de los costes unitarios, diseños genéricos representativos de HECs y análisis paramétricos de las granjas hidrocinéticas propuestas, respectivamente; y finalmente, (iv) el cálculo del OPEX de la granja, incluyendo seguros y costes fijos, mantenimiento programado o preventivo y mantenimiento no programado o correctivo, considerando datos de fiabilidad de los HECs, la definición de ventanas meteorológicas basadas en modelización numérica hidrodinámica de alta resolución (Capítulo 5) y varios procedimientos de operación y mantenimiento (O&M) dependiendo de la configuración de la granja.

De este modo, la interpretación física del índice $LCOE_{IHE}$ es sencilla. Cuanto más bajo sea el índice, y en consecuencia el parámetro coste-beneficio de la alternativa analizada (en este caso, €/kWh, ya que se lleva a cabo en términos de LCOE), mejor será el emplazamiento para la explotación de la energía hidrocinética. Además, el enfoque propuesto aborda las principales dificultades e incertidumbres a la hora de calcular los aspectos que, de una manera más destacada, afectan al CEA de las granjas de energía hidrocinética, evitando suposiciones simplistas y no fiables que puedan resultar en una sobreestimación significativa del OPEX, especialmente en el caso de grandes granjas, y mejorando en general los procedimientos actuales.

La metodología presentada es aplicada al estuario del Shannon en los Capítulos 4, 5 y 6, cada uno de ellos focalizado en un aspecto específico de su aplicación, y por tanto en un procedimiento o índice, de modo que esta puede ser totalmente desarrollada para las características de esta zona costera, así como proporcionar la información necesaria para poder aplicarla en otra región costera de interés para el aprovechamiento energético hidrocinético. Cabe destacar que su desarrollo implica hacer disponible un gran conjunto de datos de modelización numérica hidrodinámica de alta resolución y su análisis a través de procedimientos de análisis geoespacial de vanguardia, conduciendo a la aplicación de los diferentes procedimientos, cuyo objetivo final es el cálculo de una métrica o índice específico, que sirva para proporcionar un apoyo fiable en el proceso de toma de decisiones de una etapa concreta de la planificación del aprovechamiento hidrocinético, desde diseños iniciales hasta proyectos a gran escala, aumentando en complejidad y precisión a la medida que avanzan las fases del proyecto.

En el **Capítulo 4 –** ***Tidal stream energy potential in the Shannon Estuary***, se lleva a cabo el desarrollo y aplicación del índice $TSE_{ndl}$. Este constituye una adaptación del llamado índice TSE, anteriormente aplicado para la selección preliminar de emplazamientos de granjas de corrientes de marea en zonas costeras con limitación de profundidad (p.ej., parte interior o media de estuarios poco profundos), pero ahora revisado para su aplicación adecuada a zonas sin limitación de profundidad (p.ej., estuarios profundos), como el estuario del Shannon. La aplicación del índice TSE a zonas costeras sin profundidad limitada llevaría a una selección inadecuada del emplazamiento, como resultado de considerar cifras de recurso energético sobreestimadas, en consecuencia con el papel que juega la profundidad del agua, que difiere de aquel en zonas de profundidad limitada, requiriendo de una adaptación para su aplicación precisa. Con este fin, se desarrolló una nueva función de penalización-limitación, $\xi_{ndl}$, definiendo un nuevo rango en la anterior función de penalización, $\xi$, dado por un valor límite

de profundidad por encima del cual los valores de $TSE_{ndl}$ están limitados a los correspondientes a esta profundidad del agua limitada, que se estableció teniendo en cuenta las características de las tecnologías de conversión de energía actualmente disponibles. La aplicación de este procedimiento posibilita la delimitación de grandes áreas con potencialidad para el aprovechamiento de la energía hidrocinética, permitiendo así su aplicación en proyectos de ERM en fases preliminares. Como resultado de la aplicación del índice $TSE_{ndl}$ al estuario del Shannon, un total de siete áreas (Áreas I a VII) adecuadas para la conversión de energía hidrocinética fueron delimitadas de manera preliminar, considerando límites específicos del valor del índice y aplicando técnicas de análisis espacial. Con todo, los pasos siguientes en la planificación de granjas de energía hidrocinética deberían considerar no sólo el recurso energético disponible, sino también otros aspectos relevantes, como la explotabilidade de este recurso energético, junto con restricciones socioeconómicas y ambientales, cuya consideración condujo al paso inicial para el desarrollo e implementación del índice IHE.

En este sentido, en el **Capítulo 5 – *A holistic methodology for hydrokinetic energy site selection***, se presenta el desarrollo y aplicación del índice IHE. Dicho índice constituye una herramienta integrada para seleccionar las mejores zonas para la explotación de energía hidrocinética en regiones costeras, considerando la disponibilidad del recurso energético, los costes de instalación y factores socioeconómicos y ambientales, superando así las limitaciones de considerar tecnologías de conversión específicas o diseños concretos de granja y permitiendo su aplicación en proyectos de ERM en fases poco avanzadas. Su implementación implica cuatro pasos: (i) caracterizar la distribución espacial del recurso energético explotable mediante el índice de Energía Hidrocinética (HE, por sus siglas en inglés); (ii) determinar los costes de instalación resultantes de la configuración costera (esto es, profundidad del agua y distancia a la línea de costa) a través de la función de penalización geoespacial de costes ($C_{gp}$, por sus siglas en inglés); (iii) evaluar la coexistencia de la explotación de energía hidrocinética con el resto de los usos costeros existentes o potenciales mediante la implementación de la función de penalización geoespacial de uso del agua ($U_{gp}$, por sus siglas en inglés); y, finalmente, (iv) integrar los pasos anteriores (i a iii) para obtener el índice IHE. La interpretación física del índice y los términos que lo constituyen es la siguiente. Los valores de HE iguales o superiores a 1 indican aptitud para la conversión de la energía hidrocinética, sin considerar otras restricciones; en relación con los términos de penalización, $C_{gp}$ y $U_{gp}$, varían de 1 (sin restricción) a 0 (restricción total). Por consiguiente, cuanto mayor sea el índice IHE, más favorable será el emplazamiento para la explotación de la energía hidrocinética, con valores iguales o superiores a 1 indicando aptitud para tales operaciones. Como resultado de su aplicación al estuario del Shannon, el índice IHE identificó seis áreas (Área $I_{IHE}$ a Área $VI_{IHE}$) con valores de IHE superiores a 1 y, por lo tanto, indicativos de aptitud para la conversión de energía hidrocinética, que difieren de las seleccionadas en estudios anteriores. El área más adecuada, Área $IV_{IHE}$, cerca de Tarbert, ocupa una superficie menor con recursos algo inferiores y menos restricciones en comparación con la zona identificada mediante el índice $TSE_{ndl}$. Con todo, una vez identificada la mejor área para instalar una granja hidrocinética, la definición final requiere un análisis detallado de los costes de las diferentes combinaciones de convertidor y emplazamiento, para lo cual se desarrolla y aplica una metodología en términos de LCOE basada en los resultados del índice IHE, $LCOE_{IHE}$.

Así, finalmente, en el **Capítulo 6 – *A methodology for cost-effective analysis of hydrokinetic energy projects***, se presenta el desarrollo y aplicación del procedimiento conducente al cálculo del parámetro $LCOE_{IHE}$. Este constituye un procedimiento totalmente nuevo para realizar un análisis preciso y efectivo de costes de proyectos de energía hidrocinética, evitando enfoques simplificados y, por tanto, una planificación subóptima del

aprovechamiento energético. En resumen, proporciona una nueva aproximación que lleva a la selección de la combinación de convertidor y emplazamiento más adecuada dentro de un área costera de interés, posibilitando su análisis detallado en proyectos de ERM en su fase final y mejorando así los procedimientos anteriormente disponibles. Su implementación consta de cinco pasos: (i) la definición de las diferentes combinaciones de convertidor y emplazamiento factibles a través de un modelo de vanguardia para la selección de estas combinaciones basado en el índice IHE y algoritmos de análisis espacial; (ii) la evaluación de la producción de energía de las diferentes alternativas definidas en (i); (iii) el cálculo del CAPEX a través de un estudio de detalle de sus costes unitarios; (iv) la evaluación del OPEX considerando procedimientos de O&M específicos para diferentes tipos de convertidores, incluyendo el análisis de los diferentes recursos y el tiempo implicado; y, finalmente, (v) la integración de los resultados de los pasos anteriores (i a iv) para proporcionar parámetros de análisis de coste-beneficio fiables para las diferentes combinaciones de convertidor y emplazamiento, llevando a la selección de la mejor alternativa. Este procedimiento se ilustra para el estuario del Shannon, específicamente para el área de Tarbert, obteniendo los parámetros de análisis de coste-beneficio en términos de LCOE. Este análisis revela que el área con mejor rendimiento y cifras del índice IHE no es necesariamente la más rentable; por el contrario, las economías de escala favorecen a un área mayor con menos recurso disponible pero mejores cifras en términos de coste-beneficio. Consecuentemente, la combinación de convertidor y emplazamiento con mejores resultados en términos de coste-beneficio resulta de instalar la tecnología F-HEC (flotante) en el polígono C, con un $LCOE_{IHE}$ de 0.196 €/kWh. Al comparar los resultados de $LCOE_{IHE}$ con los obtenidos mediante la aplicación de procedimientos desarrollados en trabajos previos (Allan et al., 2011; Ernst, 2007; Ernst, 2010; Vázquez & Iglesias, 2015; Vázquez & Iglesias, 2016la; Vázquez & Iglesias, 2016b), se observan sobreestimaciones significativas, que van desde aproximadamente el 40% al 165%. Estas discrepancias derivan de los cálculos del OPEX, excesivamente simplificados en las metodologías anteriormente disponibles, las cuáles sobreestiman de manera significativa los costes para grandes instalaciones de aprovechamiento energético.

La metodología presentada y los procedimientos que la constituyen podrían ser utilizados para proporcionar información semejante en cualquier otra región costera de interés para la explotación de la energía hidrocinética donde estén disponibles los datos geoespaciales necesarios (condicionantes socioeconómicos, geomorfológicos y medioambientales). Finalmente, cabe mencionar que se hizo un esfuerzo intenso en los últimos meses para ampliar los procedimientos aquí desarrollados para considerar detalladamente la variabilidad intraanual en el recurso energético hidrocinético (p.ej., períodos de tiempo más cortos que las estaciones), lo que conduce a su aplicación en áreas estuarinas cuya hidrodinámica está totalmente dominada por las descargas fluviales. En este sentido, están en desarrollo nuevos parámetros que tienen en cuenta la variabilidad en el recurso hidrocinético.

This thesis develops a comprehensive methodology for the exploitation of the hydrokinetic energy resource in coastal regions —a specific type of marine renewable energy (MRE)—, providing the required information for an informed decision-making process, which is applied to the Shannon Estuary (W Ireland). The methodology comprises three different procedures, each of them resulting in a specific index designed to analyse different stages of hydrokinetic energy farm planning: (i) Tidal Stream Exploitability index adapted to non-depth-limited areas, $TSE_{ndl}$ index, for projects at preliminary stages; (ii) Integrated Hydrokinetic Energy index, IHE index, for projects at early stages; and (iii) Cost-Effective Analysis (CEA) in terms of Levelized Costs of Energy based on the IHE index, $LCOE_{IHE}$, for projects at final stages.